Defining the Oncogenic Functions of Hepatitis B Virus-Human Fusion Transcripts in Hepatocellular Carcinoma

LAU, Chi Chiu

A Thesis Submitted in Partial Fulfillment of
the Requirements for the Degree of
Doctor of Philosophy
in
Anatomical & Cellular Pathology

The Chinese University of Hong Kong

September 2011

Acknowledgement

First, I would like to express my sincere gratitude to my thesis supervisor, Prof. Nathalie Wong for her patience and guidance throughout my PhD study. I have learnt a lot from her, from scientific knowledge to logical thinking and paper writing skills. Experience gained and experimental techniques learnt from her laboratory not only broaden my vision, but is also essential for developing my career in academic research. I truly treasure all the opportunities provided and every moment in her laboratory.

I would like to acknowledge all the current and past laboratory members, Dr. Arthur KK Ching, Dr. Ball KP Lai, Dr. Amy KY Chung, Dr. Erwin TC Chan, Dr. Ibis KC Cheng, Dr. JH Chu, Dr. Queenie WL Wong, Dr. WK Ip, Mr. Bruce CK Tsang, Mr. Gary JW Chen, Mr. Wilson KC Leung, Ms. M He, Ms. Priscilla TY Law, Ms. Vanessa YI Fung, Mr. Alfa HC Bai, Ms. Emily PS Pang, Ms. Joyce BS Yuen, Ms. Navy LY Wong and Ms. PS Li, for providing a friendly working environment, help and sharings during my study. Thanks all the professors, students and supporting staff at the Department of Anatomical and Cellular Pathology and Sir Yue-kong Pao Centre for Cancer for the assistance and cooperation.

Last but not least, I would like to express my deepest gratitude to my beloved family members, especially my wife, and friends for all the unconditional support and encouragement to allow me to overcome all the challenges during my PhD study.

Abstract of thesis entitled:

Defining the Oncogenic Functions of Hepatitis B Virus-Human Fusion Transcripts in Hepatocellular Carcinoma

Submitted by: LAU, Chi Chiu
for the degree of Doctor of Philosophy in Anatomical And Cellular Pathology
at The Chinese University of Hong Kong (September 2011)

Abstract

Chronic hepatitis B (HBV) infection is a major etiologic factor in the development of human hepatocellular carcinoma (HCC). It is long recognized that viral integration into the host HCC genome can be detected in >85% cases, yet the inertional mutagenesis remains largely unclear. In an attempt to define viral integrants, our lab has previously defined recurring HBx/8p11 integration site using the technique of restriction site-polymerase chain reaction (RS-PCR). This study was elaborated by cloning the full-length HBx/8p11 chimeric transcript by 5' and 3' Rapid Amplification of cDNA Ends (RACE). Investigations conducted in this thesis revealed that this novel viral-human HBx/8p11 fusion transcript functions as long non-coding RNA (ncRNA). It regulates the epithelial-to-mesenchymal transition (EMT) and triggers Wnt signalling pathway, all of which are considered important processes in the liver oncogenesis.

The full-length HBx/8p11 chimeric transcript of 674bp contains a microhomology sequence of GTG shared at the flanking juncture. Expression of HBx/8p11 fusion transcript can be detected in 23.3% of HBV-positive HCC tumors (21 out of 90 cases), where a significant correlation with shorter patient survival (P =

0.015) and cox prognostic indicative value (P = 0.014) could be drawn. Functional knockdown of HBx/8p11 resulted in marked inhibition on cell migration (P = 0.04) and invasion (P = 0.04), with upregulation of epithelial markers E-cadherin and γ-catenin expressions, and downregulation of mesenchymal marker fibronectin, suggesting its likely role in EMT phenotype. A corresponding diminution of β-catenin nuclear localization and reduced β-catenin transactivating activity (P = 0.0076) were also revealed, which enforced a role for HBx/8p11 in the membrane-bound E-Cadherin/β-catenin complex. Conversely, ectopic expression of full-length HBx/8p11 in immortalized hepatocyte L02 promoted cell invasiveness (P = 0.005) and migration (P = 0.028) via promoting EMT. This effect was not observed in L02 transfected with empty vector, HBx component or flanking 8p11 sequence. GFP-tagged constructs further suggested protein encoded from HBx/8p11 was similar to the flanking HBx component, suggesting the functional phenotype observed on HBx/8p11 was likely attributed to a non-protein coding RNA transcript (ncRNA). Ectopic expression of full-length HBx/8p11 in L02 also induced colony growth. We further demonstrated in liver-specific transgenic model that mice with HBx/8p11 transgene were more susceptible to DEN-induced tumor formation than non-transgenic littermate. These data highlights the importance for the HBx/8p11 ncRNA transcript in conferring oncogenic advantages, and may represent an elemental predisposing factor in the initiation and progression of HCC.

During the course of RACE cloning for HBx/8p11 full-length sesquence, another viral-human transcript HBx/22q11 (477bp) was also identified. Similar to the HBx/8p11 characterizations of HBx/22q11 were also carried out. HBx/22q11 expressed in 24.9% HBV-positive HCC cases (12 out of 49 cases). However, HBx/22q11 expressions do not correlate with patients' survival and

clinicopathological parameters of these patients. Functional studies also revealed insignificant effect on cell migration, invasion and cell growth.

In summary, novel recurrent viral integration sites leading to the expression fusion transcripts were identified. In particular, HBx/8p11 functions as long ncRNA to promote cell motility, cell proliferation and tumor growth. Taken together with its high prevalence and significant effect in overall survival, HBx/8p11 fusion transcript is a possible molecular target for the development of successful therapeutic interventions in HCC.

摘要

慢性乙型肝炎病毒（HBV）感染是人類肝細胞癌（HCC）發展的主要誘因。儘管一直以來乙型肝炎病毒的整合可以在多於 85%的 HCC 病例的人類基因組中檢測出，但是插入導致的基因突變至今仍然未明。爲了嘗試確定病毒的整合位點，我們實驗室此前曾通過限制性位點-聚合酶鏈式反應（RS-PCR）技術確定了一個重複出現的 HBx/8p11 整合位點。本文進一步透過 5’ 及 3’ RACE 克隆技術，發現了全長 HBx/8p11 融合轉錄子。本論文証實此新的病毒-人類 HBx/8p11 融合轉錄子發揮長非編碼 RNA（ncRNA）的功能，能于肝臟癌變過程中調節上皮-間質轉化（Epithelial-Mesenchymal Transition, EMT）和激發 Wnt 信號通路。

全長 HBx/8p11 融合轉錄子由 674 個鹼基對組成，有一個病毒-人類序列共用的微小同源序列 GTG。在 HBV 陽性的 HCC 腫瘤病例中，23.3%的病例有 HBx/8p11 融合轉錄子的表達（90 個病例中有 21 個呈陽性表達），並証實該表達和患者的較短生存期（$P = 0.015$）及其預測性（$P = 0.014$）有顯著相關性。工能性抑制 HBx/8p11 可以導致細胞遷移能力的顯著下降（$P = 0.04$）和侵襲能力的顯著下降（$P = 0.04$），並可同時引起上皮標記物 E-cadherin 和 γ-catenin 的表達上調，間質標記物 fibronectin 的下調則提示其在 EMT 表型中可能存在的作用。此外還發現了 β-catenin 在細胞核中分佈的減少以及相應的 β-catenin 激活能力的降低（$P = 0.0076$），進一步強調了 HBx/8p11 在膜聯 E-cadherin/β-catenin 複合物中的作用。相反地，在永生肝細胞株 L02 中，全長 HBx/8p11 的異常表達會通過促進 EMT 而提高細胞的侵襲性（$P = 0.005$）和遷移能力（$P = 0.028$），然而，在含空載體，HBx 及 8p11 表達載體的 L02 細胞株中此現象並不明顯。GFP 標記實驗進一步表明，此 HBx/8p11 編碼的蛋白

與相應的 HBx 組份相似，此結果提示了在 HBx/8p11 上所觀察到的功能性表型可能是由於這一非編碼 RNA（ncRNA）。在 L02 細胞株中，全長 HBx/8p11 的異常表達亦可促進細胞生長。我們亦進一步證實了在肝組織特異性的轉基因模型中，具有 HBx/8p11 的轉基因鼠比非轉基因鼠更易於在 DEN 誘導下產生腫瘤。我們的數據指出了 HBx/8p11 ncRNA 轉錄在癌癥形成中的重要作用並且可能是 HCC 發生和進展中的重要誘發因素。

在 HBx/8p11 全長序列的 RACE 克隆過程中，另一個病毒-人類 HBx/22q11(477 個鹼基對)轉錄子亦被確定。與 HBx/8p11 類似，我們亦對 HBx/22q11 進行了功能性的實驗。在 HBV 陽性的 HCC 病例中，24.9%的病例顯示有 HBx/22q11 的表達（49 個病例中有 12 個有陽性表達）。然而，HBx/22q11 的表達與這些患者的生存期和臨床病理特徵並無顯著相關性。功能性研究結果亦顯示 HBx/22q11 表達對細胞遷移能力，侵襲能力和細胞生長並無顯著影響。

總體來說，我們發現了新的可引起融合轉錄子表達的病毒整合位點。特別是具有長 ncRNA 功能的 HBx/8p11 融合轉錄子可以促進細胞遷移能力，細胞增殖以及腫瘤的生長。綜上所述，基於 HBx/8p11 融合轉錄子在 HCC 患者中的高表達率以及其對患者總體生存率的顯著影響，HBx/8q11 可能是一個可以成功干預 HCC 發展的目標靶向分子。

Publications

Publications arising from thesis

CC Lau, AK Ching, KF To, PS Li, VY Fung, W Ng, AW Chan, JH Chu, AH Bai, SS Lee, HL Chan, DI Smith, N Wong. *De novo* transcription of chimeric non-coding RNA at the site of viral integration in human hepatocellular carcinoma. [submitted]

Table of content

List of Figures

List of Tables

Abbreviations

°C	Degree Celsius
AJCC	American Joint Committee on Cancer
ATCC	American Type Culture Collection
bp	Basepair
cDNA	Complementary DNA
CDS	Coding sequence
Chr.	Chromosome
cm	Centimetre
Ct	Threshold cycle
DAPI	4',6-diamidino-2-phenylindole
DNA	Deoxy- ribonucleic acid
dNTP	Deoxy-nucleotide Trisphosphate
dUTP	Deoxy-uracil Trisphosphate
E.coli	Escherichia coli
ECL	Enhanced chemiluminescence
EMT	Epithelial-to-Mesenchymal Transition
FITC	Fluorescein isothiocyanate
GAPDH	Glyceraldehyde-3-phosphate dehydrogenase
GFP	Green fluorescence protein
HBV	Hepatitis B virus
HCC	Hepatocellular carcinoma
HCV	Hepatitis C virus
hr	Hour
kb	Kilobase
kDa	Kilo dalton
LINE	Long interspersed nuclear element
M	Molar
Mb	Megabase
mg	Milligram
min	Minute
ml	Milliliter
mM	Millimolar
mm	Millimetre
mRNA	Messenger ribonucleic acid
MTT	3-[4,5-dimethylthiazol-2-yl]-2,5-diphenyl tetrazolium bromide
ng	Nanogram
nM	Nanomolar
nm	Nanometre
nt	Nucleotide
ORF	Open reading frame
PCR	Polymerase chain reaction
PBS	Phosphate buffered saline

qPCR	Quantitative polymerase chain reaction
RACE	Rapid Amplification of cDNA Ends
RT-PCR	Reverse transcription polymerase chain reaction
RNA	Ribonucleic acid
rpm	Rotation per minute
rRNA	Ribosomal RNA
RS-PCR	Restriction site-polymerase chain reaction
RT	Reverse transcription
SINE	Short interspersed nuclear element
SDS-PAGE	Sodium dodecyl sulfate polyacrylamide gel electrophoresis
sec	Second
siRNA	Small interfering RNA
U	Unit activity
V	Volt
µg	Microgram
µl	Microliter
µM	Micromolar

Chapter 1

Introduction

INTRODUCTION

Hepatocellular carcinoma (HCC) is the seventh most common cancer worldwide and the fourth most common cancer mortality (Ferlay et al. 2010). HCC accounts for 70-85% liver cancer cases, while cholangiocarcinoma, hepatoblastoma, angiosarcoma and hemangiosarcoma are relatively rare (Perz et al. 2006). About 748,300 new cases of liver cancer were reported and 695,500 people worldwide died from liver cancer in 2008 (Ferlay et al. 2010). In Hong Kong, HCC ranked the fourth most common cancer and number three cancer killer (Table 1.1). Males have higher HCC rates than females, with male to female ratios 3.1:1 in Hong Kong (Hong Kong Cancer Registry 2008, Hospital Authority).

Surgical resection or liver transplantation remains the most effective treatment options. For patients whose tumors cannot be surgically removed, tumor ablation and embolization are alternative methods (American Cancer Society 2010, liver cancer general treatment information). Although these advanced methods become the major treatment options of HCC, most HCC patients are still suffered from low 5-year patients' survival mainly because of the following 2 reasons: First is the HCC tumors were only diagnosed at advanced inoperable stages, often with concurrent intra- or extrahepatic metastases. Five-year patients' survival significantly dropped from 21% of patients diagnosed at early stage to only 2% when metastasis occurred in distant organs (American Cancer Society 2010, survival rates of liver cancer). Second is frequent post-operative tumor recurrences, which is resulting from micrometastasis of tumor cells prior to curative surgery (Poon et al. 2000). Although molecular targeted therapeutic agents such as sorafenib and other anti-angiogenic multi-targeted tyrosine kinase inhibitors, such as sunitinib, have been developed recently and seem to be

promising in managing patients with advanced HCC, these treatments are generally palliative in intent and most of these targeted agents have demonstrated a very low response rate when used alone. (Yau et al. 2010).

Uneven distribution of HCC cases was revealed throughout the world (Figure 1.1). More than 80% of HCC cases occur in developing countries such as Southeast Asia and sub-Saharan Africa, while China accounts for more than 50% of the cases, with 350,000 new cases of liver cancer reported per year (El-Serag et al. 2007). Increasing trend was shown in the United States.

Table 1.1 Leading cancer sites in Hong Kong in 2008 (Figures adopted from Hong Kong Cancer Registry, Hospital Authority).

Both sexes				
Rank	Site	New cases registered	Relative frequency	Crude incidence rate*
1	Lung	4,236	17.2%	60.7
2	Colorectum	4,031	16.4%	57.8
3	Breast	2,633	10.7%	37.7
4	Liver	1,745	7.1%	25.0
5	Prostate	1,369	5.6%	19.6
6	Stomach	1,058	4.3%	15.2
7	Nasopharynx	926	3.8%	13.3
8	Non-melanoma skin	717	2.9%	10.3
9	Non-Hodgkin's lymphoma	672	2.7%	9.6
10	Corpus uteri	640	2.6%	9.2
	All sites	24,635	100.0%	353.1

Both sexes				
Rank	Site	Death registered	Relative frequency	Crude mortality rate*
1	Lung	3,497	28.1%	50.1
2	Colorectum	1,686	13.5%	24.2
3	Liver	1,499	12.0%	21.5
4	Stomach	625	5.0%	9.0
5	Breast	515	4.1%	7.4
6	Pancreas	426	3.4%	6.1
7	Nasopharynx	358	2.9%	5.1
8	Oesophagus	343	2.8%	4.9
9	Non-Hodgkin's lymphoma	296	2.4%	4.2
10	Leukaemia	289	2.3%	4.1
	All sites	12,456	100.0%	178.5

* All rates are expressed per 100,000.

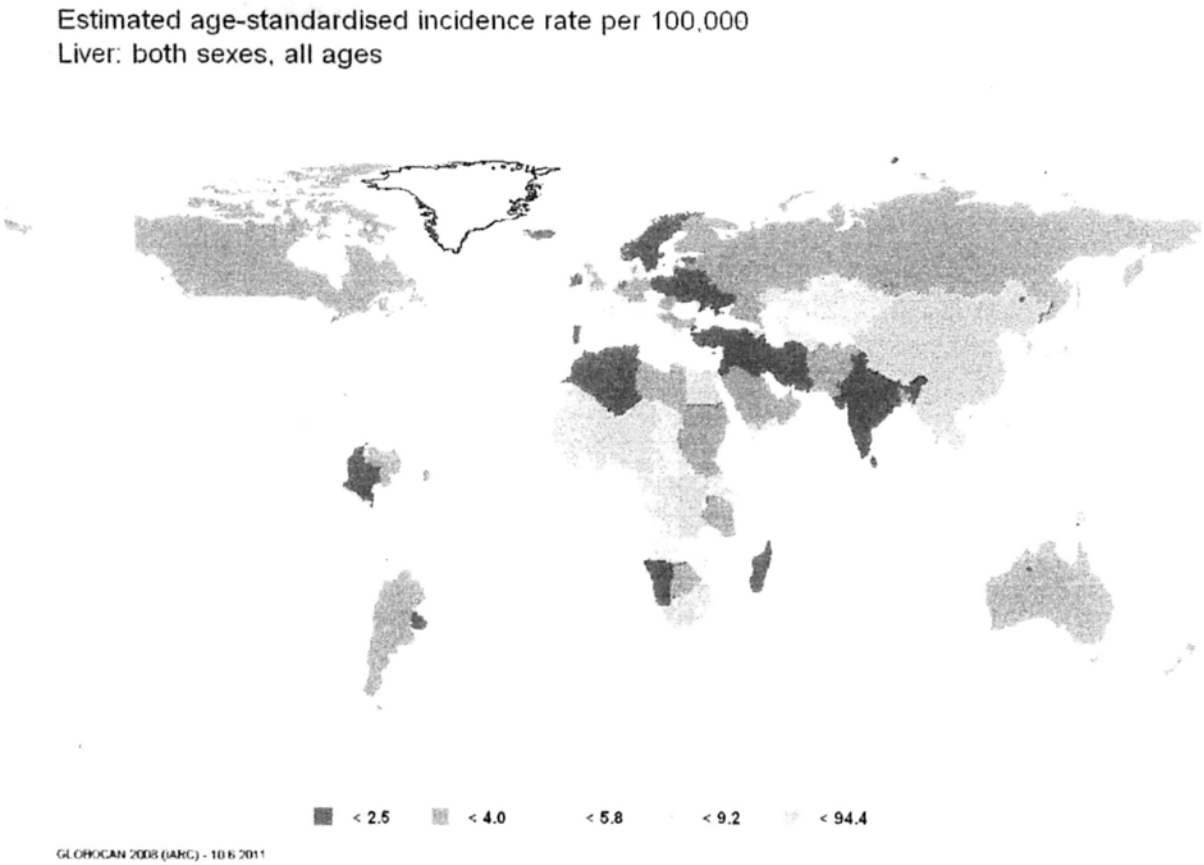

Figure 1.1 Worldwide distribution of liver cancer incidence estimated in year 2008 (GLOBOCAN2008).

1.1 ETIOLOGICAL FACTORS OF HCC

The development of HCC is commonly associated with a variety of etiological factors, including viral hepatitis infections, liver cirrhosis, aflatoxin-B1 exposure, male gender, alcoholic consumption and obesity. The prevalence of these factors varies by regions, accounting for the variation in the prevalence of HCC among different countries.

1.1.1 Viral hepatitis infection

1.1.1.1 Hepatitis B virus (HBV)

About 2 billion people worldwide have been infected with HBV and about 350 million are chronic HBV carriers (World Health Organization, http://www.who.int/mediacentre/factsheets/fs204/en/index.html). HBV infection is endemic, the overall prevalence of chronic hepatitis B infection is more than 8% in Hong Kong and other southeast Asian countries (Figure 1.2). Chronic HBV carriers are subjected to 5- to 15-fold increased risk of HCC development compared with the population without HBV infection. Moreover, around 70% to 90% of HBV-related HCC developed from the patients with cirrhosis (El-Serag et al. 2007). These figures demonstrated HBV infection is associated with higher risk of HCC development.

HBV is divided into genotypes A-H, according to the homogeneity of the viral sequence based on the variation of 8% in the complete nucleotide sequence among genotypes (Chan et al. 2005). Genotype B and C are the most common genotype in Asia, with genotype Ce is associated with higher risk of HCC development (Chan et al 2008).

HBV is classified within the Hepadnaviridae family, characterized as a 42 nm partially double stranded DNA virus, composed of a 27 nm nucleocapsid, surrounded by an outer lipoprotein coat (also called envelope) containing the surface antigen (Figure 1.3A). HBV contain a 3.2kb of relaxed circular, partially duplex DNA with four overlapping open reading frames (ORFs). Polymerase gene encodes reverse transcriptase (pol) that can repair the partially double stranded DNA template. Precore and core region encode HBeAg and HBcAg respectively (Figure 1.3B). Surface gene encodes large, middle and small surface proteins (HBsAg) and X gene encodes X protein (HBx).

Strong association between chronic infection with HBV and the development of HCC have been clearly demonstrated (McMahon. 2009; Beasley. 1988). HBV chronic carriers are subjected to a 5-15 folds increased risk of developing HCC when compared to non-carriers (El-Serag et al. 2007). It is proposed that direct and indirect mechanisms on the viral induction are involved HCC development. HBV proteins expression and viral replications are known to stimulate the host immune response, leading to liver inflammation, cirrhosis and ultimately cancer (Chisari et al. 1995). In addition, based on the fact that over 85-90% of HBV-related HCC tumors harbour one or more sites of HBV insertion which usually precede the development of HCC, a more direct oncogenic effect of HBV integrations on the hepatic carcinogenesis has also been proposed (Buendia, 1992; Bréchot et al. 2000). Majority of HCC tissue also exhibits clonal expansion of tumoral cells carrying the same integration site (Gozuacik et al. 2001).

On the other hand, due to the high replication efficiency and lack of proof-reading activity of polymerase of HBV, mutations occur frequently along the HBV genome. Some mutations affect HBV replication cycle or HBV infection, resulted in enhanced HBV replication or immunological escape to host's immune response. Double mutations A1762T and G1764A in the core promoter region (Takahashi et al. 1998) and G1896A in the precore region lead to HBeAg negativity (Carman et al. 1989). Amino acid change G145R in S gene induced by vaccine cause escape mutant of HBV (Carman et al. 1990). Prolonged therapy with lamivudine has been associated with the development of mutations in a region of the polymerase gene coding for the YMDD (Bock et al. 2002).

HBx is believed to play a key role in hepatocarcinogenesis. HBx is 154 amino acids in size, with a molecular mass of 17kDa. Apart from regulating viral replication, different studies demonstrated that HBx acts as a transcriptional trans-activator. HBx transactivates some signaling pathways by binding to nuclear transcription factors, including cAMP response element binding (CREB), activating transcription factor 2 (ATF-2), Oct-1 and TATA box binding protein (TBP) to activate protein kinase C (PKC), JAK/STAT, PI3K, stress-activated protein kinase (SAPK)/c-Jun NH2-terminal kinase (JNK), Ras/Raf mitogen-activated protein kinase (MAPK), activator protein-1 (AP-1), AP-2, nuclear factor-κB (NF-κB) and Smad. Upregulation of cytoplasmic β-catenin and its downstream genes c-myc and cyclin-D1 suggested the activation of Wnt signaling pathway (Cha et al. 2004). HBx was also shown to activate cellular signal-transduction pathways such as Ras/Raf mitogen-activated protein kinase (MAPK) cascade and Src kinases (Lev et al. 1995). HBx can bind to p53 and inhibit several p53-mediated cellular

processes, including DNA sequence-specific binding, transcriptional transactivation, and apoptosis (Elmore et al. 1997). Figure 1.4 summarized the involvement of HBx in the signaling pathways of hepatocytes (Kremsdorf et al. 2006).

Moreover, increasing number of evidences suggested that C-terminal truncation of HBx enhances the transforming ability of liver cells (Tu et al. 2001, Ma et al. 2008). Among the 80% of HBV integrations into human genome in HBV infected HCC patients, C-terminal HBx truncation was the most frequently detected HBV integrations.

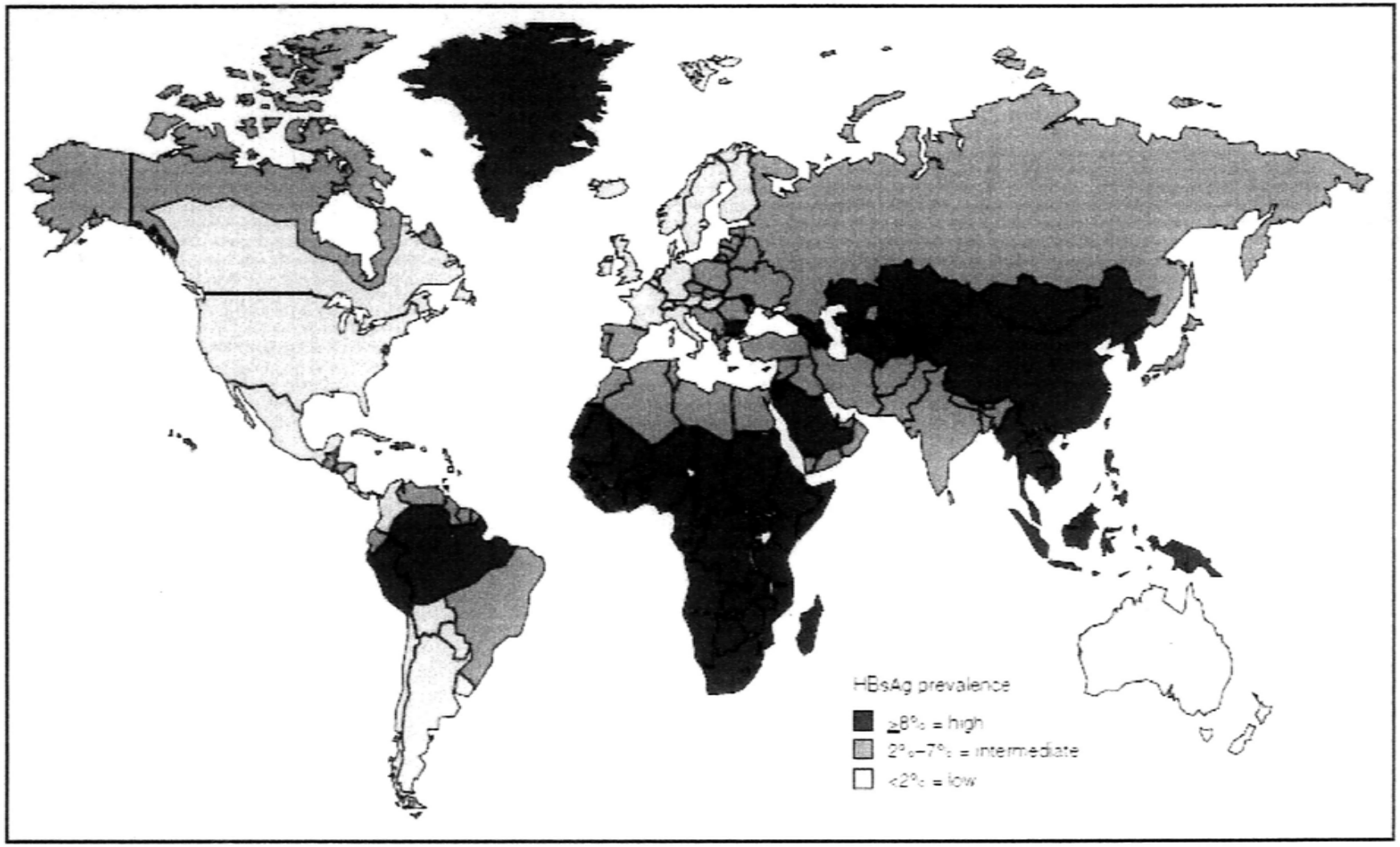

Figure 1.2 Geographic distribution of chronic hepatitis B virus (HBV) infection - worldwide, 2006 (Adopted from CDC, 2008. Available at http://www.cdc.gov/hepatitis/HBV/PDFs/HBV_figure3map_08-27-08.pdf).

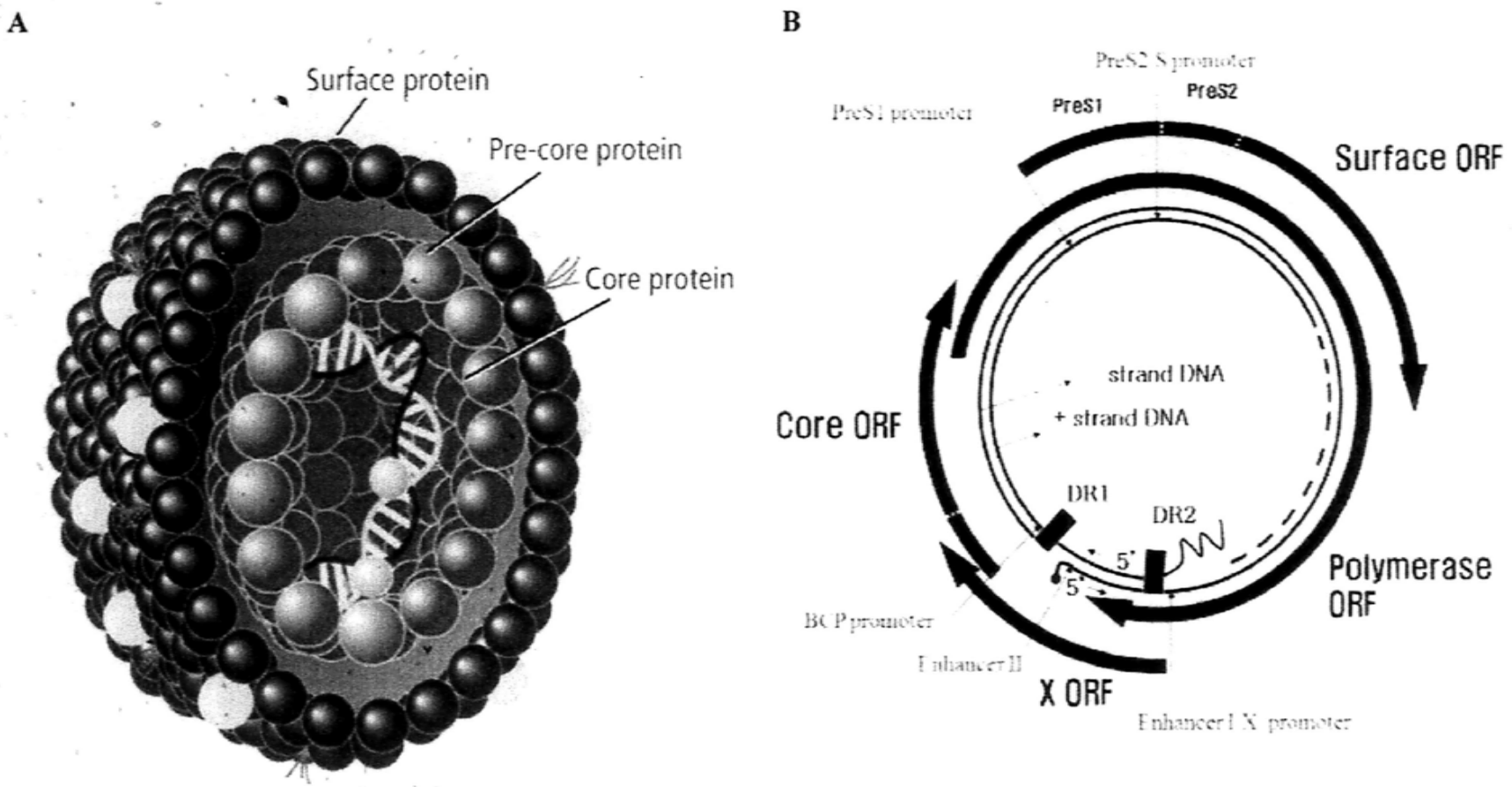

Figure 1.3 Schematic diagram of hepatitis B virus. (A) Structure of HBV (Adopted from Elgouhari et al. 2008). (B) Genomic organization of HBV (Adopted from Yim et al. 2008)

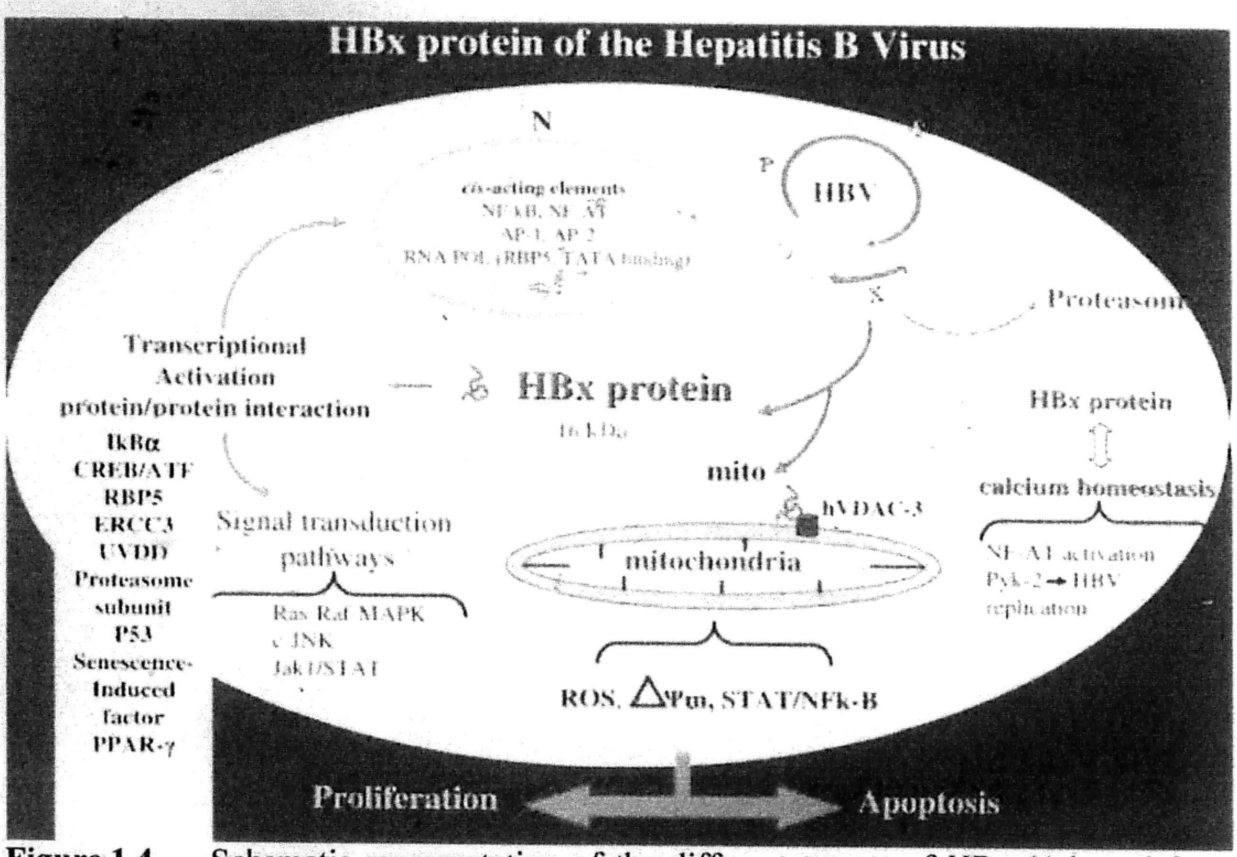

Figure 1.4 Schematic representation of the different targets of HBx (Adopted from Kremsdorf et al. 2006).

1.1.1.2 Hepatitis C virus (HCV)

Hepatitis C virus (HCV) belongs to the Flaviviridae family (Choo et al. 1989). It is a small enveloped positive-stranded RNA virus comprised of six major genotypes that differ in the nucleotide sequence by 30-35%. There are currently 130-170 million people worldwide to be infected with HCV (Lavanchy. 2009). About 50-85% individuals exposed to HCV develop chronic infection, with the associated risks of fibrosis, cirrhosis, and HCC (Hoofnagle. 2002).

The RNA genome of HCV is approximately 9.6kb that encodes a single, large polyprotein of about 3,000 amino acids. The HCV-encoded polyprotein is cleaved post-translationally into several structural and nonstructural peptides: structural components consist of a nucleocapsid core (C) and E1 and E2 envelope glycoproteins. Nonstructural components consist of proteins p7, NS2, NS3, NS4A, NS4B, NS5A and NS5B (Figure 1.4). Although specific functions of the individual NS proteins remain unclear, it is known that NS2 and NS3 have protease and helicase activities, while the NS5 region contains the RNA dependent RNA polymerase activity essential for RNA viral replication. The 5' untranslated region has an internal ribosomal entry site (IRES) essential to initiate viral protein translation. The 3' untranslated region has structured RNA elements essential for both viral replication and translation (Figure 1.5).

Rapid viral replication and the absence of proofing activity of the viral polymerase account for the frequent HCV RNA genome mutations, leading to the presence of high genetic variability of HCV population. This genetic variability of HCV

may contribute to the development of chronic infection and immunological escape due to the rapid changes of the envelope protein in response to immune pressure.

Both structural and nonstructural HCV proteins contribution to the dysregulation of signaling pathways and disrupt the cell physiology. HCV core protein interacts with cellular tumor suppressors such as p53, p73 and pRb. HCV core protein also upregulates the expression of TGF-β (Shin et al. 2005) and activate the Raf/MAPK signaling pathway (Erhardt et al. 2002). E2 activates the MAPK/ERK pathway, including the downstream transcription factor ATF-2 to maintain survival and growth of target cells (Zhao et al. 2005). NS3 inhibits the activity of the $p21^{WAF1}$ promoter (Kwun et al. 2001). NS5A is involved in many cellular functions, including apoptosis, signal transduction, transcription, transformation and ROS production (Majumder et al. 2003).

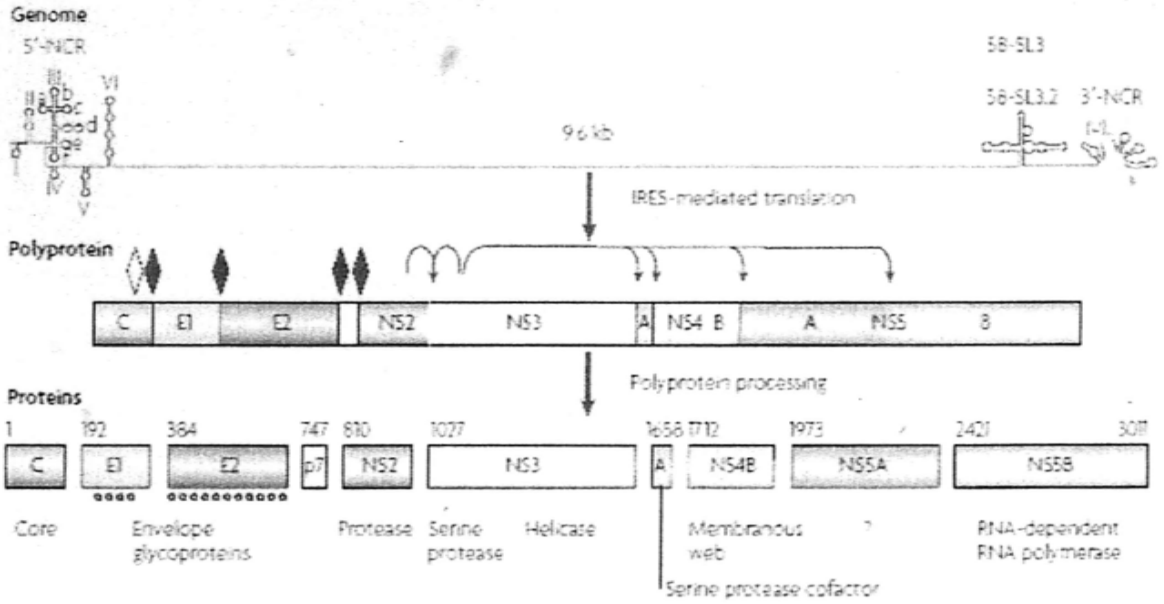

Figure 1.5 Genetic organization and polyprotein processing of HCV (Adopted from Moradpour et al. 2007).

1.1.2 Liver cirrhosis

Cirrhosis is present in 80-90% of HCC patients worldwide which constitutes the largest single risk factor and can be considered a premalignant condition (Caldwell et al. 2009). It is the most advanced stage of fibrosis, characterized by not only more scar than fibrosis, but also distortion of the liver parenchyma associated with septae and nodule formation, altered blood flow, and risk of liver failure. To initiate fibrosis during liver injury, hepatic stellate cells are activated into myofibroblasts and responsive to proliferative PDGF (Friedman et al, 1989; Pinzani, 1996) and fibrogenic TGF-β (Matsuzaki, 2009) cytokines, which are upregulated in fibrogenesis and modulate inflammatory signaling from infiltrating immune cells (Parsons et al. 2007). As a result, the myofibroblasts become proliferative, contractile, and fibrogenic. Over time, bone marrow (which gives rise to circulating fibrocytes), portal fibroblasts, and epithelial mesenchymal transition (EMT) from hepatocytes and cholangiocytes contribute to fibrogenic populations in liver (Friedman et al. 2008). Moreover, cirrhosis is associated with telomere shortening followed by chromosomal instability, deletion of checkpoints (Satyanarayana et al. 2004) and decreased natural killer cell function, which also correlated with HCC development (Friedman, 2008).

1.1.3 Aflatoxin B_1 exposure

Aflatoxin B_1 (AFB_1) is a mycotoxin produced by the *Aspergillus* fungus that grown on corn and peanuts. AFB_1 causes mutation in TP53 codon 249 AGG^{arg} to AGT^{ser} upon metabolized to an active intermediate, AFB_1-*exo*-8,9-epoxide. AFB_1 can also bind to DNA to form the promutagenic N7dG adduct (Buss et al. 1990, Guengerich et al. 1996) and cause oxidative and nitrosative stress, which may indirectly induce TP53 249^{ser} mutations by lipid peroxidation. This mutation induced by AFB_1 exposure is predominant in China and Africa, which was detected in 30% - 60% of HCC tumors (Hsu et al. 1991, Bressac et al. 1991, Turner et al. 2002).

1.1.4 Chronic alcohol consumption

Heavy alcohol intake has been recognized as a cause of steatohepatitis, cirrhosis and eventually HCC. It is reported that HCC risk increased in a linear fashion with daily intake of more than 60g (Donato et al. 2002). Synergistic effect of heavy alcohol consumption with viral hepatitis infection even increase HCC risk for additional 2-fold. The effect of alcohol could be involved in the development of HCC by both direct (genotoxic) and indirect mechanisms. For genotoxic mechanism, proinflammatory cytokines such as TNFα, IL-1β and IL-6, are released from Kupffer cells or infiltrating neutrophils and macrophages and elicit apoptosis of parenchymal cells (Hoek et al. 2002). An indirect mechanism includes the development of cirrhosis, the presence of cirrhosis increase the risk of developing HCC among alcoholics (Kuper et al. 2001).

1.1.5 Male gender

Men are about three to five times more likely to develop HCC than women (Bosch et al. 2004). In 2008, the number of registered cases of HCC in male is 1,319 versus 426 in female (Table 1.2, Hong Kong Cancer Registry 2008, Hospital Authority). The major reason is due to the presence of androgen receptor (AR) in male liver. Androgen/AR signals may modulate many biological events via interaction with various AR coregulators (Heinlein et al. 2002). Conditional knockout hepatic AR mouse with HCC induced by diethylnitrosamine (DEN) demonstrated that AR may play a pivotal role in HCC development (Ma et al. 2008). HBx also contributes the disparity of HCC development between sexes by enhancing the transcriptional activity of the AR in an androgen concentration–dependent manner. Moreover, DEN administration induced greater increases in serum IL-6 concentration in males than it did in females (Naugler et al. 2007) and in turn lead to HCC development (Abiru et al. 2006).

Table 1.2 Incidence of liver cancer in male and female of Hong Kong in 2008 (Figures adopted from Hong Kong Cancer Registry, Hospital Authority).

	Male	Female
Number of cases registered	1,319	426
Rank	4	7
Relative Frequency (%)	10.0	3.7
Male : Female Ratio	3.1	1
Median age (years)	62	70
Crude Rate	40	11.6
Age-standardized rate (World*)	27.4	7.6
Cumulative life-time risk (0-74 yrs)	1 in 33	1 in 134

*The age-standardized rate (World) is calculated based on the world standard population published in the 1997-99 World Health Statistics Annual, WHO.

*All rates are expressed per 100,000.

1.2 HBV INTEGRATION

1.2.1 Proposed mechanisms of HBV integration

Several mechanisms have been proposed for the integration of HBV sequences into the human host genome. Firstly, integration of the viral DNA at a site of single-stranded gap allowed the DNA polymerase switches from human genomic DNA strand to the 5' end of single stranded region of HBV genome. Subsequent recombination joins the long strand of HBV genome with human genomic DNA by end filling and ligation resulted in the full integration of HBV sequence into the human genome (Koshy et al. 1983) (Figure 1.6A). Secondly, partial sequence homology between HBV DNA and the human genomic DNA determined the site of viral integrations. During replication of cellular DNA, the DNA polymerase switches to the partial sequence homology of single-stranded region of the HBV DNA molecule. This is followed by recombination, which leads to integration of the viral DNA (Figure 1.6B) (Koch et al. 1984).

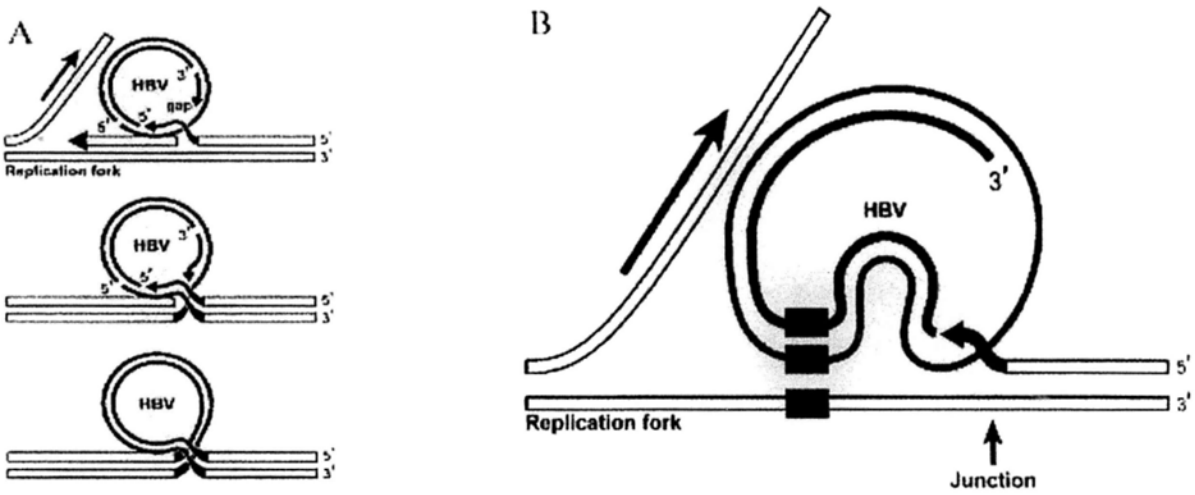

Figure 1.6 Proposed mechanisms of HBV integration. (A) HBV integration through single-stranded gap. (B) HBV integration at the partial sequence homology shared by HBV and human genome.

1.2.2 HBV integration into human genome

HBV integration was found in up to 90% of HCC cases (Koch et al. 1984, Tokino et al. 1987). Although HBV integration into human genome has been suggested to correlate with HCC development and allow the persistence of viral genome (Bréchot 2004), yet the underlying molecular mechanisms remain unclear. In the past years, HBV integrations were identified in different locations within human genome, suggesting the integration is a random event (Matsubara et al. 1990). However, identification of HBV integrations in earlier years was difficult due to limited information available from human genome project.

During liver regeneration, such integrations may promote genetic instabilities such as amplification of cellular DNA, chromosomal deletions, transpositions of viral-human flanking sequences and production of fusion transcripts (Dandri et al. 2002, Wang et al. 1998). Dysregulation of oncogenes, tumor suppressor genes or microRNAs in cancer associated regions and alternation of signaling pathways during tumor development and cancer progression were also described (Feitelson et al. 2007). Under selective clonal advantage, tumor cells bearing viral integrations with growth advantage and anti-apoptotic ability exhibit clonal expansion and become the carrier of the same integration site (Gozuacik et al. 2001). With the accumulation of DNA mutations during the course of HBV infection, the cells carrying such viral integrations may eventually result in a tumor proliferation.

HBV integrations are more likely to occur near or within common fragile sites or repetitive sequences which are highly recombinogenic that are prone to breaks, deletions,

gene amplification and chromosomal rearrangements. These repeat regions include long interspersed nuclear element 1 (LINE1) and short interspersed nuclear elements (SINE), for example, Alu sequences. When viral integrations occur into these repetitive sequences, it can be difficult to locate the site of integration within the genome unless there is sufficient flanking sequence to allow placement at a unique genomic locus. Thus the identification of viral integrations remains not much described, which may result in missing important information.

1.2.3 Gene targets of HBV integration

Many researchers had focused on investigating the relationship between viral integrations and HCC development. Alu-PCR analyses by Gozuacik et al. 2001 and Paterlini-Bréchot et al. 2003 and other research groups had identified the HBV integration sites in vicinity of genes involved in cancer or are key regulators of cell proliferation and death (Figure 1.7): IL-1R associated kinase 2 (IRAK2), p42 mitogen-activated protein kinase 1 (MAPK1) and mevalonate kinase (Graef et al., 1994) are involved in Ras signalling; neurotropic tyrosin receptor kinase 2 (NRTK2), inositol 1,4,5-triphosphate receptor (IP3R) type 1 and 2 and sarco/endoplasmic reticulum calcium ATPase1 (SERCA1) are involved in calcium signalling; thyroid hormone receptor associated protein 150 alpha (TRAP 150), thyroid hormone uncoupling protein (TRUP), control of gene transcription; nuclear matrix protein p84 (NMP 84p) and Cyclin A (Wang et al., 1990) play a role in the control of cell cycle; minichromosome maintenance protein (MCM)-related gene (MCM8) and human telomerase reverse transcriptase (hTERT) are involved in the control of DNA replication. With HBV integration in IP3R and hTERT

recurrently found in different tumors and similar findings from Ferber et al., preferential targets of HBV integration was firstly suggested (Paterlini-Bréchot et al. 2003). In 2005, Murakami et al. conducted a large scaled analysis on 50 HCC cases and again revealed recurrent HBV integration in hTERT in three cases, which further illustrated the preferential HBV integration and allowed the recognition of common cell signaling pathways activated in hepatocarcinogenesis (Murakami et al. 2005).

Similar study was conducted by Saigo et al. suggested recurrent HBV integrations into intron 3 of the mixed-lineage leukemia 4 (MLL4) and expression of HBx/MLL4 chimeric fusion transcript. Subsequent detection of chromosomal translocation between intron 3 of MLL4 and a specific region of chromosome 17p11.2 in HCC samples indicated intron 3 of the MLL4 is one of the sites of translocation break point that served as a preferential target for HBV integration.

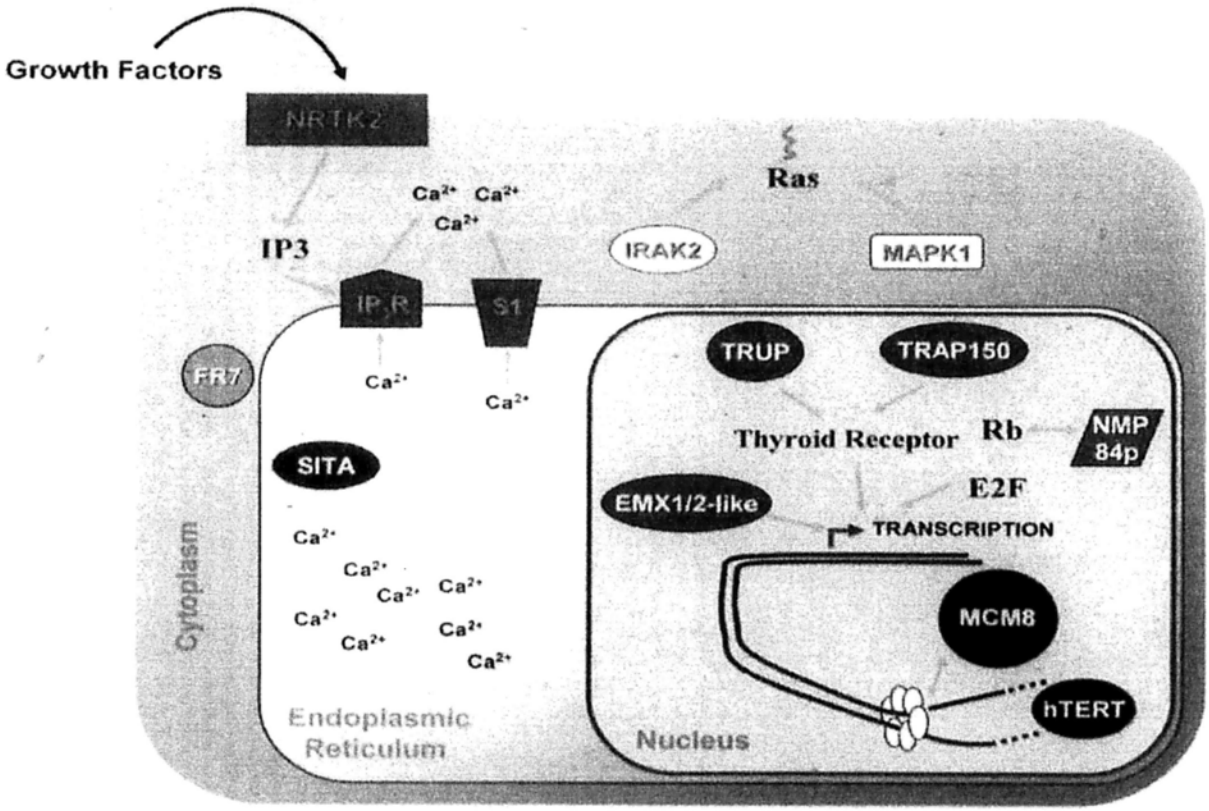

Figure 1.7 Cellular genes targeted by HBV-DNA integration (Adopted from Paterlini-Bréchot et al. 2003).

1.2.4 Truncated HBx integration

Full-length HBx has been strongly implicated in hepatocarcinogenesis by regulating transcription, signaling pathways, cell-cycle control, apoptosis and carcinogenesis. However, COOH-terminal truncations of HBx due to viral integration were also frequently reported. Hong et al. suggested the COOH-terminal truncated HBx enhanced the transforming ability of ras and myc. Similar study conducted by Wang et al. reported that 10 out of 14 HBV integrations within or close to human repetitive sequence. Larger cohort of HCC samples recruited by the same group (Ma et al. 2008) further suggested the high frequency of COOH-terminal truncated HBx, which showed the ability to regulate gene expressions that control cell proliferation and apoptosis. Alternation of Wnt signaling pathway by COOH-terminal truncated HBx was suggested (Liu et al. 2008). Truncated HBx retain their ability to bind to p53, and attenuate DNA repair and p53-mediated apoptosis (Hussain et al. 2007).

1.2.5 Techniques for the identification of HBV integration into human genome

Earlier studies employed Southern blotting and conventional cloning strategies (Matsubara et al. 1990, Bréchot et al. 2000) for the identification of HBV integration sites. However, the low resolution and small scale of detection restricted the understanding on the relationship between HBV integration and hepatocarcinogenesis. Although PCR-based technique such as Alu-PCR was developed for large scale and higher sensitivity of detection, these studies were frequently associated with the identification of Alu repeat sequences or non-Asian HBV genotype (Gozuacik et al. 2001, Paterlini-Bréchot et al. 2003). Thorland et al. utilized restriction site PCR (RS-PCR) for the identification of HPV16 integrations in cervical tumors. Later on Ferber et al. adopted the same approach for the identification of HBV integrations in HCC. A set of HBV specific primers were designed based on published HBV genomic sequence (AB032432) isolated from chimpanzees. Together with the restriction site oligonucleotide primer (RSO primers) containing a T7 RNA polymerase promoter recognition site, 10 random nucleotides and bases specific for restriction sites, nested PCR were performed and HBV-human flanking sequences were amplified. The previous study of our lab utilized this method for the identification of HBV integration sites.

1.2.6 Previous study of our lab using RS-PCR for the identification of HBV integration sites

Although HBV-human flanking sequences had been reported by other group using RS-PCR (Ferber et al. 2003), the redesign of HBV specific primers would increase the sensitivity and specificity of detection. Based on the alignment and consensus sequences of 56 HBV genomes isolated from the patients with chronic hepatitis B infection (genotype B and C) in Hong Kong and China, 8 HBV specific primers were designed 400bp apart from each other on HBV genome (Fig 1.8A). With 6 different restriction-site oligonucleotides, HBV-human flanking PCR products were obtained (Fig 1.8B). Based on our laboratory's previous study, RS-PCR analysis of 15 HBV-positive cell lines and 50 primary tumors (representative results summarizing HBV integrations in cell lines and primary cases wers shown in Table 1.3A and Table 1.3B respectively), a recurring integration site of exact flanking sequences were identified. This HBV integration site was found in cell lines HKCI-4 and primary cases H210T, with HBx integrated into human chromosome 8p11. Microhomology sequence GTG was shared between the viral and human sequence (Figure 1.9). UCSC BLAT analysis suggested the human 8p11 sequence is classified to long interspersed nuclear elements (LINE), which belongs to non-long terminal repeat (LTR) retrotransposable elements.

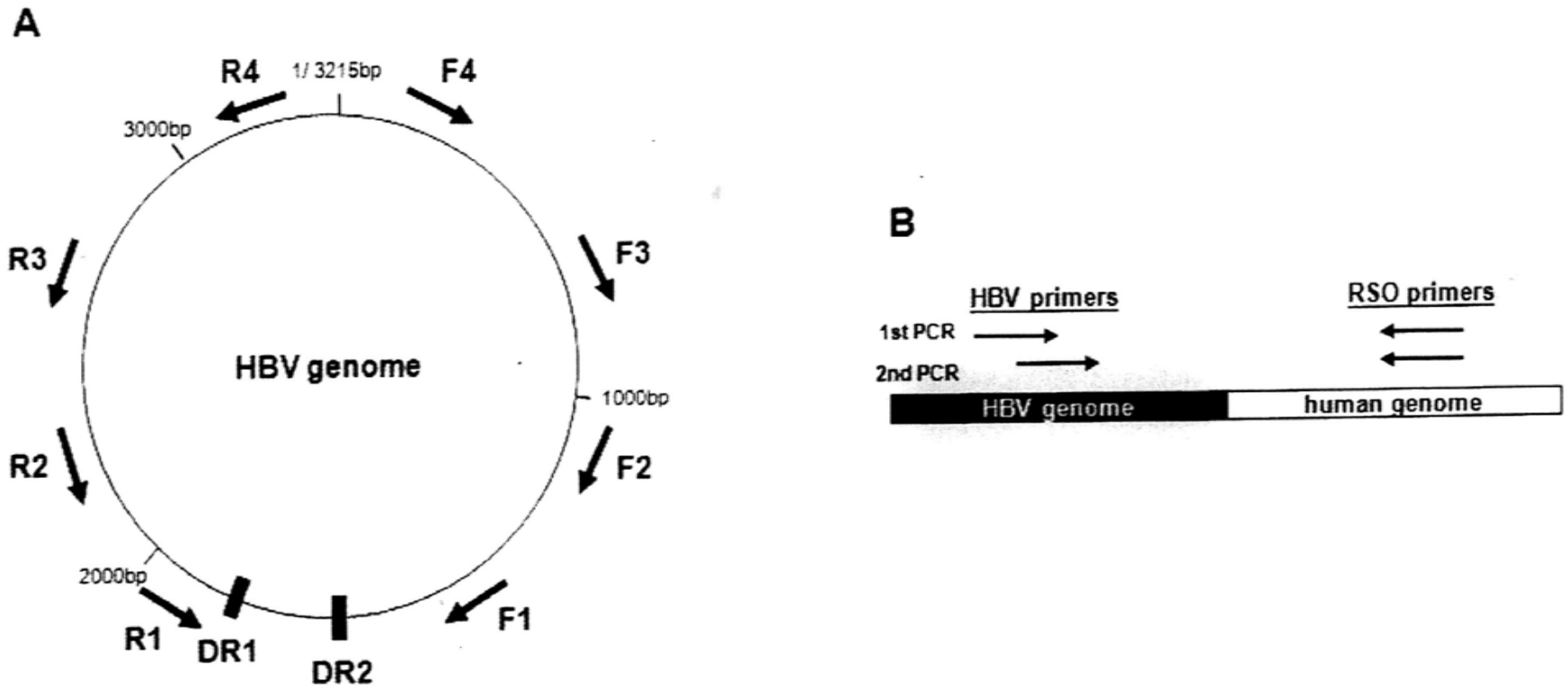

Figure 1.8 Restriction-site PCR (RS-PCR). (A) HBV specific primers design on HBV genome. (B) RS-PCR amplification of HBV-human flanking sequences using HBV-specific and RSO primers.

Table 1.3A Identification of HBV integrations in HCC cell lines in the previous study.

	HBV Junctions		Human Junctions	
	ORF Interrupted	**Sequence corresponding to HBV genome**	**Chromosomal location**	**Known gene interrupted**
HKCI-3	Core	2359-1991	2p23.3 25,156,691-25,157,032 (+)	1st intron of EFR3B
HKCI-4	Polymerase	360-926	2q14.2 119,490,768-119,490,891 (-)	
	Precore/ Core	2135-1824	2q14.1 118,342,743-118,342,936 (+)	
	X	1496-1823	6p12.1 56,633,375-56,633,507 (-)	
	X	1167-1622	8p11.21 41,613,080-41,613,201 (+)	
	X/ Precore	1853-1428	2q36.3 228,942,254-228,942,404 (-)	
	Polymerase	2752-2232	13q34 114,086,130-114,086,285 (+)	8th intron of UPF3A
HKCI-7	X	1488-1811	4q23 100,168,208-100,168,598 (-)	1st intron of METAP1
	Core	2800-2139	4q23 100,168,634-100,168,750 (+)	1st intron of METAP1
	X/Core	2352-1842	11q13.2 68,644,153-68,644,354 (+)	
	Polymerase/ X	1167-1405	11q13.2 68,609,461-68,609,584 (-)	19th intron of TPCN2
	S	3108-2331	13q21.1 57,560,886-57,561,238 (+)	

Table 1.3B Identification of HBV integrations in primary HCC tumors.

	HBV Junctions		Human Junctions	
	ORF Interrupted	**Sequence corresponding to HBV genome**	**Chromosomal location**	**Known gene interrupted**
H206	X	1471-1643	16q12.1 46,717,545-46,717,955 (-)	9th intron of ABCC12
	X	1476-1825	5p13.2 37,858,573-37,858,901 (+)	2nd intron of GDNF
	Core	2806-2163	5p13.2 37,858,573-37,858,890 (+)	2nd intron of GDNF
	X	1471-1982	19q13.12 40,905,088-40,905,196 (+)	3rd intron of MLL4
H227	X	1458-1751	14q21.3 45,219,307-45,219,460 (-)	
	S/ Polymerase	786-1077	15q23 68,832,032-68,832,247 (-)	1st intron of UACA
	X	1472-1740	5p13.2 38,285,703-38,285,939 (-)	
	S	774-811	5p15.33 1,348,675-1,349,055 (-)	516bp upstream to hTERT
H125	X	1476-1736	14q12 23,638,476-23,638,889 (+)	6th exon of PCK2
H210	X	1841-1655	1p12 118,937,910-118,938,347 (+)	
	X	1493-1622	8p11.21 41,613,080-41,613,201 (+)	
H216	X	1857-1684	16q11.2 44,949,428-44,949,675 (-)	
	X	1814-1684	16q11.2 44,949,345-44,949,675 (-)	
	X	1459-1762	2q35 215,993,667-215,993,700 (-)	10th exon of FN1
	Polymerase	1179-1405	17q21.31 39,693,887-39,694,068 (-)	4th intron of SLC4A1
	X	1855-1761	8p23.2 5,113,325-5,114,067 (+)	

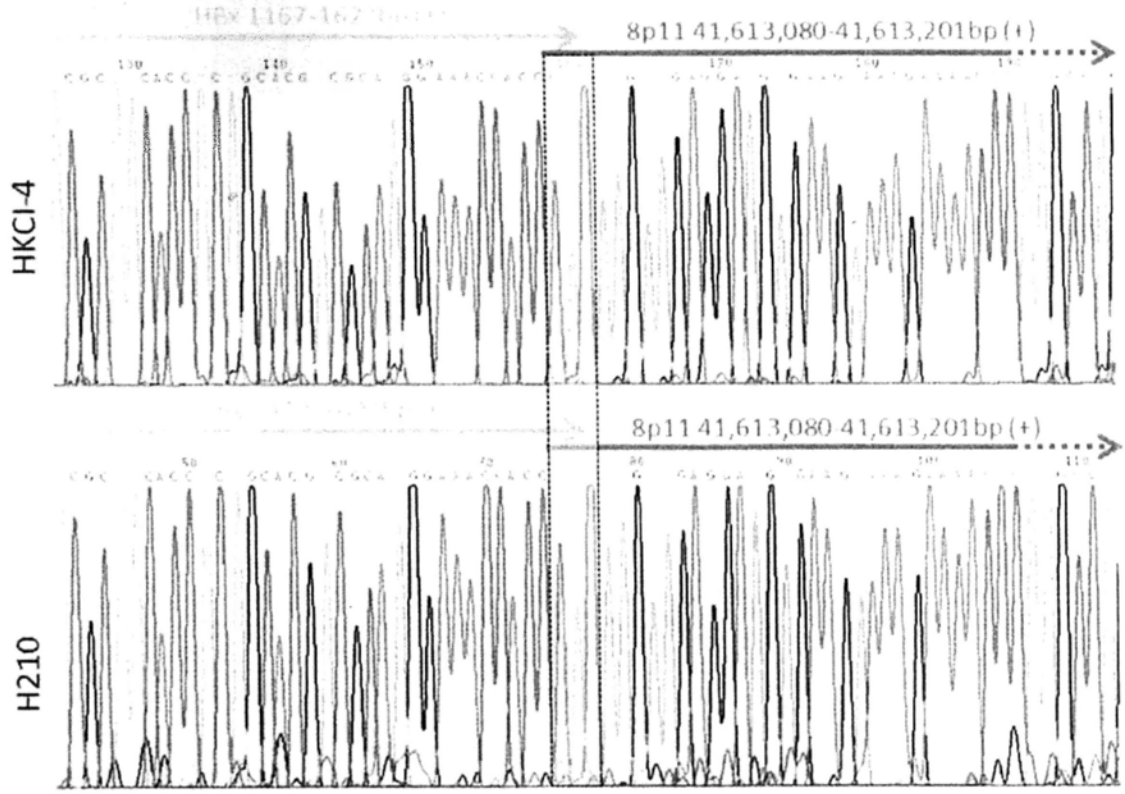

Figure 1.9 HBx/8p11 flanking sequence in cell line HKCI-4 and primary cases H210. Microhomology sequence GTG between HBx and chr8p11 were boxed.

1.2.7 HBV Integration into chromosome 8p11 and 22q11

Molecular genetic studies and cytogenetic analysis showed frequent genomic imbalances in chromosome 8 (Chan et al. 2006; Parada et al. 1998; Moinzadeh et al. 2005). Such chromosomal abnormalities not only found in liver cancer, but also described in hepatoblastoma (Parada et al. 1997), colon carcinoma (Bardi et al. 1995), pancreatic cancer (Gorunova et al. 1998) and in other solid tumor types (Mertens et al. 1997). Viral integrations into such unstable genomic region may be responsible for generation of additional chromosomal alternations such as chromosomal deletions, translocations, amplification of cellular DNA and genomic instability (Ogata et al. 1990; Feitelson et al. 2007; Bonilla et al. 2005), eventually contributing to the carcinogenic process.

HBV integration into the intronic region of Clathrin (CLTCL1) in chr22q11 was revealed. This gene is a member of the clathrin heavy chain family and has important functions in membrane trafficking, endocytosis and mitosis (Schmid. 1997; Okamoto et al. 2000; Doherty et al. 2008). Although CLTCL1 expression is upregulated in skeletal muscle, its expression is very low in most cells (Blixt et al. 2011). The functional roles of CLTCL1 in cancer have not been described.

1.3 THESIS OBJECTIVES

HBV DNA integration can be found in up to 90% of HBV positive HCC and clonal viral insertions have been observed (McMahon. 2009, Gozuacik et al. 2001). Although HBV DNA integration is generally believed to be a random event, few recurred HBV integration resulted in the disruption of genes and possibility of generating fusion transcripts (Gozuacik et al. 2001, Ferber et al. 2003, Murakami et al. 2005, Saigo et al. 2008) have been reported. Therefore, the identification of HBV integrations juxtaposed to cellular genes that participate in liver carcinogenesis may provide an important insight of the relationship between HCC development and chronic HBV infection. Previous RS-PCR study identified recurred HBx/8p11 integration site. Realizing that 8p-arm abnormalities are frequent and important in the liver carcinogenesis, the 8p11 integration site was further investigated in this thesis.

The first objective is to identify the expression of HBV-human fusion transcripts by rapid amplification of cDNA ends, based on the recurred HBV integration site found in RS-PCR analysis. The second objective is to establish the prognostic value of these fusion transcripts by correlating its expression in primary HCC with clinicopathological features and patients' survival. The third objective is to characterize the functional roles exerted by these fusion transcripts by knockdown in HKCI-4 and ectopic expression in immortalized hepatocyte L02. Further characterization of fusion transcript in vivo transgenic model reveals more functional implications contributed by the fusion transcript. Finally, the fourth objective is to identify the molecular mechanism and signaling pathway by which the fusion transcript exert its functions as well as to delineate whether the viral component,

human sequence or the full-length fusion transcript contribute the functional advantages.

Chapter 2

Materials and Methods

2.1 MATERIALS

2.1.1 Reagents

Reagents	Company
Bio-Rad Protein Assay	Bio-Rad Laboratories
Chloroform	Merck & Co., Inc.
Diethyl pyrocarbonate (DEPC)	Sigma-Aldrich Company
Dimethyl sulfoxide (DMSO)	Sigma-Aldrich Company
Ethanol	Merck & Co., Inc
Formaldehyde (37%)	Sigma-Aldrich Company
GelRed™ nucleic acid gel stain, 10,000X in water	Biotium Inc.
Glycerol	Sigma-Aldrich Company
H_2O (Molecular biology reagent)	Sigma-Aldrich Company
Hematoxylin solution, Harris modified	Sigma-Aldrich Company
Hi-Di™ formamide	Applied Biosystems
Isopropanol	Merck & Co., Inc.
LipofectamineTM 2000	Gibco Invitrogen Corporation
Methanol	Merck & Co., Inc.
Mountant	Sigma-Aldrich Company
N,N,N',N'-tetramethylethylenediamine (TEMED)	Sigma-Aldrich Company
Precision Plus Protein™ Standards (dual color)	BioRad Laboratories
RNase ZAP®	Ambion Inc.
Triton X-100	Sigma-Aldrich Company
TRIZOL® reagent	Gibco Invitrogen Corporation
Trypan blue	Gibco Invitrogen Corporation
Tween 20	Sigma-Aldrich Company
Vectorshield anti-fade reagent	Vector Laboratories
Xylene	Riedel-de Haën

2.1.2 Chemicals

Chemicals	Company
3-(4,5-Dimethylthiazol-2-yl)-2,5-diphenyltetrazolium bromide (MTT)	Sigma-Aldrich Company
4',6-Diamidino-2-phenylindole (DAPI)	Sigma-Aldrich Company
Agarose, regular	USB Corporation
Albumin, from bovine serum (BSA)	Sigma-Aldrich Company
Ammonium persulfate (APS)	Sigma-Aldrich Company
Ampicillin sodium salt	USB Corporation
Bromophenol blue	Sigma-Aldrich Company
Crystal violet	Sigma-Aldrich Company
Ethylenediaminetetraacetic acid (EDTA)	Sigma-Aldrich Company
Glycine	Sigma-Aldrich Company
LB agar	USB Corporation
LB broth	USB Corporation
Leupeptin	Sigma-Aldrich Company
Paraformaldehyde	Sigma-Aldrich Company
Pepstatin A	Sigma-Aldrich Company
Phenyl methyl sulfonyl fluoride (PMSF)	GE Healthcare
PhosSTOP	Roche Diagnostics
Protease inhibitor cocktail tablets	Roche Diagnostics
Sephadex™ G-50 Fine	GE Healthcare
Sodium deoxycholate	Sigma-Aldrich Company
Sodium Dodecyl Sulfate (SDS)	USB Corporation
Sodium chloride (NaCl)	Sigma-Aldrich Company
Trizma base	Sigma-Aldrich Company

2.1.3 Buffers

Buffers	Company
Phosphate buffer saline (PBS), pH7.4	Sigma-Aldrich Company
Tris acetate EDTA buffer (TAE), pH7.4	Sigma-Aldrich Company
Tris borate EDTA buffer (TBE), pH7.4	Sigma-Aldrich Company
ULTRAhyb®-oligo hybridization buffer	Ambion Inc.

Prepared buffers	Reagents
Transfer Buffer (Western)	25mM Tris, 200mM glycine, 20% methanol (pH 8.3)
Laemmli sample buffer (5X) (Western)	60mM Tris-HCl, 2% SDS, 25% glycerol, 0.1% bromophenol blue, 5% 2-Mercaptoethanol
Tris-HCl for resolving gel (Western)	1.5M Tris-HCl (pH 8.8)
Tris-HCl for stacking gel (Western)	1M Tris-HCl (pH 6.8)
Running buffer (Western)	25mM Tris, 200mM glycine, 1% SDS (pH8.3)
RIPA Cell Lysis Buffer (Western)	20 mM Tris-HCl (pH7.4), 150mM NaCl, 1mM EDTA, 1mM EGTA, 0.1% SDS, 1% Triton X-100, 1% sodium deoxycholate
Tris buffered saline (TBS)	150mM NaCl, 50mM Tris, (pH 7.5)
Tris buffered saline tween (TBST)	150mM NaCl, 50mM Tris, 0.1% Tween, (pH 7.5)

2.1.4 Cell Culture

Reagents	Company
AIM-V	Gibco Invitrogen Corporation
DMEM	Gibco Invitrogen Corporation
Fetal bovine serum (FBS)	Gibco Invitrogen Corporation
Geneticin (G418)	Gibco Invitrogen Corporation
L-Glutamine 200mM (100X)	Gibco Invitrogen Corporation
MEM Non-essential amino acids solution 10mM (100X)	Gibco Invitrogen Corporation
Opti-MEM®I Reduced Serum Medium	Gibco Invitrogen Corporation
Penicillin-Streptomycin, liquid contains 10,000 units of penicillin and 10,000µg of streptomycin	Gibco Invitrogen Corporation
6.5mm Transwell® with 8.0µm Pore Polycarbonate Membrane Insert	Corning Incorporated
Matrigel Invasion Chambers in two 24-well plates, 8.0µm	Becton Dickinson
Trypsin-EDTA	Becton Dickinson
Tissue culture flask (150, 75cm^2)	Becton Dickinson
Tissue culture dish (150, 100, 60 mm)	Becton Dickinson
Tissue culture plate (96-, 24- and 6-well)	Becton Dickinson

2.1.5 Nucleic Acids

Nucleic Acids	Company
1 kb Plus DNA Ladder	Gibco Invitrogen Corporation
All custom designed primers/oligos	Tech Dragon Limited
BLOCK-iT Fluorecent Oligo	Gibco Invitrogen Corporation
BLOCK-iT Fluorecent Oligo	Gibco Invitrogen Corporation
Deoxynucleotide Trisphosphate Set, PCR grade	Applied Biosystems
Green Fluorescence Protein expression vector (pEGFP-C2)	Clontech, Becton Dickinson
Human normal total liver RNA	Ambion Inc
Human normal total liver RNA	Clontech, Becton Dickinson
Human normal total liver RNA	Stratagene, Agilent Technologies
Stealth RNAi™ siHBx/8p11	Gibco Invitrogen Corporation
Stealth RNAi™ siRNA Negative Control Med GC	Gibco Invitrogen Corporation
TaqMan probes	Applied Biosystems

2.1.6 Enzymes

Enzymes	Company
AmpliTaq Gold DNA polymerase	Applied Biosystems
Pfu DNA polymerase	Stratagene, Agilent Technologies
Protease K	Qiagen
RQ1 RNase-free DNase	Promega Biotech Co., Ltd
RNase A	Roche Diagnostics
SuperScript™ II Reverse Transcriptase	Gibco Invitrogen Corporation
T4 DNA ligase	Gibco Invitrogen Corporation
EcoRI	New England Biolabs
SalI	New England Biolabs

2.1.7 Equipments

Equipments	Company
ABI PRISM® 3100XL Genetic Analyzer	Applied Biosystems
Centrifuge 5415R	Eppendorf International
CM3000-Cryostat	Leica Corporation
Gene Amp PCR System 9700	Applied Biosystems
GloMax®-Multi Microplate Multimode Reader	Promega
Geliance 200 Imaging System	Perkin Elmer
StepOnePlus™ Real-Time PCR Systems	Applied Biosystems
Leitz DM RB fluorescence microscope	Leica Corporation
LSM 5 PASCAL	Carl Zeiss
ND-1000 UV-VIS Spectrophotomer	NanoDrop Technologies
Thermomixer 5435	Eppendorf International
Victor3^{TM} multilabel counter	Perkin Elmer

2.1.8 Kits

Kits	Company
BigDye Terminator Cycle Sequencing Kit	Applied Biosystems
ECL Western blotting detection reagents	GE Healthcare
Dual Luciferase Reporter® Kit	Promega
One Shot® TOP10 Chemically Competent *E. coli*	Gibco Invitrogen Corporation
QIAamp DNA Mini Kit	Qiagen
QIAquick Gel purification Kit	Qiagen
QIAGEN Plasmid Maxi Kit	Qiagen
QIAGEN Plasmid Mini Kit	Qiagen
QIAquick PCR Purification Kit	Qiagen
SMART RACE cDNA Amplification Kit	BD Biosciences
SYBR Green PCR Reagents	Applied Biosystems
TaqMan Universal PCR master mix	Applied Biosystems
TaqMan Universal PCR master mix, No Amperase® UNG	Applied Biosystems
TOPO TA Cloning® Kit	Gibco Invitrogen Corporation

2.1.9 Antibodies

Primary/Secondary antibodies	Company
Active β-catenin mAb (Mouse)	Millipore
β-catenin mAb (Mouse)	BD Biosciences
c-Myc mAb (Mouse)	Santa Cruz Biotechnology
Cyclin D1 mAb (Mouse)	Cell Signaling Technology
E-cadherin mAb (Rabbit)	Cell Signaling Technology
E-cadherin mAb (Mouse) (IF)	Zymed, Invitrogen Corporation
N-cadherin mAb (Mouse) (IF)	Zymed, Invitrogen Corporation
N-cadherin mAb (Mouse)	Santa Cruz Biotechnology
α-catenin pAb(Rabbit)	Cell Signaling Technology
γ-catenin pAb(Rabbit)	Cell Signaling Technology
Cytokeratin 18 mAb (Mouse)	Dako
Fibronectin pAb (Rabbit)	Sigma-Aldrich Company
GAPDH mAb (Mouse)	Chemicon, Millipore Corporation
Vimentin mAb (Mouse) (sc-51721)	Santa Cruz Biotechnology
Vimentin mAb(Mouse) (IF) (sc-6260)	Santa Cruz Biotechnology
Alexa Fluor® 488 goat-anti-mouse IgG ab	Invitrogen Corporation
Alexa Fluor® 488 goat-anti-rabbit IgG ab	Invitrogen Corporation
Anti-rabbit conjugated HRP IgG	Santa Cruz Biotechnology
Anti-mouse conjugated HRP IgG	Santa Cruz Biotechnology

2.1.10 Softwares

Softwares	Company
ABI PRISM® 3130 Genetic Analyzer Data Collection Software v1.1	Applied Biosystems
AxioVision LE ver 4.5	Carl Zeiss
Chromas 2.33	Technelysium Pty Ltd
DNA sequencing analysis software v3.7	Applied Biosystems
GeneSnap	Perkin Elmer
GraphPad PRISM ver 3.02	GraphPad Software Incorporation
LSM 5 PASCAL	Carl Zeiss
LSM Image Browser	Carl Zeiss
MedCalc® ver 11.0.1.0	MedCalc Software bvba
Primer Express 3.0	Applied Biosystems
Quantity One	Bio-Rad

2.1.11 Web Resources

Web Resources	URL
BioMath Calculators	http://www.promega.com/resources/tools/biomath-calculators/
National Center for Biotechnology Information (NCBI)	http://www.ncbi.nlm.nih.gov/
Life science tools	http://www.fr33.net
NEBcutterv2.0	http://tools.neb.com/NEBcutter2/index.php
Primer3	http://frodo.wi.mit.edu/primer3/
UCSC Genome Bioinformatics	http://www.genome.ucsc.edu/
BioMath Calculators	http://www.promega.com/resources/tools/biomath-calculators/

2.2 CELL LINES

HCC cell lines HKCI-3, -4, -5a, -5b, -7, -8 and -9 were previously established from our lab. SNU387, SNU398, SNU423, SNU449, SNU475 and Hep3B were obtained from the American Type Culture Collection (ATCC, Rockvilled, MD). Immortalized normal human liver cell, L02 was obtained from Shanghai Institute of Cell Biology.

The series of HKCI cell lines were cultured in AIM-V medium supplemented with 10% fetal bovine serum (FBS), 1% L-glutamine and 1% penicillin-streptomycin according to the method described (Pang et al, 2000). SNU387, SNU398, SNU423, SNU449, SNU475, Hep3B and L02 were cultured in Dulbecco's modified Eagle's medium (DMEM) supplemented with 10% FBS, 1% MEM non-essential amino acids and 1% penicillin-streptomycin (Invitrogen, Carlsbad, CA). All cultures were maintained in a humidified incubator at 37°C in an atmosphere of 5% CO_2.

2.3 PATIENTS

Tumorous liver tissues were collected from HCC patients who underwent curative surgery for HCC at the Prince of Wales Hospital, Hong Kong. Informed consent was obtained from all patients recruited. A diagnosis of HCC was confirmed from histology examination. Relevant clinical and pathologic information were retrieved from the hospital database.

Ninety patients were recruited (median age: 55; 86% male). All patients are chronic HBV carriers, 74 out of 90 cases (82%) with cirrhosis. Sixty cases were graded as stage T1, 18 cases as stage T2 and 12 cases as stage T3 according to American Joint Committee on Cancer (AJCC) staging system.

2.4 RAPID AMPLIFICATION OF cDNA ENDS

The BD SMART™ RACE cDNA amplification kit provides a method for performing both 5' and 3'-rapid amplification of cDNA ends (RACE) to generate full-length cDNAs in reverse transcription reactions Figure 2.1 showed the procedural overview of RACE.

2.4.1 Total RNA extraction from cell lines

Cells at 80% confluence were subjected to RNA extraction. Cells were washed with DEPC-treated PBS and lysed with TRIZOL reagent (Invitrogen, Carlsbad, CA). Total RNA was extracted by chloroform and precipitated by isopropanol according to the manufacturer's protocol. RNA pellet was washed with cold ethanol and air-dried for 10 min prior the resuspension in DEPC-treated water. RNA integrity was assessed by agarose gel electrophoresis and the concentration and purity was measured by ND-1000 UV-Vis spectrophotometer.

2.4.2 3'-RACE PCR-ready cDNA synthesis

For 3'-RACE cDNA synthesis, 5μl of reaction mixture containing 1μg of total RNA isolated from HKCI-4 and 1μl 3'-CDS primer A was incubated at 70°C for 2 min for RNA denaturation and followed by cooling on ice for 2 min. Two microliters of 5X first-strand buffer (Invitrogen, Carlsbad, CA), 1μl of 20mM DTT, 1μl of 10mM dNTP mix and 1μl SuperScript™ II reverse transcriptase (Invitrogen, Carlsbad, CA) were mixed with the denatured RNA and incubated at 42°C for 90 min. For 3'-RACE cDNA amplification, the first-strand reaction product was diluted with 100μl Tricine-EDTA buffer. Fifty microliters of first round PCR reaction containing 2.5μl of diluted 3'-RACE cDNA, 1μl of 10μM 3'-RACE gene-specific primers, 5μl of 10X universal

primer A mix, 5μl of 10X PCR buffer, 1μl of 10 mM dNTP mix and 1μl of 50X BD Advantage 2 Polymerase mix was subjected to thermal cycling condition of 94°C for 30 sec, 68°C for 30 sec and 72°C for 3 min by 25 cycles. Nested PCR was performed similarly as first round PCR except 2.5μl of first round PCR product, 1μl of 10μM nested 3'-RACE gene-specific primers and 1μl of 10μM nested universal primer were added. Primer sequences for 3'-RACE were listed in Table 2.1 and 2.2.

2.4.3 5'-RACE-ready cDNA synthesis

For 5'-RACE cDNA synthesis, 5μl of reaction mixture containing 1μg of total RNA isolated from HKCI-4, 1μl 5'-CDS primer and 1μl BD SMART II A oligo was incubated at 70°C for 2 min for RNA denaturation and followed by cooling on ice for 2 min. Two microliters of 5X first-strand buffer (Invitrogen, Carlsbad, CA), 1μl of 20mM DTT, 1μl of 10mM dNTP mix and 1μl SuperScript™ II reverse transcriptase (Invitrogen, Carlsbad, CA) were mixed with the denatured RNA and incubated at 42° C for 90 min. For 5'-RACE cDNA amplification, the first-strand reaction product was diluted with 100μl Tricine-EDTA buffer. Fifty microliters of first round PCR reaction containing 2.5μl of diluted 5'-RACE-Ready cDNA, 1μl of 10μM 5'-RACE gene-specific primers, 5μl of 10X universal primer A mix, 5μl of 10X PCR buffer, 1μl of 10 mM dNTP mix and 1μl of 50X BD Advantage 2 Polymerase mix was subjected to thermal cycling condition of 94°C for 30 sec, 68°C for 30 sec and 72°C for 3 min by 25 cycles. Nested PCR was performed similarly as first round PCR except 2.5μl of first round PCR product, 1μl of 10μM nested 5'-RACE gene-specific primers and 1μl of 10μM nested universal primer were added. Primer sequences for 5'-RACE were listed in Table 2.1 and 2.2.

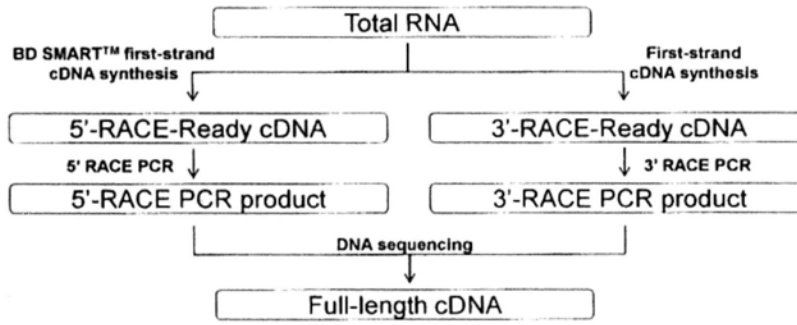

Figure 2.1 Procedural overview of rapid amplification of cDNA ends.

Table 2.1 Primer sequences for RACE.

BD SMART II™ A Oligonucleotide (12 µM)	5′-AAGCAGTGGTATCAACGCAGAGTACGCGGG-3′
3'-RACE CDS Primer A (3'-CDS; 12 µM)	5′-AAGCAGTGGTATCAACGCAGAGTAC(T)$_{30}$VN-3′ (N = A, C, G, or T: V = A, G or C)
5'-RACE CDS Primer (5'-CDS; 12 µM)	5′-(T)$_{25}$VN-3′ (N = A, C, G, or T: V = A, G or C)
5'- & 3'-RACE PCR	
10X Universal Primer A (NUP; 10µM)	
Long (0.4µM)	5′-CTAATACGACTCACTATAGGGCAAGCAGTGGTATCAACGCAGAGT-3′
Short (2µM)	5′-CTAATACGACTCACTATAGGGC-3′
Nested Universal Primer A (NUP; 10µM)	5′- AAGCAGTGGTATCAACGCAGAGT-3′

Table 2.2 Primer sequences for Gene specific primers.

	HBx/8p11	HBx/22q11
3′-GSP	5′-TGCTGCCAACTGGATCCTGCG-3′	5′-TGCTGCCAACTGGATCCTGCG-3′
3′-NGSP	5′-ACGTCCTTTGTTTACGTCCCGTC-3′	5′-ACGTCCTTTGTTTACGTCCCGTC-3′
5′-GSP	5′-TCTCCATGCTGTTTTCCACA-3′	5′-TGCATCCCCCGATTTAACTA-3′
5′-NGSP	5′-ATTCCTACCAAGAGCAGGCA-3′	5′-TCCTCCAAAGTGCACGAGTT-3′

The PCR product was subjected to 1% agarose gel electrophoresis. All the visible bands were excised from the gel and subjected to gel purification using QIAquick Gel Extraction Kit (Qiagen, Valencia, CA) according to the manufacturer's protocol.

2.4.4 TOPO TA cloning

The purified PCR products were cloned into pCR®2.1-TOPO® vector using TOPO TA Cloning Kit® (Invitrogen, Carlsbad, CA) according to the manufacturer's protocol. Five microliters of ligation product was transformed into One Shot® TOP10 competent *E.coli* (Invitrogen, Carlsbad, CA) according to manufacturer's protocol. Transformed *E.coli* was spread on the LB plate with 100μg/ml ampicillin and incubated at 37°C overnight. Ten individual colonies were picked from the LB plate and inoculated in 5ml LB broth with 100μg/ml ampicillin and incubated at 37°C overnight for subsequent plasmid purification and DNA sequencing analysis.

2.4.5 Plasmid purification

Plasmids containing the 5'RACE and 3'RACE PCR products were purified using QIAprep Spin Miniprep Kit (Qiagen, Valencia, CA) according to manufacturer's protocol.

2.4.6 Cycle Sequencing

The DNA sequencing reaction was performed using the BigDye Terminator Cycle Sequencing kit (ABI, Foster City, CA). Ten microliters of sequencing reaction containing 2μl of purified plasmid, 3.22μM primer, 2μl Sequencing buffer and 1μl Big Dye were subjected to 45 cycles of thermal cycling conditions as follows: 1 min at 96°C for 10 sec, annealing at 50°C for 5 sec and extension at 60°C for 4 min. Unincorporated nucleotides were removed using Sephadex™ G-50 fine column. Then 10μl of Hi-Di formamide (ABI, Foster City, CA) was added to the purified product and the DNA was denatured at 95°C for 5 min. The denatured DNA was chilled on ice for 5 min prior to the sequencing analysis by the automated ABI PRISM® 3100XL Genetic Analyzer (ABI, Foster City, CA).

The sequencing data were analyzed by ABI PRISM® 3100 Genetic Analyzer Data Collection Software 1.1 and DNA sequencing analysis software v3.7 (ABI, Foster City, CA). The sequence was searched against UCSC BLAT Search and NCBI Basic Local Alignment Tool for the identification of HBV and human sequence.

2.5 RT-PCR ANALYSIS ON CELL LINES AND PRIMARY TISSUES

2.5.1 Total RNA Extraction from Cell Lines and Tumors

The cells at 80% confluence were subjected to RNA extraction. Cells were washed with DEPC-treated PBS and lysed with TRIZOL reagent (Invitrogen, Carlsbad, CA). Total RNA was extracted by chloroform and precipitated by isopropanol according to the manufacturer's protocol. The RNA pellet was washed with cold ethanol and air-dried for 10 min prior the resuspension in DEPC-treated water. The total RNA integrity was assessed by agarose gel electrophoresis and the concentration and purity was measured by ND-1000 UV-Vis spectrophotometer.

OCT embedded HCC tumors were sectioned with the thickness of 50μm by cryostat. Sectioned tissue was homogenized in 1ml TRIZOL® reagent (Invitrogen, Carlsbad, CA) for RNA extraction following the procedures above.

2.5.2 Reverse Transcription

HBx/8p11 and HBx/22q11 expression in cell lines and primary tumors was analyzed by RT-PCR. First, total RNA was converted to cDNA. Ten microliters of reaction mixture containing 2μg of total RNA, 1U/μl of DNase and 1μl of DNase reaction buffer (Promega, Madison, WI) was incubated at 37°C for 10 min followed by 65°C for 5 min for DNase treatment to eliminate the genomic DNA contamination. DNase-treated RNA was subjected to PCR reaction using primers targeting genomic β–globulin gene to ensure no DNA contamination.

DNase-treated total RNA was subjected to RT reaction using SuperScript™ II reverse transcriptase (Invitrogen, Carlsbad, CA). Twelve microliters of mixture containing 2μg DNase-treatd total RNA, 1μl of 50μM random hexamers and 1μl of

10μM dNTP was heated to 65°C for 5 min. Then 4μl of 5X first-strand buffer, 2μl of 0.1M DTT, 1μl of water was added into the RT mixture and incubated at 25°C for 2 min. One microliter of 200 units SuperScript™ II reverse transcriptase was added to the RT mixture and incubated at 25°C for 10 min, 42°C for 50 min and 70°C for 15 min.

2.5.3 Semi-nested PCR

HBx/8p11 and HBx/22q11 were amplified by semi-nested PCR. Two microliters of first strand cDNA was added to 23μl PCR reaction mix containing 2.5μl of 10X PCR buffer, 1.5mM $MgCl_2$, 0.25mM of dNTP, 0.2μM of each primer and 0.5U of AmpliTaq Gold DNA Polymerase (ABI, Foster City, CA). No template reaction mixture was served as negative control. The PCR reaction mixture was subjected to 30 cycles of thermal cycling condition as follow: 95°C for 30 sec, 58°C for 30 sec and 72°C for 30 sec. Two microliters of the first round PCR product was added to 23μl PCR reaction mix containing the same content as the first round PCR and subjected to 30 cycles of thermal cycling condition as follow: 95°C for 30 sec, 60°C for 30 sec and 72°C for 30 sec. The primers used for amplifying HBx/8p11 and HBx/22q11 were listed in Table 2.3.

Table 2.3 Primers for PCR amplification of HBx/8p11 and HBx/22q11.

	Primer	Sequence (5′ → 3′)	product size (bp)	Tm (°C)
1st round	HBx/8p11 1F	5′-GGACTCTACCGTCCCCTTCT-3′	283	58
	HBx/8p11 1R	5′-AGTAGGGGACTGCTGGATCA-3′		
2nd round	HBx/8p11 2F	5′-CCGTCTGTGCCTTCTCATCT-3′	211	60
	HBx/8p11 1R	5′-AGTAGGGGACTGCTGGATCA-3′		
1st round	HBx/22q11 1F	5′-GGACTCTACCGTCCCCTTCT-3′	160	58
	HBx/22q11 1R	5′-TGCATCCCCGATTTAACTA-3′		
2nd round	HBx/22q11 2F	5′-TACCGTCCCCTTCTTCGTCT-3′	154	60
	HBx/22q11 1R	5′-TGCATCCCCGATTTAACTA-3′		

2.6 FUNCTIONAL ANALYSIS

2.6.1 Evaluation of Transfection Efficiency of Cell Lines

Transfection efficiencies of cell lines were evaluated by transfecting FITC-labeled double stranded RNA (BLOCK-iT Fluorescent Oligo) (Invitrogen, Carlsbad, CA) or Green Fluorescence Protein expression vector (pEGFP-C2) (BD, Franklin Lakes, NJ) mimicking siRNA and plasmid respectively, using Lipofectamine™ 2000 (Invitrogen, Carlsbad, CA). FITC or GFP signal from transfected cells were observed under fluorescence microscope at 24 hr after transfection. The transfected cells were then fixed in 70% ethanol followed by resuspension in PBS for the evaluation of transfection efficiencies using flow cytometry analysis. Representative images and flow cytometry spectra of GFP-vector or FITC-oligo transfected cells were shown in Figure 2.2.

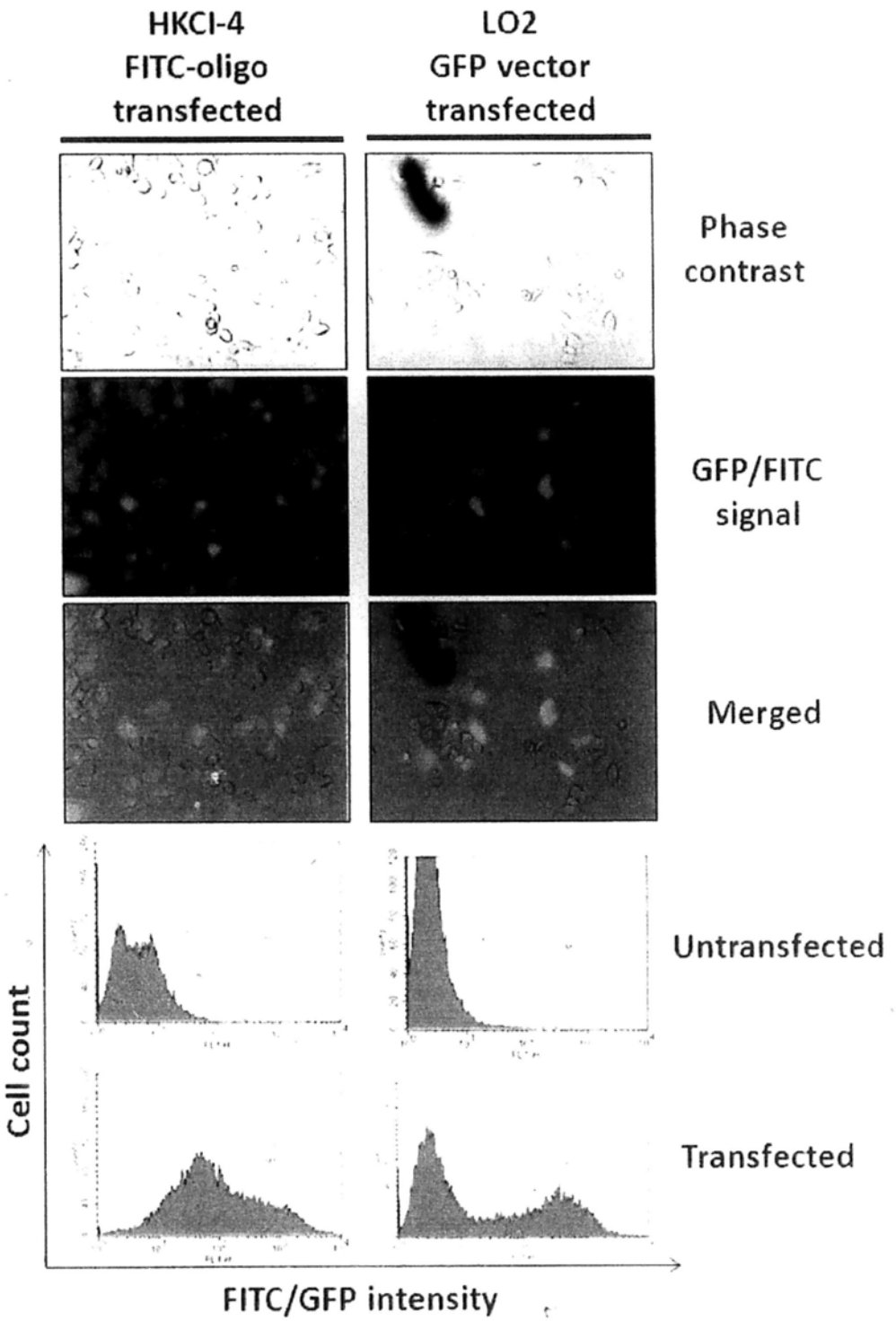

Figure 2.2 Representative images and flow cytometry spectra of GFP-vector or FITC-oligo transfected cells.

2.6.2 Cloning

The effects of HBx/8p11 and HBx/22q11 expressions were studied by overexpressing the full-length HBx/8p11 in immortalized human liver cell lines L02. For HBx/8p11 cloning, full-length HBx/8p11$^{1-674}$, HBx$^{1-297}$ and 8p11$^{295-674}$ were cloned individually to determine the functional sequences on this fusion transcript. As there is a stop codon introduced by chr.8p11, leading to the additional 5 amino acids in the HBx C-terminal, sequence contributing to 5 amino acids from chr.8p11 together with HBx sequence was cloned and designated as HBx+5aa^{1-312*} individually to investigate the functional roles of HBx/8p11 protein. Similarly, for full-length HBx/22q11, HBx/22q11$^{1-477}$, HBx$^{1-303}$, 22q11$^{304-477}$ were cloned. Due to the stop codon in chr.22q11 which introduced 3 amino acids into HBx sequence, 22q11+3aa^{1-315*} was also cloned to mimic HBx/22q11 protein expression. Schematic diagram of different clones of HBx/8p11 and HBx/22q11 were shown in Figure 2.3A and 2.3B respectively.

Overexpression of HBx/8p11, HBx/22q11 and their different clones were performed by cloning these sequences into the derivative of pEGFP-C2 vector, pEGFP-C2R(-), with a deleted EGFP coding. Primers containing restriction sites for amplifying specific sequences of HBx/8p11 and HBx/22q11 were listed in Table 2.4. These sequences were amplified using HKCI-4 DNA as template. Fifty nanograms of DNA was added to 23µl PCR reaction mix containing 2.5µl of 10X PCR buffer, 1.5mM $MgCl_2$, 0.25mM of dNTP, 0.2µM of each primer and 0.5U of Pfu DNA polymerase (Strategene, Aligent, Cedar Creek, TX). The PCR reaction mixture was subjected to 30 cycles of thermal cycling condition as follow: 95°C for 30 sec, 60-65°C for 30 sec and 72°C for 1 min. The PCR products and vector double digested

with EcoRI and SalI (NEB, Ipswich, MA) at 37°C overnight. The digested DNAs were purified using QIAquick PCR Purification Kit (Qiagen, Valencia, CA) according to the manufacturer's protocol. The inserts were ligated to the digested vector in insert/vector molar ratio of 3:1 by T4 DNA ligase (Invitrogen, Carlsbad, CA) at 16°C overnight. Five microliters of ligation product was transformed into TOP-10 *E.coli* competent cells (Invitrogen, Calsbad, CA) and incubated on ice for 30 min, followed by heat shock at 42°C for 30 sec and chilled on ice for 2 min. Transformed cells were recovered by adding 200μl of SOC medium and incubated at 37°C for 1 hr. SOC medium containing transformed cells were spread on LB agar plate with amplicillin (100μg/ml) and incubated at 37°C overnight. Three individual colonies were picked from each plate and subjected to colony PCR to confirm the presence of inserts. Colonies with insert were inoculated in LB broth with amplicillin (100μg/ml) and incubated overnight at 37°C. The plasmids were extracted using QIAprep Spin Miniprep Kit (Qiagen, Valencia, CA). All the plasmids were subjected to DNA sequencing verification and large scale plasmid extraction using Maxiprep Kit (Qiagen, Valencia, CA) for the downstream transfection.

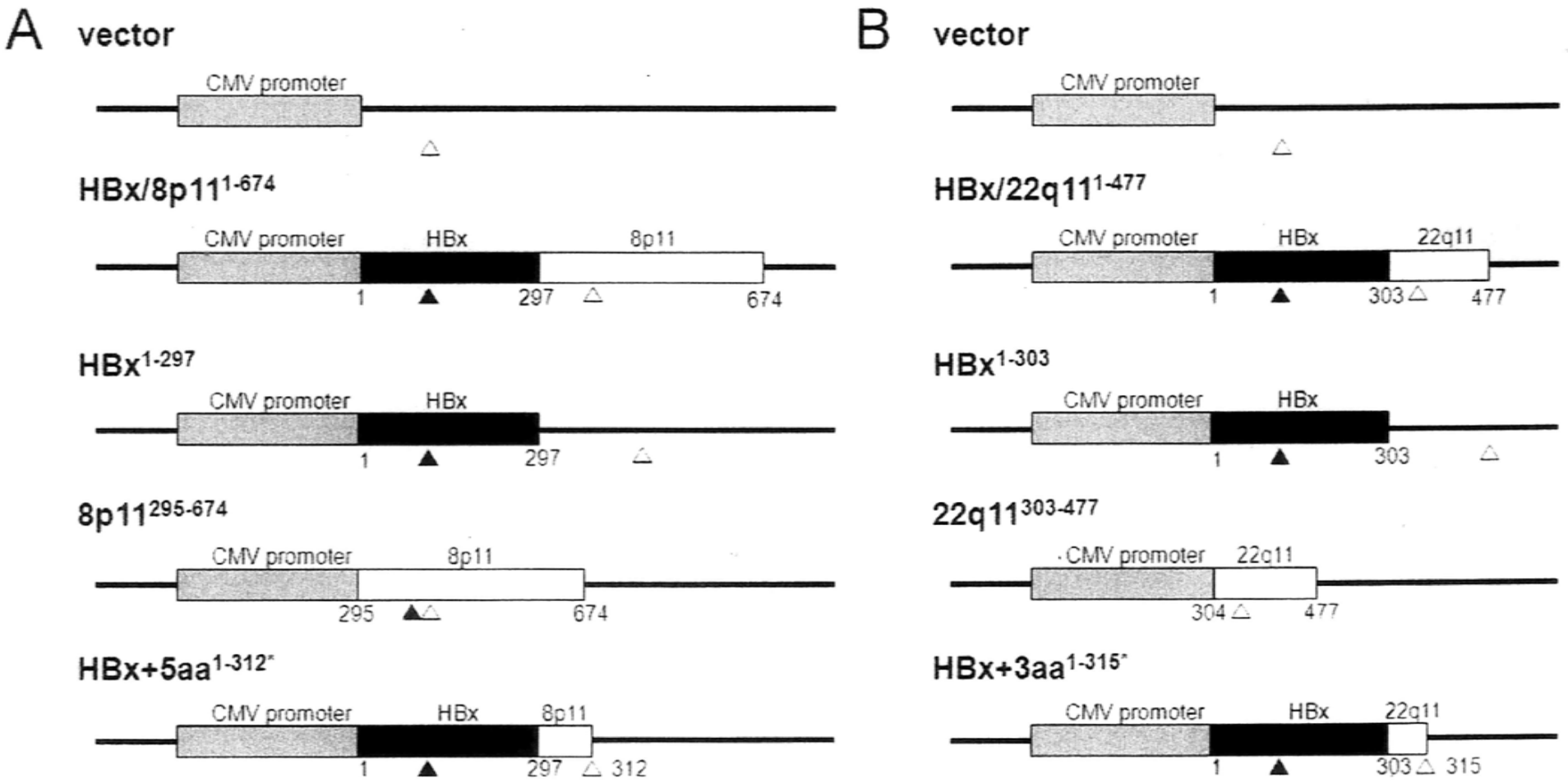

Figure 2.3 Expression contructs of HBx/8p11 and HBx/22q11. (A) Expression constructs of full-length HBx/8p11$^{1-674}$, HBx$^{1-295}$, 8p11$^{295-674}$ and HBx+5aa^{1-312*}. (B) Expression constructs of full-length HBx/22q11$^{1-477}$, HBx$^{1-303}$, 22q11$^{304-477}$ and HBx+3aa^{1-315*}. ▲ and Δ denote start and stop codon respectively.

Table 2.4 Primer sequences for the cloning of HBx/8p11.

Sequence	Primers	Size (bp)	Tm (°C)
HBx/8p11$^{1-674}$	5′-CCGGAATTCCGGAACCGACAACTCTGTTGT-3′ (Forward) 5′-ACGCACGCGTCGACTCCTGTGATTGATTTATTTTAC-3′ (Reverse)	697	60
HBx$^{1-297}$	5′-CCGGAATTCCGGAACCGACAACTCTGTTGT-3′ (Forward) 5′-ACGCACGCGTCGACCACGGTGGTTTCCATGCGAC-3′ (Reverse)	320	65
8p11$^{295-674}$	5′-CCGGGATCCGTGTTGTTGAGGATGTGAAG -3′ (Forward) 5′-ACGCACGCGTCGACTCCTGTGATTGATTTATTTTAC-3′ (Reverse)	403	65
HBx+5aa^{1-312*}	5′-CCGGAATTCCGGAACCGACAACTCTGTTGT-3′ (Forward) 5′-ACGCACGCGTCGACTCACATCCTCAACAACACGG-3′ (Reverse)	335	65
HBx/22q11$^{1-477}$	5′-CGGACTAGTGATCCATACTGCGGAACTCCT-3′ (Forward) 5′-CCGCTCGAGATTGCAGGTGTGAGCCACTG-3′ (Reverse)	495	60
HBx$^{1-303}$	5′-CGGACTAGTGATCCATACTGCGGAACTCCT-3′ (Forward) 5′- CCGCTCGAGCGAGAAGGCACAGACGGGGAGA-3′ (Reverse)	321	65
22q11$^{304-477}$	5′- CGGACTAGTCATGGAAAGTAACTCGTGCAC-3′ (Forward) 5′-CCGCTCGAGATTGCAGGTGTGAGCCACTG-3′ (Reverse)	192	65
HBx+3aa^{1-315*}	5′-CGGACTAGTGATCCATACTGCGGAACTCCT-3′ (Forward) 5′- CCGCTCGAGTTACTTTCCATGCGAGAAGGC-3′ (Reverse)	333	65

2.6.3 Transfection

Ectopic expression of full-length HBx/8p11$^{1-674}$, HBx$^{1-295}$, 8p11$^{295-674}$ and HBx+5aa^{1-312*} was performed to investigate the functional roles of these clones. These clones were transiently expressed in L02 cells by transfecting the cells of 80% confluence for 6 hr using Lipofectamine^{TM} 2000 according to the manufacturer's protocol. The expression of these clones was revealed by semi-quantitative RT-PCR (Figure 2.4A).

Knockdown of HBx/8p11 in HKCI-4 using Stealth Select RNAi^{TM} (Invitrogen, Carlsbad, CA) siHBx/8p11-1 and siHBx/8p11-2 against the sequence 289-313bp or 622-646bp of HBx/8p11 respectively was performed by transfecting the cells of 80% confluence for 24 hr using Lipofectamine^{TM} 2000 according to manufacturer's protocol. The knockdown efficiency was evaluated by qPCR or semi-quantitative RT-PCR (Figure 2.4B). Primers amplifying the specific sequences arised from HBx/8p11 were listed in Table 2.3.

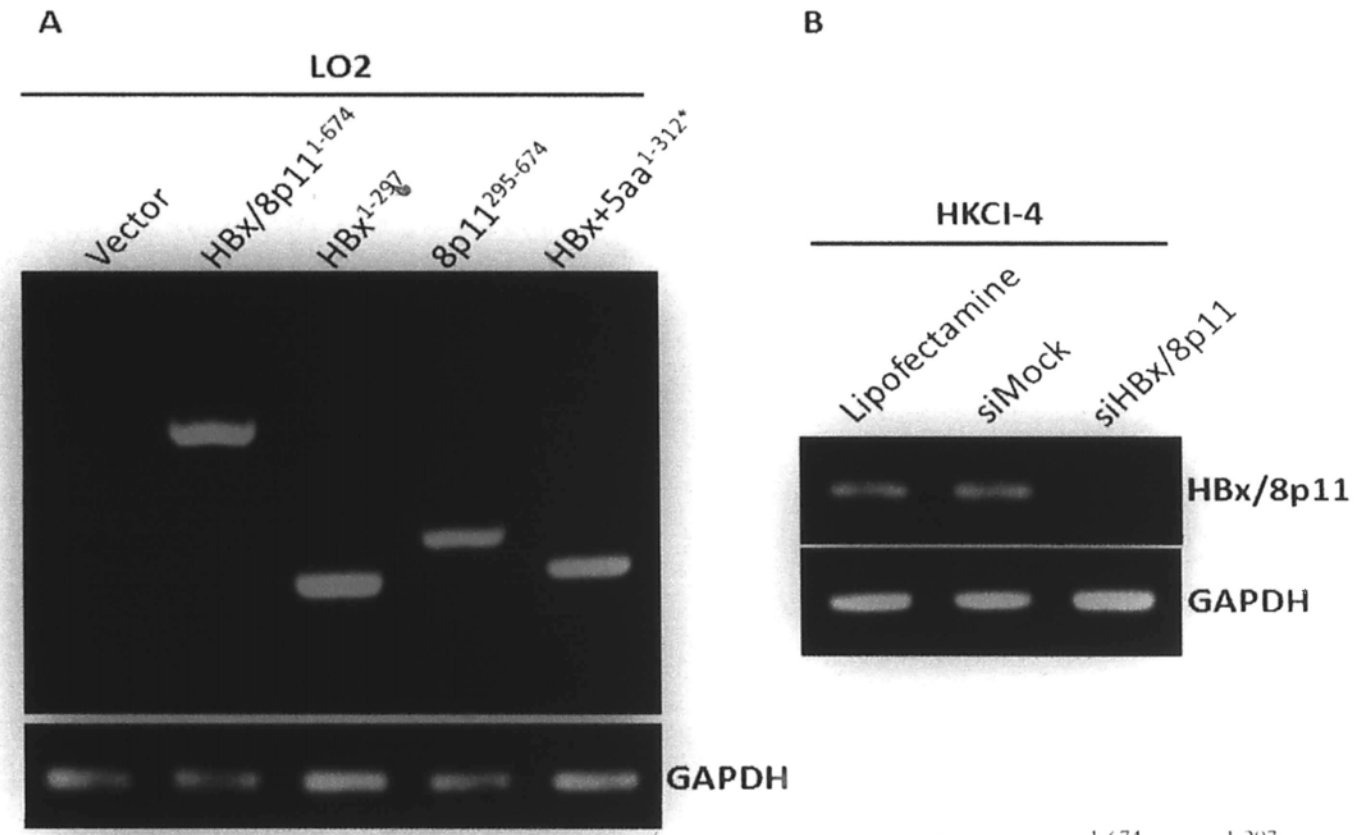

Figure 2.4 Semi-quantitative RT-PCR. (A) Expression of HBx/8p11$^{1-674}$, HBx$^{1-297}$, chr.8p11$^{295-674}$ and HBx+5aa^{1-312*} in L02. (B) HBx/8p11 knockdown was demonstrated in HKCI-4.

2.6.4 Cell Viability Assay

The effect of HBx/8p11 on cell viability was assessed by 3-(4,5-Dimethylthiazol-2-yl)-2,5-diphenyltetrazolium bromide MTT assay. HKCI-4 and L02 were seeded at a density of 2 X 10^3 cells/well in 96-well plate in 5 replicates for 7 days. Cells were incubated with 500μg/ml of MTT (Sigma-Aldrich, St. Louis, MO) for 2 hr at 37°C. Water soluble MTT was converted into insoluble purple formazan salt by living cells and dissolved in 100μl dimethyl sulfoxide (DMSO, Sigma-Aldrich, St. Louis, MO) and the absorbance was measured at 570nm and 630nm using Victor^{3TM} multilabel counter (Perkin Elmer, Waltham, MA).

2.6.5 Colony Formation Assay

L02 transfected with plasmids were seeded in a density of 2 X 10^4 cells/well in 6-well culture plate. The cells were selected in 0.5mg/ml of G418 (Gibco Invitrogen, Carlsbad, CA) for 21 days. Colonies were washed with PBS, fixed and stained by 1% crystal violet (Sigma-Aldrich, St. Louis, MO) in methanol for 15 min and washed by H_2O. Colonies with >50 cells were scored.

2.6.6 Matrigel Invasion and Cell Migration Assay

The effect of HBx/8p11 on cell motility was accessed by Matrigel invasion and cell migration assay. BioCoat™ Matrigel™ Invasion Chamber (8μm membrane pores) (BD, Franklin Lakes, MJ) was used for Matrigel invasion assay and Costar Transwell® (8μm membrane pores) (Corning Incorporation, Cambridge, MA).

The Matrigel™ Invasion Chamber and Costar Transwell® were rehydrated using plain DMEM (L02) or AIM-V (HKCI-4) for 2 hr. L02 (5 X 10^4 for Matrigel Invasion assay, 2 X 10^4 for cell migration assay) and HKCI-4 (2 X 10^4 for both

Matrigel invasion assay and cell migration assay) were resuspended in plain medium and seeded into the chambers. The chambers were immersed in DMEM or AIM-V supplemented with 10% FBS for 24 (HKCI-4) or 48hr (L02). After incubation, the cells remained in the chambers were wiped off and the cells invaded/migrated through the membranes were fixed with 100% methanol for 5 min and stained with haematoxylin (Sigma-Aldrich, St. Louis, MO) for 20 min. The membranes were then washed by ddH_2O, followed by dehydration in 80% ethanol, 100% ethanol and xylene for 2 min each and mounted on glass slides.

The number of cells invaded/migrated from 20 microscopic fields (400X) were scored. Each experiment was performed in duplicated and results were averaged from 3 independent experiments.

2.7 EXPRESSION ANALYSIS BY QUANTITATIVE RT-PCR (qPCR)

RNA extracted from cell lines were converted to cDNA as stated above, followed by quantitative RT-PCR (qPCR) with either gene-specific TaqMan Probes (ABI, Foster City, CA) or SYBR® qPCR.

Twenty microliters of PCR reaction mix containing 1.5µl of cDNA, 1µl of 20X TaqMan probe (ABI, Foster City, CA) and 10µl of TaqMan® Universal PCR Master Mix with AmpErase UNG (ABI, Foster City, CA) or SYBR® Green PCR mix (ABI, Foster City, CA) were subjected to thermal cycling condition in 96-well optical tray in StepOnePlus™ Real-Time PCR System (ABI, Foster City, CA) as follow: 50°C for 2 min, 95°C for 10 min and 40 cycles of 95°C for 15 sec and 60°C for 1 min. Each experiment for detecting the threshold cycle of the target gene was performed in triplicates. Target gene expressions were normalized with 18S rRNA. No template control reaction was included in each reaction. The relative expression level (defined as fold change) of target gene is given by $2^{-\Delta\Delta Ct}$ ($\Delta Ct = \Delta Ct^{target} - \Delta Ct^{18S}$). TaqMan probe against HBx/8p11 was designed by Primer Express® software v3.0, with the forward primer 5'-GCTTCACCTCTGCACGTC-3', reverse primer 5'-TAATTTACATTCCTACCAAGAGCAGG-3' and TaqMan probe 5'-ATGGAAACCACCGTGTTGTTGAGGATGT-3'. Primer-probe mix was prepared by mixing 1.5µl of 100µM forward and reverse primer, 1µl of 100µM TaqMan probe and 16 µl H_2O. TaqMan gene expression assays and SYBR® qPCR analysis were listed in Table 2.5 and 2.6 respectively.

Table 2.5 TaqMan Assays for qPCR

E-cadherin repressors	TaqMan Gene Expression Assay (ABI, Foster City, CA)
SNAI1 (SNAIL)	Hs00195591_m1
SNAI2 (Slug)	Hs00950344_m1
ZEB1	Hs00611018_m1
ZEB2	Hs00207691_m1
TWIST1	Hs00361186_m1
TCF3	Hs01012685_m1
18S rRNA (Internal control)	Hs99999901_s1

Table 2.6 Primer designs of neighboring genes for SYBR® qPCR analysis

Genes	Primer sequences
ZMAT4	Forward 5'-TTTATTCACAGACAGTTACTGCAAGGT-3'
	Reverse 5'-GACTTTGCTTGCATGTTTTCGA-3'
SFRP1	Forward 5'-ACGTCTGCATCGCCATGAC-3'
	Reverse 5'-GCCTCAGATTTCAACTCGTTGTC-3'
GOLGA7	Forward 5'-TCCGGAAAGGTGTTCATTCAG-3'
	Reverse 5'-GCTGCCTATCAATCCGGTTCT-3'
ANK1	Forward 5'-CTGAGAGCAGCAAGATCAGGTAAC-3'
	Reverse 5'-GCAAGCCATTCAACCCATTC-3'
MYST3	Forward 5'-GGCTCAACACTAAAGCAACCAA-3'
	Reverse 5'-GGCTTATCCTTTTCATGTGGAAGA-3'
PLAT	Forward 5'-GAGGCCAGACGCCATCAG-3'
	Reverse 5'-CTTCCCCGCCTTAAAGACGTA-3'
POLB	Forward 5'-GGCCGCCATGAGCAAAC-3'
	Reverse 5'-TTGGCTCACGTTCTTCTCAAAG-3'
c8orf40	Forward 5'-CCTTGTTAGCTTCGGTCTCTTCA-3'
	Reverse 5'-TTGGGCTCTGACAAAGTTTCCT-3'
DKK4	Forward 5'-GAGCTCTGGTCCTGGACTTCA-3'
	Reverse 5'-CTGGTATTGCAGTCCGTGTCA-3'
GINS4	Forward 5'-GAACGCCCCGTCCTTACC-3'
	Reverse 5'-GAAATCCACTTCTTCGGTCATCTT-3'
IKBKB	Forward 5'-CGTCCCTGCCGACAGAGTTA-3'
	Reverse 5'-TCCCAAGGCGCTCTTTCAT-3'
AGPAT6	Forward 5'-AGCCATTTTTGGAGTCTCCTTTG-3'
	Reverse 5'-CTTGGCTCCTCGCTCCATT-3'
AP3M2	Forward 5'-CCTGTCCGCGCCTAGGA-3'
	Reverse 5'-TTTCAAGACCAGGCCCAATC-3'
VDAC3	Forward 5'-CACAGCCAAATCCAAACTGTCA-3'
	Reverse 5'-TCCAAATTCAGTGCCATCGTT-3'
SLC20A2	Forward 5'-TGTACAACGAGACGGTGGAGACT-3'
	Reverse 5'-ATTGGAAGCCTCAGGAAGGAA-3'
NKX6-3	Forward 5'-GGGGAAGAAGCAGACACTCC-3'
	Reverse 5'-GCTCTTCTTCCGCCACTTG-3'
miR-486	hsa-miR-486 (TaqMan Gene Expression Assay (ABI, Foster City, CA)

2.8 WESTERN BLOTTING

Total protein were extracted from the cells by RIPA lysis buffer containing protease inhibitor cocktail and phosSTOP (Roche Applied Science, Penzberg, Germany). The protein concentration was quantitated by using Bradford reagent (Bio-Rad, Hercues, CA) by measuring the absorbance at 595nm using Victor^{3TM} multilabel counter (Perkin Elmer, Waltham, MA).

Twenty micrograms of total protein were separated by 8-12% SDS polyacrylamide gel electrophoresis. The protein was transferred to Hybond^{TM}-P PVDF membrane (GE Healthcare, Piscataway, NJ) using semi-dry electrophoretic transfer (Bio-Rad, Hercues, CA). Non-specific bindings of antibodies were blocked by 5% non-fat dry milk for 1 hr. The blots were probed against primary antibodies at 4°C overnight. Primary antibodies were listed in Table 2.7. After 2 times of washing with TBST buffer by gentle agitation, the blots were probed against horseradish peroxidase conjugated secondary antibodies in a dilution of 1:5000 (1:20000 for GAPDH) (Santa Cruz Biotechnology, Santa Cruz, CA) for 1 hr. Protein bands were visualized on X-ray film using enhanced chemiluminescence detection (GE Healthcare, Piscataway, NJ).

Table 2.7 Primary antibodies for Western blot.

Features	Antibodies/ markers	Size (kDa)	Companies	Sources	Dilutions
Epithelial	E-cadherin	135	Cell Signaling Technology	Rabbit	1:500
	α-E-catenin	100	Cell Signaling Technology	Rabbit	1:1000
	γ-catenin	83	Cell Signaling Technology	Rabbit	1:1000
	Cytokeratin 18	45	Dako	Mouse	1:1000
Mesenchymal	Fibronectin	220	Sigma-Aldrich Company	Rabbit	1:1000
	N-cadherin	135	Santa Cruz Biotechnology	Mouse	1:1000
	Vimentin	57	Santa Cruz Biotechnology	Mouse	1:500
	Smooth muscle actin	42	Sigma-Aldrich Company	Mouse	1:1000
Wnt Signaling	β-catenin	92	BD Biosciences	Mouse	1:1000
	Active β-catenin	92	Millipore	Mouse	1:1000
House keeping	GAPDH	37	Millipore	Mouse	1:20000

2.9 IMMUNOFLUORESCENT IMAGING

Cells were seeded in a density of 1.5 X 10^5 cells on a cover-slip (22 X 22mm) in a 6-well culture plate overnight. Cells were transfected according to the protocol. The cells were washed with PBS twice and fixed with 4% paraformaldehyde (Sigma-Aldrich, St. Louis, MO) for 20 min. The cells were washed twice with PBS for 5 min followed by permeabilization by 0.1% Trition X-100 (Sigma-Aldrich, St. Louis, MO). The cells were blocked by 3% goat serum (Invitrogen, Carlsbad, CA) to prevent non-specific binding. The cells were probed against primary antibodies for 3 hr at room temperature and washed twice with PBS after incubation. Primary antibodies were listed in Table 2.8. Secondary antibodies conjugated with Alexa-Fluor® 488 (Invitrogen, Carlsbad, CA) were allowed to probe against the primary antibodies for 2 hr at room temperature. Cells were counterstained by DAPI (Sigma-Aldrich, St. Louis, MO) in anti-fade solution (Vector Laboratories, Burlingame, CA) and images were captured by LSM PASCAL confocal microscopy (Carl Zeiss, Gottingen, Germany).

Table 2.8 Primary antibodies for immunofluorescence imaging.

Features	Antibodies/ markers	Companies	Sources	Dilutions
Epithelial	E-cadherin	Cell Signaling Technology	Rabbit	1:100
	α-E-catenin	Cell Signaling Technology	Rabbit	1:100
	γ-catenin	Cell Signaling Technology	Rabbit	1:100
	Cytokeratin 18	Dako	Mouse	1:500
Mesenchymal	Fibronectin	Sigma-Aldrich Company	Rabbit	1:200
	N-cadherin	Zymed	Mouse	1:100
	Vimentin	Santa Cruz Biotechnology	Mouse	1:100
	Smooth muscle actin	Sigma-Aldrich Company	Mouse	1:100
Wnt Signaling	Active β-catenin	Millipore	Mouse	1:100

2.10 TOP/FOPFLASH LUCIFERASE REPORTER ASSAY

TCF-dependent luciferase activity in HKCI-4 and L02 cells following siHBx/8p11 treatment or full-length HBx/8p11$^{1-674}$ ectopic expression were measured. Five hundred nanograms of pTOPflash or pFOPflash with 20ng of Renilla plasmid were co-transfected. The activities of firefly and Renilla luciferases were detected using Dual-Luciferase® Reporter Assay System (Promega). Relative luciferase activities were calculated by normalizing the ratios of TOP/FOP with the Renilla luciferase activities.

2.11 ANIMAL STUDY

2.11.1 Construction of HBx/8p11 Transgene

Full-length HBx/8p11 was cloned into expression vector containing liver-specific transthyretin (TTR) promoter (kindly provided by Van Dyke TE) to generate HBx/8p11 transgene (Figure 2.5). Fill-length HBx/8p11 was amplified using the forward and reverse primer containing NruI restriction site. The HBx/8p11 PCR product was cloned into the expression vector by conventional cloning approach as stated above.

2.11.2 Transgenesis

Transgenic mice were made following the standard protocol outlined in references (Hogan et al. 1986; Pinkert 1994). F2 zygotes of F1CB mouse strain (F1 of BALB/C male crossed with C57BL/6 female) were used for microinjection. TTR-HBx/8p11 was microinjected into F2 zygotes. Surviving zygotes after the injection were transferred to the oviducts of foster mothers (ICR mouse strain). After weaning, the pups were ear-tagged and tail biopsies were obtained for PCR screening.

2.11.3 Preparation of Transgene DNA for Microinjection

Transgene DNA for microinjection was prepared using Qiagen Plasmid Maxi kit (Qiagen, Valencia, CA) according to the manufacturer's protocol. The DNA dissolved in TE buffer was then cut with EcoRI overnight. The digested DNA was resolved by 0.8% agarose gel electrophoresis. The TTR-HBx/8p11 fragment was cut and gel purifified by QIAquick gel purification kit (Qiagen, Valencia, CA). The concentration was measured

by ND-1000 UV-Vis spectrophotometer. The injection DNA concentration was adjusted to 1ng/μl.

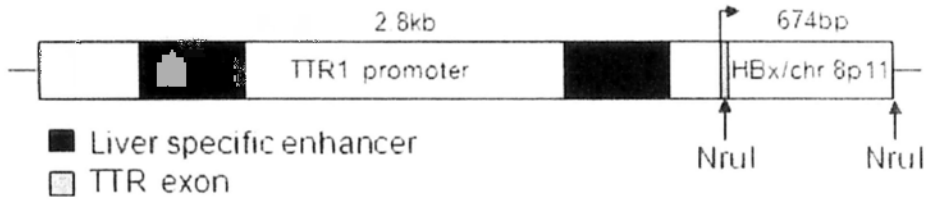

Figure 2.5 Schematic diagram of liver-specific TTR-HBx/8p11.

2.11.4 F1CB Production and Superovulation

C576L/B female mice were mated with BALB/C mice to generate F1CB mice. Superovulation of adult F1CB female mice were induced by injecting hormone by the following time schedule: On day 1, 5 I.U. of pregnant mare serum gonadotropin (PMSG) was injected i.p. at 4 p.m. On day 3 before noon, 5 I.U. of human chorionic gonadotropin (HCG) was injected and each injected female was kept with one male F1CB. Copulation was confirmed by the presence of mating plug in female genital opening.

2.11.5 Preparing foster ICR

Adult ICR male were vasectomized and kept individually in separate cages. Vasectomized mice were allowed to mate with adult female mice for several times to confirm sterility and mating ability. Only those could plug female mice but without causing pregnancy were to be used. One vasectomized ICR mouse was allowed to mate with two adult ICR female mice on the day before microinjection.

2.11.6 Preparation of Embryo Culture Medium

M2 and M16 media were prepared by addition of appropriate volume of diluent into the medium powder. After all the powder was dissolved, the liquid medium was stored in aliquots at 4°C. Each vial was used only once. Drop culture was set up one day before egg harvesting. Seven to eight drops of M16 medium, each around 30µl were added on a 35mm petri dish. Parafilm oil was laid on top of the drops and left in a CO2 incubator overnight for pH equilibration.

2.11.7 Recovery of Fertilized Eggs

Plugged F1CB female mice were sacrificed by cervical dislocation. Oviducts were cut out and put onto a petri dish containing M2 medium to wash away debris and transferred into a watch glass containing M2 medium. The swelling ampullae were located and the eggs with cumulus cells were released by tearing the oviduct wall. A drop of hyaluronidase was added into the watch glass. When the cumulus cells were detached, the single egg was transferred to a new petri dish with M2 medium to wash away the enzyme. Residual enzyme was removed by repeating the washing step for 2 more times. The washed eggs were transferred into the M16 drop culture equilibrated previously and incubated at 37°C in a 5% CO_2 incubator for until microinjection.

2.11.8 Microinjection of Mouse Egg Pronuclei

After 2-3hrs of incubation, eggs with clearly visible pronuclei were subjected to microinjection. Twenty to 25 eggs were transferred to depression slide containing a drop of mineral oil covered M2 medium. Eggs were injected one by one using a micromanipulators-controlled injection pipette and a holding pipette under a DIC equipped inverted microscope at 200x magnification. Concentration of DNA solution used for microinjection was around 1ng/µl. Microinjected eggs were transferred back to the M16 drop culture equilibrated previously and incubated in a CO_2 incubator for recovery. Another batch of 20-25 eggs was transferred to the injection chamber and the microinjection procedure was repeated until all the eggs were done. Healthy eggs were picked for oviduct transfer to ICR foster mothers on the same day or the day after.

2.11.9 Oviduct Transfer

ICR foster mice were anaesthetized with ketamine and xylazine mixture. A small incision was made in the lateral size area located between the spine and the pelvic girdle. The fat pad attached to the ovary was located and the tissue pulled out gently from the abdominal cavity. The tissue was kept in position by a bulldog type serrefine. A hole was made on the membrane embraced the ovary and oviduct. Infundibulum was stabilized by a twister gently. Healthy eggs after transferring into M2 medium were sucked into a mouth pipette together with a bubble at each end and blown into the oviduct. Presence of two bubbles inside the oviduct, indicates successful transfer. The ovary and oviduct were put back inside the abdominal cavity carefully. The wound was stitched up by surgical needle. About 15 eggs were transferred into each oviduct. Oviduct transfer was then repeated at the other side. The foster mothers were kept in a warm quiet place after the operation to allow recovery from anesthesia. The pups born of the foster mothers were then screened for the presence of transgene after weaning.

2.11.10Screening of Transgenic Mouse

Screening of the pups for transgenesis was performed by PCR using genomic DNA extracted from tail clippings. Genomic DNA was extracted using DNeasy Tissue Kit (Qiagen, Valencia, CA). The tissues were digested with proteinase K (Qiagen, Valencia, CA) and 4 µl RNase A (100 mg/ml) and genomic DNA was extracted according to the manufacturer's instruction. For PCR screening, primers HBx/8p11 1F and HBx/8p11 1R with the thermal cycling condition same as RT-PCR stated above.

2.11.11 Induction of HCC Development in Transgenic Mice

HCC development was demonstrated in male mice at 8 months when diethylnitrosamine (DEN) was administrated by intraperitoneal injection in male mice of age 15 days (Nakatani et al, 2001). Mice of age 15 days received a single intraperitoneal injection of DEN (5 mg/kg body weight; Sigma-Aldrich, St. Louis, MO). Mice were sacrificed after 8 months and liver RNA was extracted to confirm HBx/8p11 expression by qPCR. The presence of surface nodules were evaluated and recorded. HCCs were confirmed histologically by an experienced pathologist. All experiments in the current study were conducted in accordance with guidelines by the Animal Experimentation Ethics Committee of the Chinese University of Hong Kong.

2.12 STATISTICAL ANALYSIS

Data are presented as mean ± S.E.M., unless otherwise indicated. Kaplan-Meier plots and log-rank tests were used for survival analysis. Correlations with patient's survival were investigated by Cox regression using MedCalc (MedCalc Software, Mariakerke, Belgium). Correlation of HBx/8p11 or HBx/22q11 expression with clinicopathological parameters of HCC patients were calculated by Chi-square or Mann Whitney test (specifically for tumor size and age) using PRISM (GraphPad Software). The independent Student's t test was used to compare the functional effects, gene expression levels and luciferase reporter readings between groups. A P value less than 0.05 was considered statistically significant.

Chapter 3

De novo Transcription of Chimeric non-coding RNA at the Site of Viral Integration in Human Hepatocellular Carcinoma

3.1 INTRODUCTION

Although the details on HBV-induced carcinogenetic changes remain elusive, implication of viral integrants in the development of HCC has been long suggested. Low-resolution approaches of Southern blotting and cloning strategies in earlier reports suggested HBV integrations to occur randomly throughout the whole genome, leading to the presumption that there are no preferential sites of insertion (Matsubara et al. 1990). In recent years, high-resolution analysis demonstrated many HBV integrants occur in the proximity of important cancer-related genes, within or near chromosome fragile sites that have been postulated to prone genetic instability (Kremsdorf et al. 2006). Preferential integrations in the cellular genome at sites that harbour genes involved in regulating cell signaling, proliferation and viability were further highlighted recently (Murakami et al. 2005). In the previous study, our laboratory had attempted to explore the HBV DNA junctures in primary HCC tumors and cell lines using restriction-site PCR (RS-PCR) screening (Thorland et al. 2003). The detection of recurrent 8p11 insertional site of exact viral-human sequences prompted the further cloning for the full-length transcript. In this chapter, a novel viral-human chimeric sequence of 674bp transcribed from the site of insertion was discovered by the combination of 5' and 3' RACE. The fusion transcript comprised of the HBx open reading frame (297bp) and intergenic sequence from 8p11 (380bp), sharing a 3bp micro-homology (GTG) between the viral and human sequences. Investigation of HBV/8p11 chimeric sequence in HCC tumors and cell lines revealed a remarkable incidence of ~25%, which further suggesting this integration is a non-random event. Functional characterization of HBx/8p11 demonstrated its role in promoting metastatic potentials of HCC cells through regulating the Epithelial-Mesenchymal

Transition (EMT). More suprisingly, HBx/8p11 exerts it oncogenic effects as a long non-coding RNA (ncRNA), which is usually defined at a size of greater than 200 bp (Hung et al. 2010).

Recent genome-wide studies have highlighted the non-protein-coding RNAs (ncRNAs), including miRNAs, siRNA and various classes of long ncRNAs, are transcribed in the mammalian genome in high abundancy. Increasing evidences also revealed vital roles for ncRNA in regulating cellular processes as well as their aberrant expressions in contributing to disease phenotypes. However other than miRNAs, only a handful of long ncRNAs have been studied in the hepatocarcinogenesis (Matouk et al. 2007; Matouk, et al. 2009; Oliva et al. 2009; Panzitt et al. 2007). The present study on HBV-related insertional mutagenesis has allowed isolation of previously undescribed viral-human chimeric ncRNA that confers advantages in tumor growth and cell motility implicated in liver pathogenesis.

3.2 RESULTS

3.2.1 Cloning of Full-length HBx/8p11 and Expression in HCC

Based on the previous findings on high-throughput PCR-based RS-PCR, particular interest was the finding of a recurring HBV integration that displayed the exact viral human flanking sequence. In primary tumor H210 and cell line HKCI-4, HBV enhancer I and HBx promoter sequences (HKCI-4: 1167-1622; H210T: 1493-1622) were found to insertion at the precise position on chr.8p11.21, which is a LINE1 region (chr.8: 41,613,080-41,613,201) (Table 1.3A and 1.3B). In all cases, the 3'-end of integrated HBx sequence shared a common microhomology GTG with the 5'-end of chr.8p11 region (Figure 1.10). Next the effect of viral integration on the transcription of HBx and 8p11 sequences was examined. By 5' and 3' RACE cloning in HKCI-4, we isolated a 3'-end transcript of 8p11 that contained a polyadenylation signal AATAAA and poly(A) tail (Figure 3.1A), and a 5'-end transcript entailing the HBx sequence (Figure 3.1B). In addition, the juncture sequence that flanked the HBx and chr.8p11 was identical to the RS-PCR sequence obtained. By combining the results obtained from the 3'and 5' -end RACE, a full-length HBx/8p11 fusion transcript of 674bp was identified (Figure 3.2A). The transcript comprised of 297bp from HBx, ranged from 1326-1622bp of HBV genome (accession no.: NC_003977), and 380bp of chr.8p11 that ranged from 41,613,080-41,613,459bp; the overlapping 3bp GTG homology was also present in the transcribed sequence (Figure 3.2B).

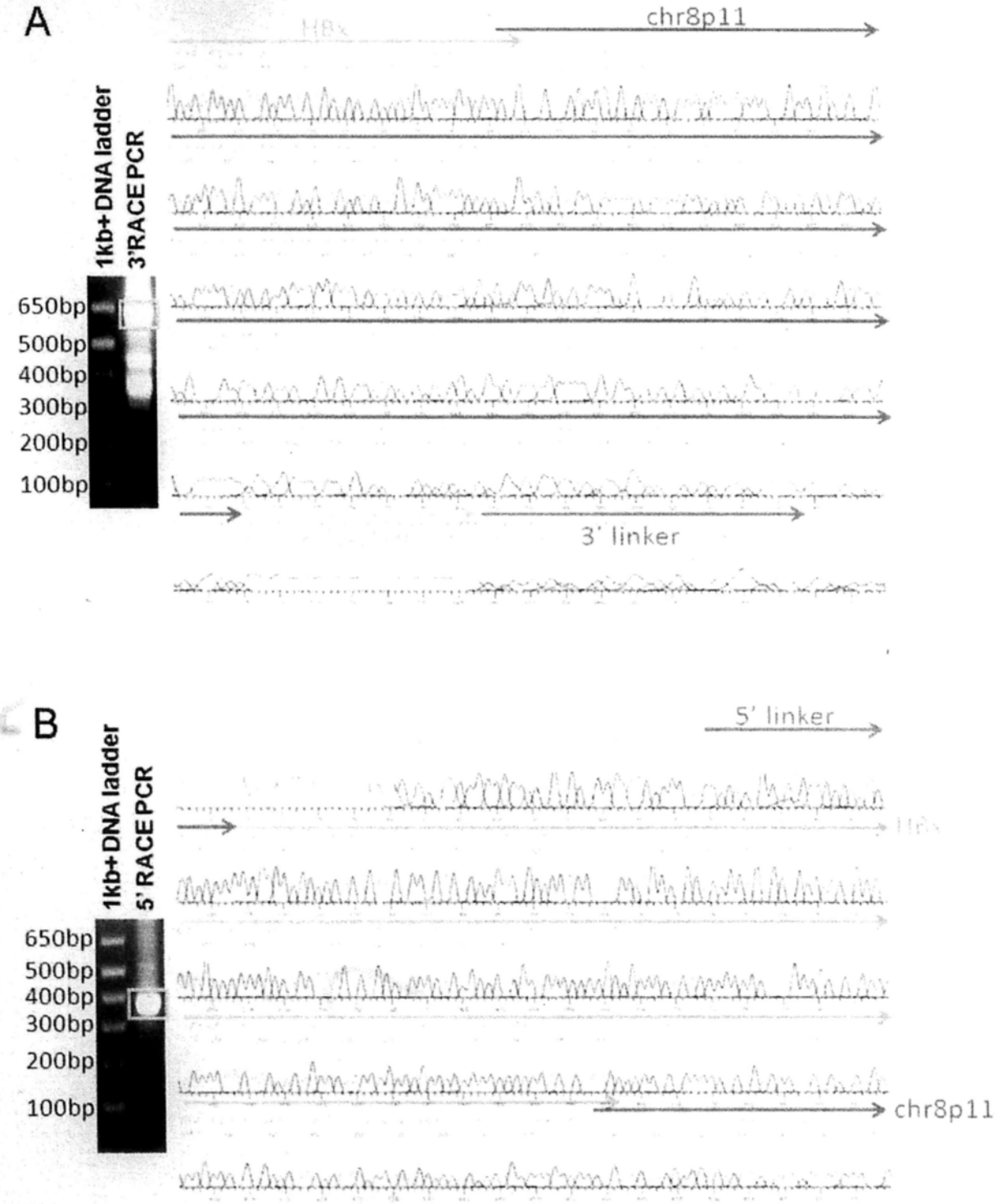

Figure 3.1 RACE for identification of HBx/8p11 fusion transcript. (A) 3' RACE identified the 3' end of HBx/8p11 (red box) consists of HBx, chr.8p11, PolyA signal and PolyA tail. (B) 5' RACE identified the 5' end of HBx/8p11 consists of HBx chr.8p11 sequence (red box). The presence of 5' linker suggested the achievement of 5' end.

A

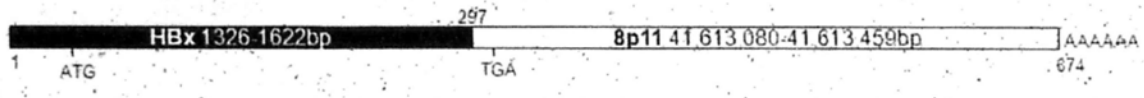

B

GTG TGG

V

301bp TTG AGG ATG TGA AGT AAA GAA AAC CCT TGC CTG CTC TTG GTA GGA ATG TAA ATT AGA TTA

85aa L R M *

361bp GCT ATT GTG GAA AAC AGC ATG GAG ATT CCT AAA ACT AAA ACC AGA GCT TCC ATA TGA TCC

421bp AGC AGT CCC CTA CTA GGA AAG GAA ATC AAT ATA TCA AAG AGA TAC CTG CAC TCC CAT GTT

481bp TAT TGC AGC ACT ATT CAC AAT GAC CAA GAT TTG GAA TCA ACT TGT GTC CAT CAT AGA TGA

541bp GTA GAT AAG GAA AAT GTG GTA TAT GTC ATC ATG GAA TAT TAT TCG GTG TTA AAA AAG AAG

601bp GAA ATC CTG TCA TTT GCG ACA TCG TGG ATG GAA TCG AAG AAC ATT ATG CTA AGT AAA ATA

661bp AAT CAA TCA-CAG GA

Figure 3.2 Schematic diagram of HBx/8p11. (A) Full-length HBx/8p11 fusion transcript. (B) Translation of HBx/8p11 fusion transcript. Microhomology GTG between HBx and chr8p11 (black) was maintained in transcribed sequence.

3.2.2 Expression of HBx/8p11 fusion transcript in HCC cell lines and primary tumors

Due to the limitation of RS-PCR in selecting prominent gel bands for sequencing, the expression of HBx/8p11 fusion transcript in HCC cell lines previously subjected to RS-PCR analysis were re-examined. Results obtained from RT-PCR affirmed HBx/8p11 expression in HKCI-4; in addition HKCI-3, -5a, -5b, -8, and SNU 387 were also shown to be positive for the presence of this transcript (Figure 3.3). To eliminate the possibility that HBx/8p11 insertion was introduced as a result of prolonged in-vitro culture, the parental tumor of 2 cell lines HKCI-3 and HKCI-4, which have established from in-house, was examined for the same integration site. Cell lines HKCI-3 and HKCI-4 and their parental HCC tumors showed consistent presence of this fusion transcript, while HKCI-9 served as a negative control (Figure 3.3).

Encouraged by findings from cell lines, the incidence of HBx/8p11 chimeric transcript was further examined in a cohort of 90 HBV-positive HCC tumors. RT-PCR analysis indicated common HBx/8p11 expression in 21 of 90 (23.3%) of tumors (Figure 3.4A). To confirm the presence of HBx/8p11, all PCR products in primary HCC tumors and cell lines were also sequence verified (Figure 3.4B). The correlation between HBx/8p11 expression and the prognosis of patient were investigated. Kaplan-Meier analysis indicated the expression of HBx/8p11 could predict a shorter overall survival of HCC patients (P = 0.015, log-rank test; hazard ratio, 2.243; 95% confidence interval, 1.214 - 6.239; Figure 3.5A), although it does not correlate with disease-free survival (Figure 3.5B). Cox regression analysis further suggested HBx/8p11 expression remained

a significant predictor of HCC development (P = 0.014) in addition to the presence of micro-vascular invasion (P = 0.004) and tumoral lesions (P = 0.030, Table 3.1). Clinicopathological correlations of HBx/8p11 expression were shown in Table 3.2.

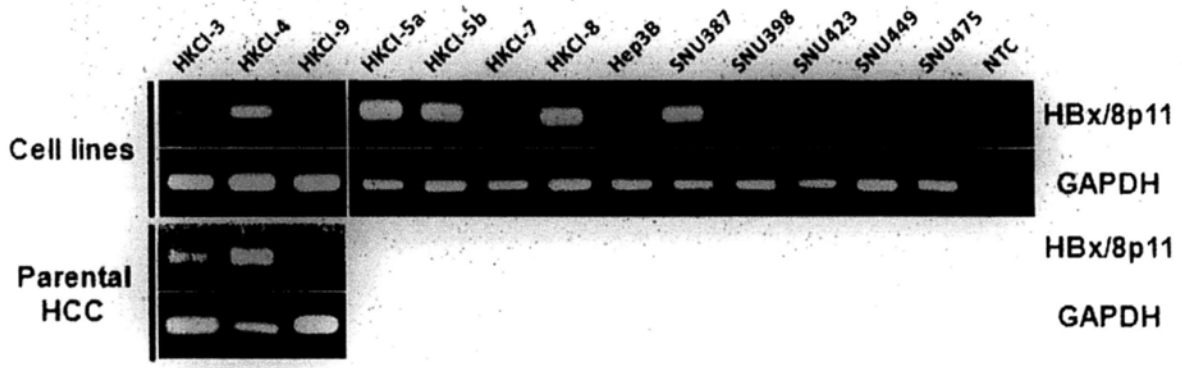

Figure 3.3 RT-PCR analysis demonstrated HBx/8p11 fusion transcript expression in cell lines and parental primary tumors.

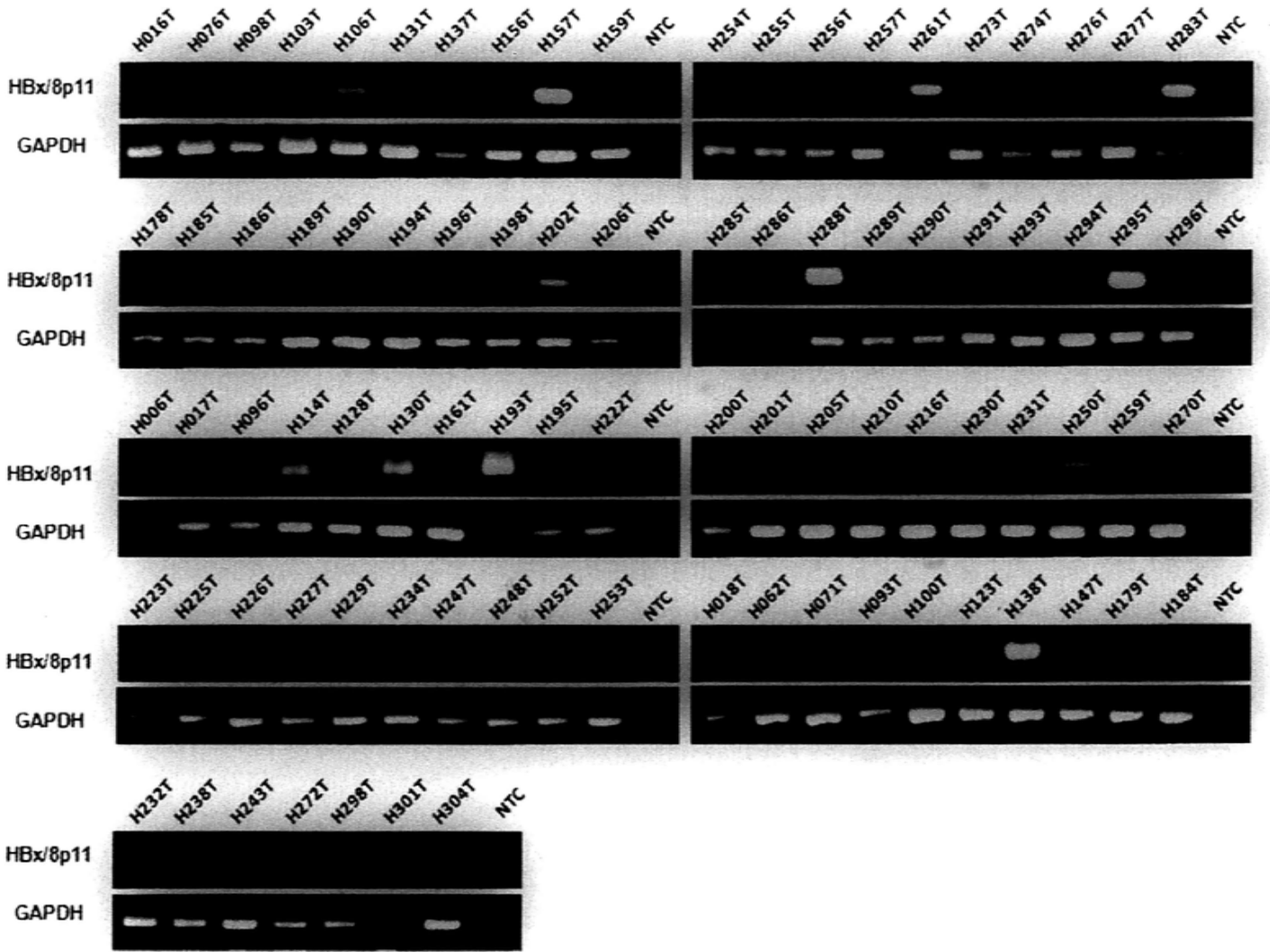

Figure 3.4A RT-PCR analysis demonstrated HBx/8p11 fusion transcript expression in HCC primary tumors.

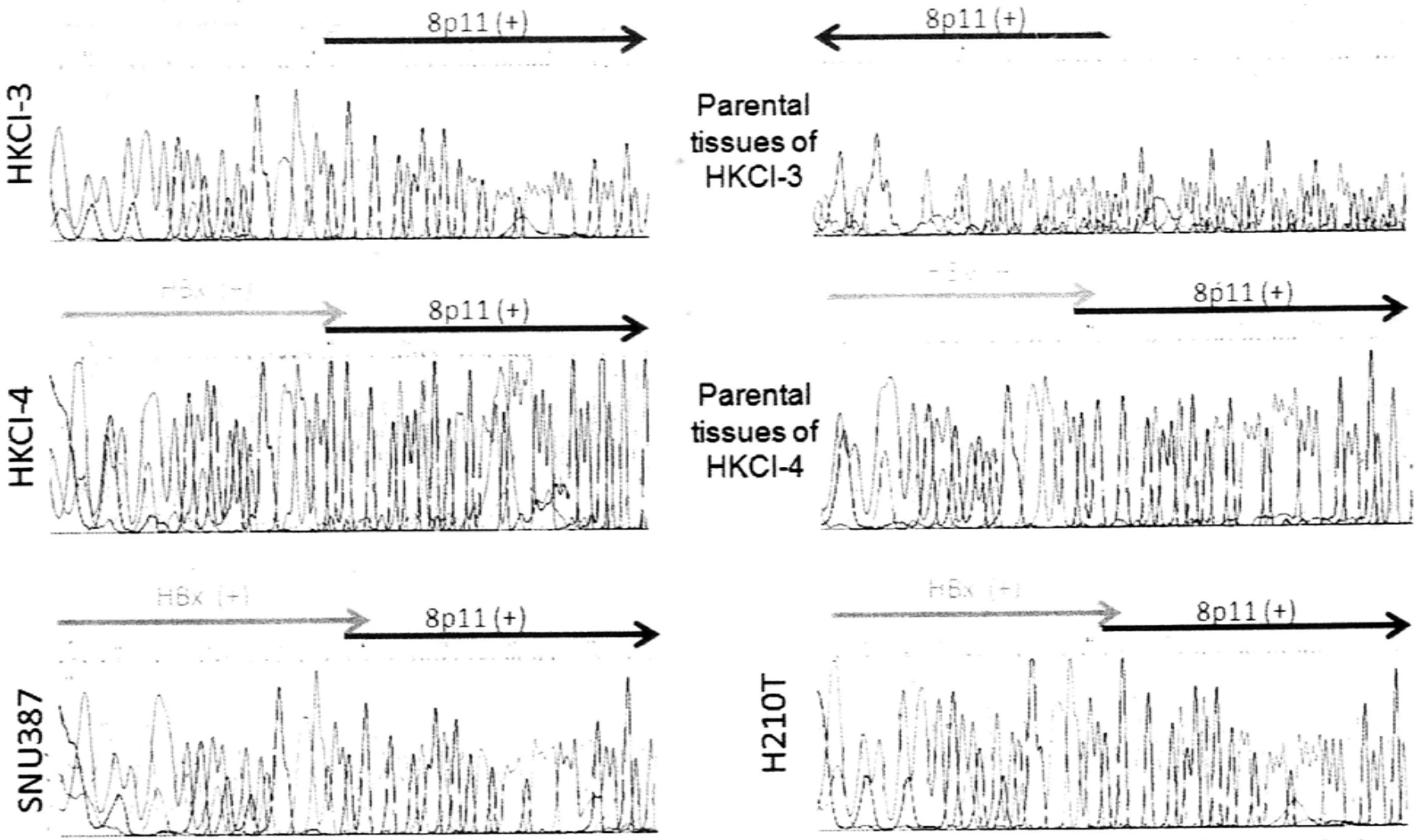

Figure 3.4B Representative sequencing verification of HBx/8p11 fusion transcript expression in cell lines (left panel) and primary tissues (right panel).

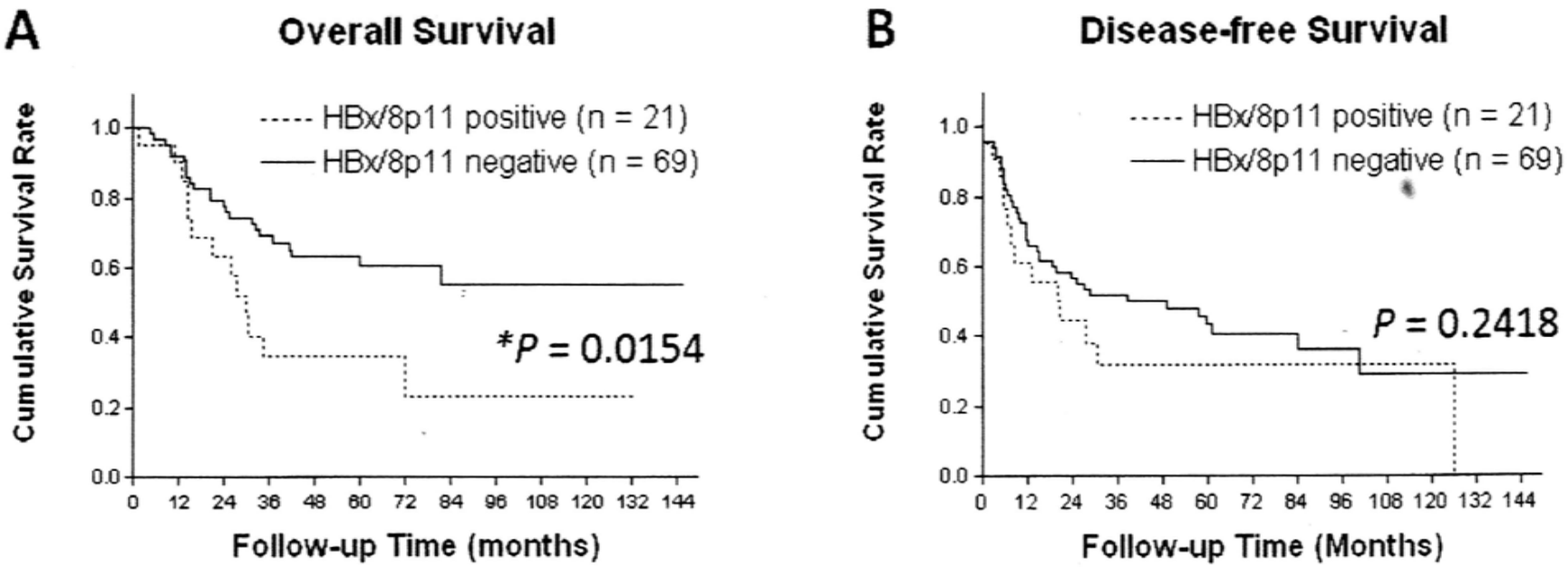

Figure 3.5 Kaplan-Meier analyses of 90 HCC patients. (A) Overall survival curve. (B) Disease-free survival curve.

Table 3.1 Cox regression analysis of HBx/8p11 expression in HCC primary tumors.

Variable	Overall survival		
	Hazard ratio	95% CI	*p* value
HBx/8p11			
Positive	2.626	1.224 - 5.630	0.014*
Negative	-	-	-
Age	1.029	0.996 - 1.063	0.083
Gender	0.209	0.028 - 1.576	0.131
Clinical Stage[@]	0.932	0.425 - 2.046	0.862
Tumor Grade[#]	1.282	0.610 - 2.694	0.514
Macro-vascular invasion^	0.589	0.122 - 2.853	0.513
Micro-vascular invasion^	4.587	1.630 - 12.904	0.004**
Cirrhosis^	1.209	0.486 - 3.006	0.685
Tumoral lesions[I]	3.061	1.121 - 8.360	0.030*

@ Clinical stage: T1 versus T2 versus T3.The disease stage of tumors was classified according to the American Joint Committee on Cancer tumor-node-metastasis staging criteria (Greene et al., 2002).

Tumor grade: poorly differentiated versus moderately differentiated versus well-differentiated.

^ Macro-vascular invasion; micro-vascular invasion; cirrhosis: presence versus absence.

I Tumoral lesions: solitary versus multiple.

Table 3.2 Correlation of clinicopathological parameters with HBx/8p11 expression.

Clinicopathological parameters		HBx/8p11 expression		*P* value
		Positive	Negative	
Sex	Male	17	60	0.49
	Female	4	9	
Age (years, mean±SD)		56.6±11.8	54.6±10.8	0.47
Clinical stage[@]	T1	14	46	0.98
	T2	4	14	
	T3	3	9	
Macrovascular invasion	Yes	1	5	0.65
	No	20	64	
Microvascular invasion	Yes	1	13	0.12
	No	20	56	
Cirrhosis	Yes	17	52	0.60
	No	4	17	
Tumor size (cm, mean±SD)		4.6±2.91	5.0±2.75	0.29
Tumor Grade[#]	1	3	4	0.10
	2	14	60	
	3	4	5	
Tumoral lesions[I]	Yes	7	17	0.57
	No	14	52	

@ Clinical stage: T1, T2 and T3 disease stage of tumors was classified according to the American Joint Committee on Cancer tumor-node-metastasis staging criteria (Greene et al., 2002).

\# Tumor grade: 1: well-differentiated; 2: moderately differentiated; 3: poorly differentiated

I Tumoral lesions: solitary versus multiple.

3.2.3 Knockdown of HBx/8p11 inhibits cell motility and invasion through repression of EMT

It is postulated that the high prevalence of HBx/8p11 expression in HCC may hold biological relevance. To elucidate the potential functional contributions from this fusion transcript, transient knockdown of HBx/8p11 in HKCI-4 were performed using siRNA siHBx/8p11-1 or siHBx/8p11-2. Real-time PCR analysis suggested the successful knockdown of HBx/8p11 by either siRNA (Figure 3.6). While siRNA mediated targeting of HBx/8p11 did not seem to affect the cell viability as indicated from MTT assay (Figure 3.7A), more apparent effects on cell motility were indicated from Transwell migration and Matrigel invasion assays. Knockdown of HBx/8p11 significantly reduced the cell migratory ($P = 0.040$, Student's t test) (Figure 3.7B and 3.7C) and invasiveness properties ($P = 0.040$, Student's t test) of HCC cells (Figure 3.7D and 3.7E) when compared to siMock control. As EMT is a major molecular mechanism by which cancer cells acquire motile ability to invade the tumor microenvironment, the effect of HBx/8p11 expression on the modulation of EMT was further investigated. Western blotting of siHBx/8p11 treated HKCI-4 revealed increase expression of cohesive epithelial markers E-cadherin and γ-catenin, and a corresponding diminution of mesenchymal specific protein fibronectin (Figure 3.8). These findings were further substantiated in immunofluorescence analysis, which corroborated the augmented expression of epithelial E-cadherin and γ-catenin, and their prominent accumulation at the cell membrane when compared to the more diffused cytoplasmic localization of these markers in both lipofectamine-treated and siMock control. A decrease in the level of cytoplasmic fibronectin was also observed in siHBx/8p11 treated cells (Figure 3.9).

E-cadherin expression is transcriptionally controlled by several EMT transcription factors such as SNAIL1, SLUG, ZEB1, ZEB2, TWIST1 and TCF3) by binding to the E-box elements on the promoter of E-cadherin (Giroldi et al; 1997; Hennig et al, 1995). In this regard, expressions of these transcription factors were analysed upon HBx/8p11 knockdown. qPCR revealed the downregulation of ZEB1, Twist1 and TCF3 in siHBx/8p11-1 treated cells (Figure 3.10A). Downregulation of ZEB1 and Twist1 were further confirmed by Western blot (Figure 3.10B).

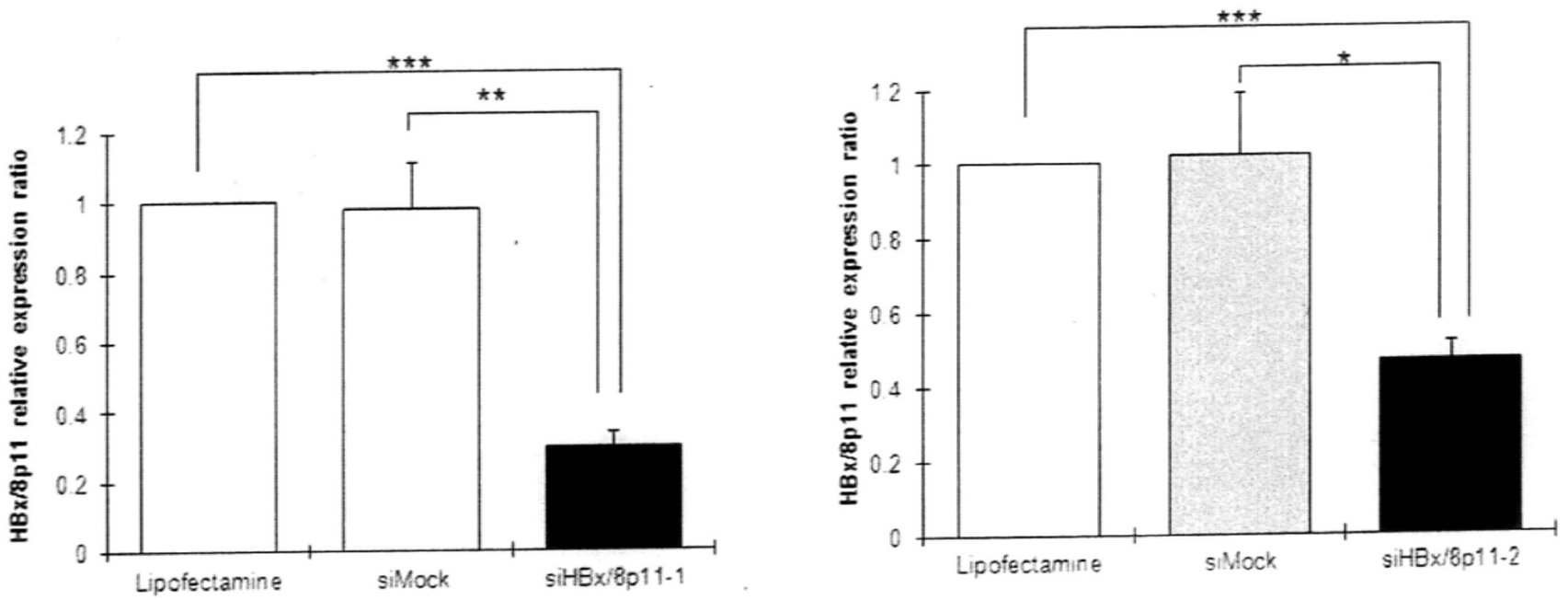

Figure 3.6 Transient knockdown of HBx/8p11 fusion transcript using (A) siRNA siHBx/8p11-1 or (B) siHBx/8p11-2 in HKCI-4 was confirmed by qPCR.

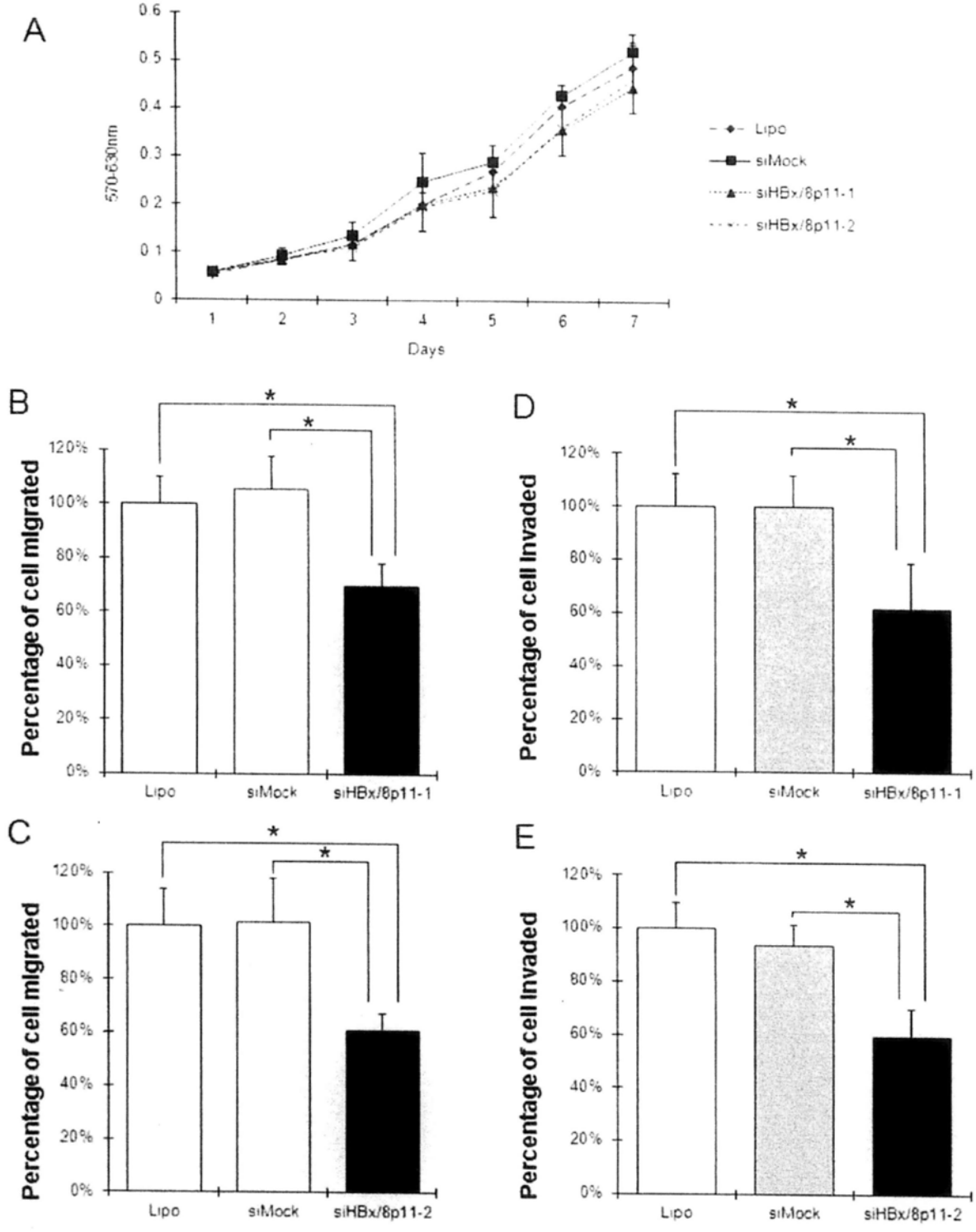

Figure 3.7 Knockdown of HBx/8p11 inhibits cell migration and invasion. (A) Knockdown of HBx/8p11 do not affect cell viability. Percentage of lipofectamine-treated, siMock-treated and HBx/8p11 knockdown HKCI-4 passed through the transwells in (B and C) migration assay and (D and E) Matrigel invasion assay.

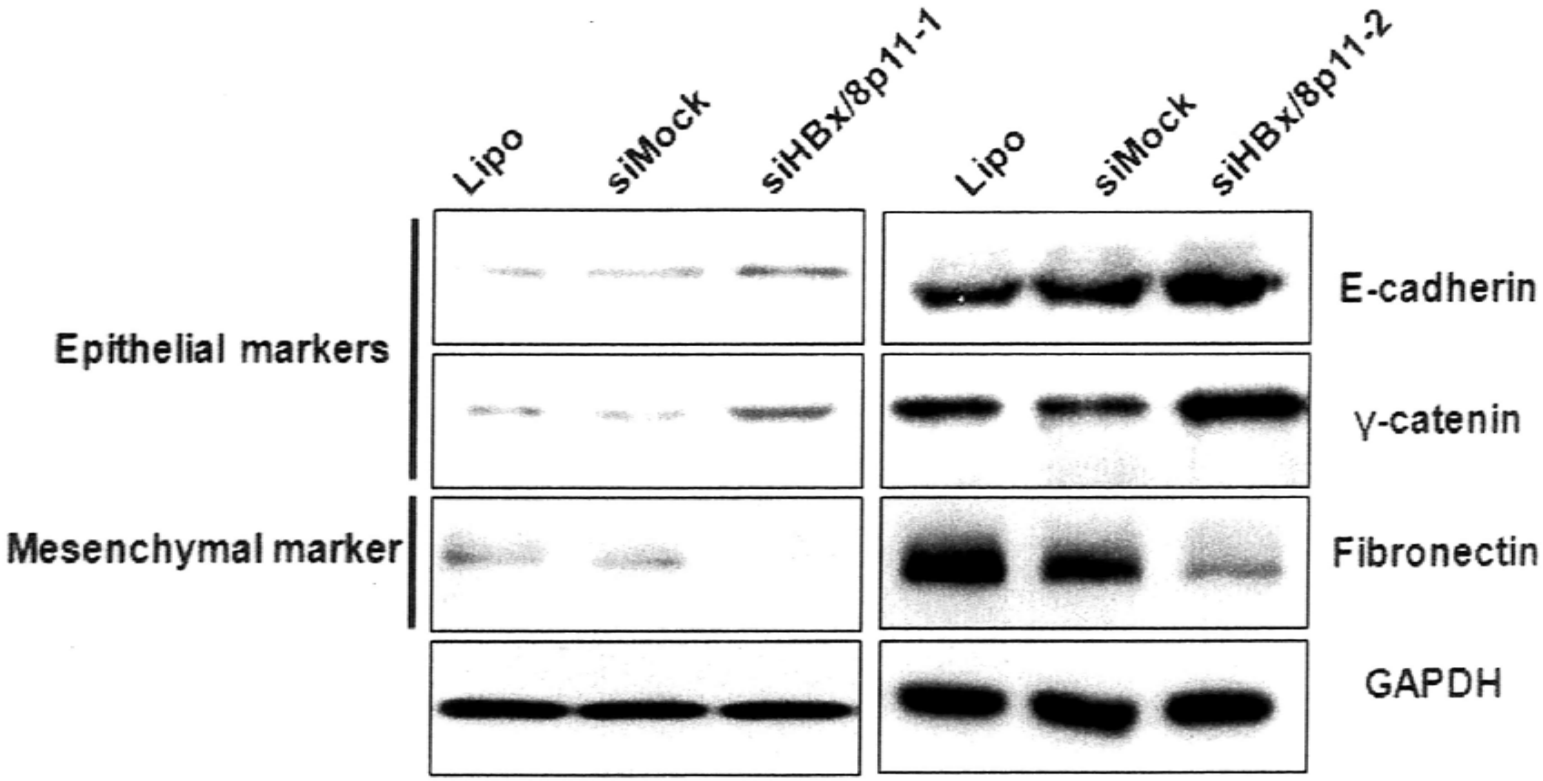

Figure 3.8 Knockdown of HBx/8p11 inhibits cell migration and invasion through repression of EMT. Expression of epithelial markers (E-cadherin and γ-catenin) and mesenchymal marker (fibronectin) were compared between lipofectamine-treated, siMock control and HBx/8p11 knockdown in HKCI-4 by Western blotting.

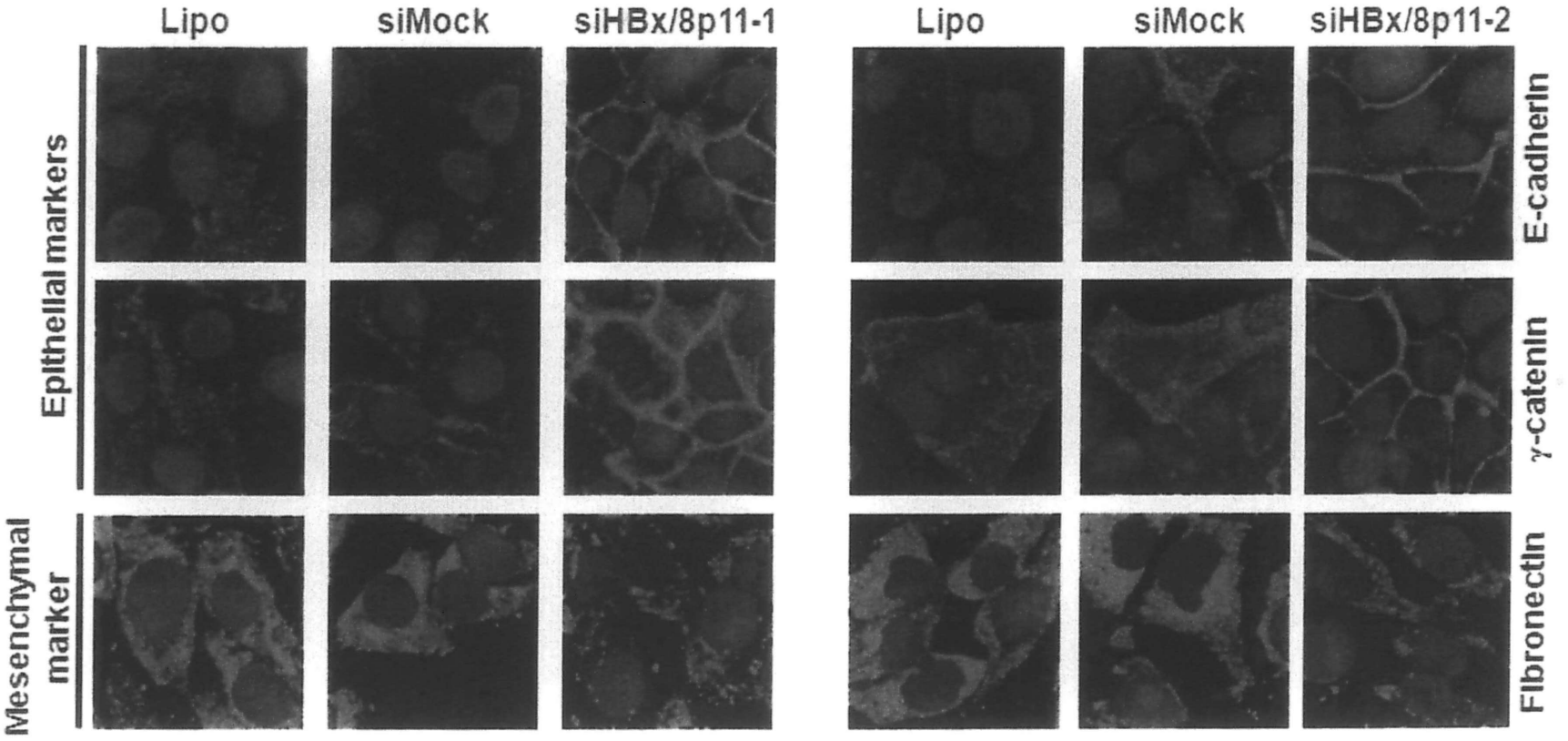

Figure 3.9 Knockdown of HBx/8p11 inhibits cell migration and invasion through repression of EMT. Expression of epithelial markers (E-cadherin and γ-catenin) and mesenchymal marker (fibronectin) were compared between lipofectamine-treated, siMock control and HBx/8p11 knockdown in HKCI-4 by immunofluorescence staining: nuclei were counterstained with DAPI.

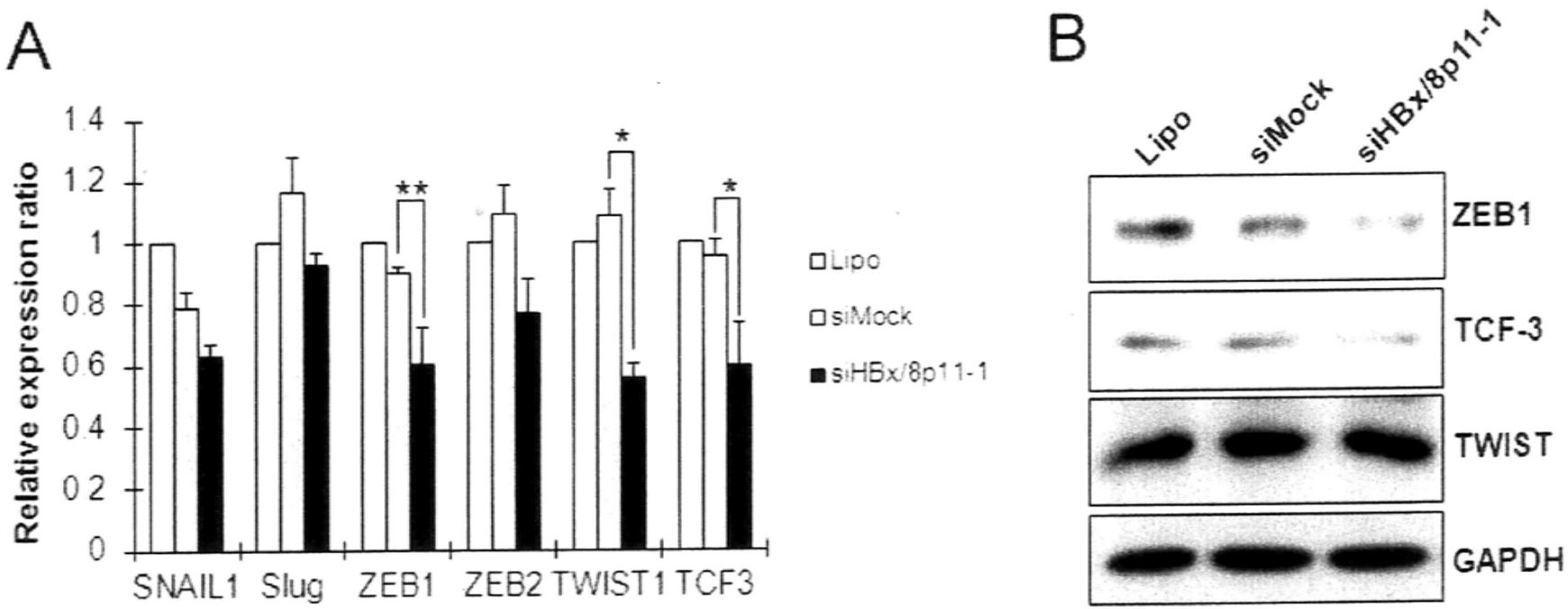

Figure 3.10 Expression of E-cadherin transcription factors in HBx/8p11 knockdown cells. (A) qPCR revealed the downregulation of ZEB1, TWIST1 and TCF3. (B) Western Blot confirmed ZEB1 and TCF3 downregulation.

3.2.4 HBx/8p11 fusion transcript targets Wnt signaling pathway

It is known that β-catenin forms a membranous complex with the cell adhesion protein E-Cadherin and other catenin proteins. During the process of EMT, β-catenin is dissociated from the membrane-associated E-Cadherin complex and translocates to the nucleus where it coactivates transcription of target genes through the formation of transcriptional complex with TCF/LEF (Nusse. 2005). To examine the plausible effect of HBx/8p11 on the β-catenin signaling, the nuclear localization and transactivity of β-catenin under the influence of HBx/8p11 were examined. In HKCI-4 cells treated with siHBx/8p11-1, an effect on the total cellular β-catenin protein was not suggested, although marked reduction in the level of active β-catenin was readily shown from Western blot (Figure 3.11A). β-catenin target genes cyclin-D1 and c-Myc were also found to display a concordant downregulation in the presence of HBx/8p11 siRNA (Figure 3.11A). By TOP/FOPflash luciferase reporter assay, a consistent reduction in the transactivation activity of β-catenin following HBx/8p11 knockdown was found, which is in line with the reduced active β-catenin protein determined ($P = 0.0076$, Student's t test) (Figure 3.11B). Cellular distribution of β-catenin as revealed from immunofluorescence staining indicated much reduced nuclear localization of active β-catenin in siHBx/8p11-treated cells, whereas lipofectamine-treated and siMock control cells showed more intense accumulation of β-catenin within the nucleus (Figure 3.11C).

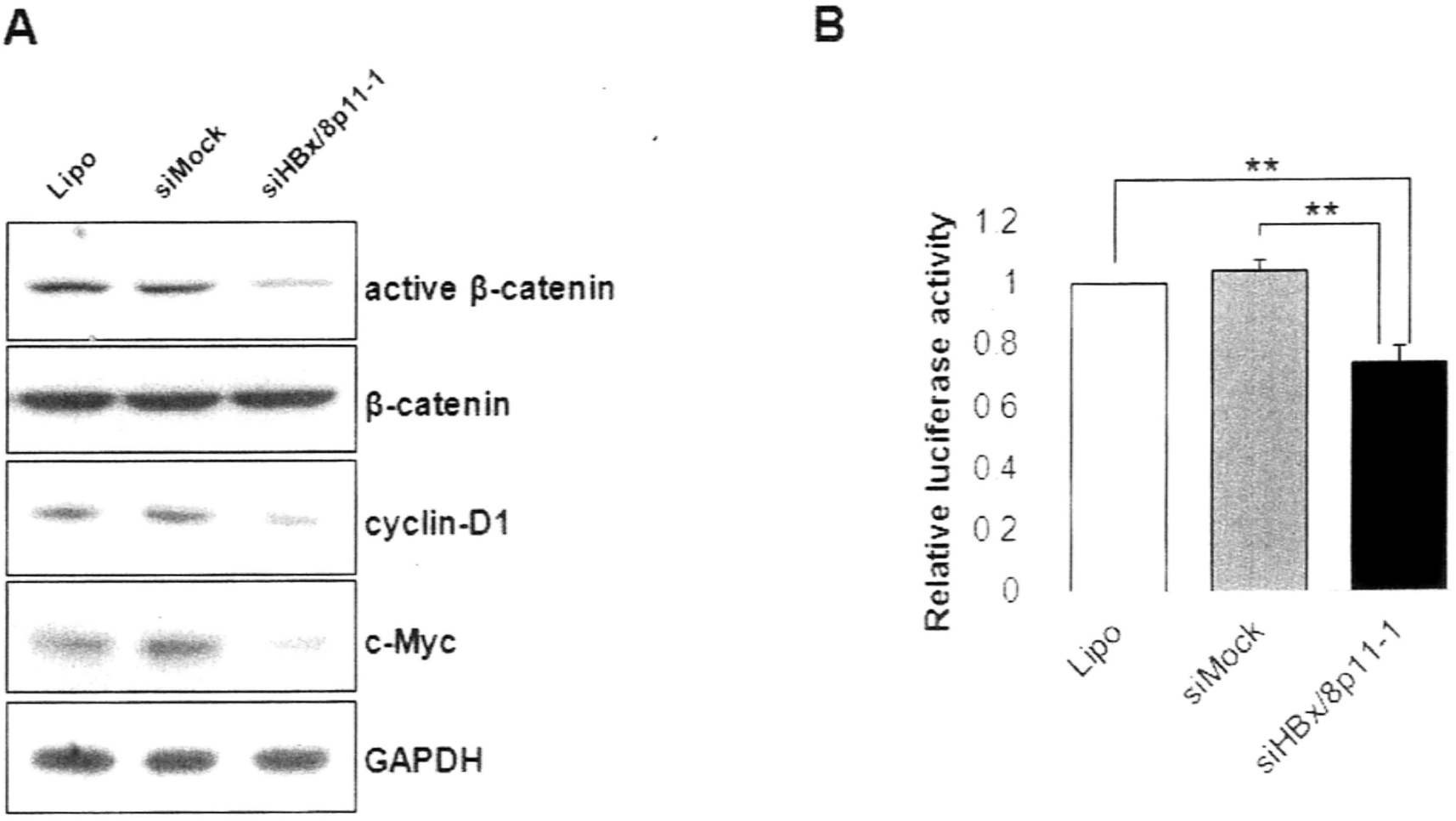
A
Lipo
siMock
siHBx/8p11-1
active β-catenin
β-catenin
cyclin-D1
c-Myc
GAPDH
B
Relative luciferase activity
1.2
1
0.8
0.6
0.4
0.2
0
**
**
Lipo
siMock
siHBx/8p11-1

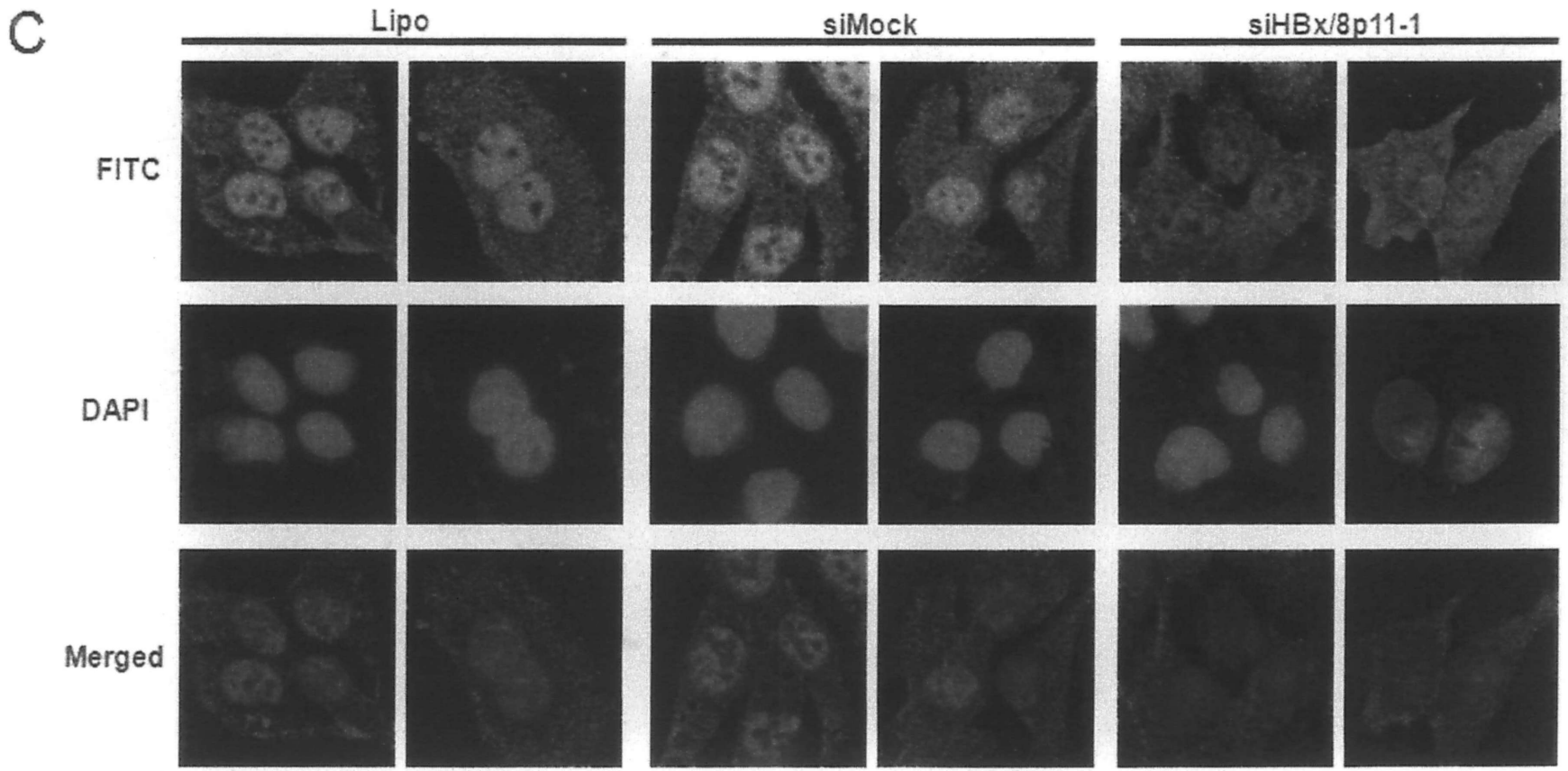

Figure 3.11 HBx/8p11 targets Wnt signaling pathway. (A) Western blot analysis showed downregulation of active β-catenin and its target gene cyclin-D1 and c-Myc after HBx/8p11 knockdown. (B) TOP/FOPflash luciferase reporter assay revealed the reduction of β-catenin activity in HBx/8p11 knockdown cells. (C) Immunofluoresence staining of active β-catenin. Nuclei were counterstained by DAPI.

3.2.5 HBx/8p11 exerts functional effects as ncRNA

To determine whether viral components, human sequence or the full-length HBx/8p11 underlie the functional effects observed, the HBx/8p11$^{1-674}$, HBx$^{1-297}$, 8p11$^{295-674}$, HBx+5aa^{1-312*} for translated protein were cloned and expressed, and the functional roles of these expressing vectors in immortalized human hepatocyte cell line L02 were examined (Figure 3.12A). The GFP-fused protein expressed from these clones showed protein sizes in accordance to prediction, where minimal differences could be identified between proteins translated from HBx/8p11$^{1-674}$, HBx$^{1-297}$, 8p11$^{295-674}$, HBx+5aa^{1-312*} (Figure 3.12B). Protein translated from full-length HBx/8p11$^{1-674}$ and HBx+5aa^{1-312*} revealed translation of 87 amino acids at 9.57 kDa, both including 5 amino acids contributed from the chr.8p11 sequence prior to a stop codon, whereas the flanking viral HBx$^{1-297}$ and human 8p11$^{295-674}$ components expressed proteins at 9.13 kDa and 0.55 kDa, respectively (Figure 3.12B). The slight increase in size of HBx$^{1-297}$ when compared with full-length HBx/8p11$^{1-674}$ and HBx+5aa^{1-312*} is due to the lack of stop codon in HBx$^{1-297}$. Sequence from multiple cloning site prior to the stop codon was integrated into HBx$^{1-297}$. However in functional investigations, only L02 cells expressing the full-length HBx/8p11$^{1-674}$ presented prominent in-vitro advantages, such as promotion of cell migration (P = 0.028, Figure 3.13A) and cell invasion (P = 0.005, Figure 3.13B). Overexpressing HBx$^{1-297}$, 8p11$^{295-674}$ and HBx+5aa^{1-312*} in L02, on the other hand, showed similar functional behaviors as vector control. Western blot analysis indicated downregulation of epithelial marker CK18 and upregulation of mesenchymal protein N-cadherin and vimentin in cells expressing HBx/8p11$^{1-674}$ compared to HBx$^{1-297}$, 8p11$^{295-674}$ and HBx+5aa^{1-312*} treated cells (Figure 3.13C). This suggested the likely involvement

of EMT in L02 cells expressing HBx/8p11$^{1-674}$. Similarly, although HBx/8p11$^{1-674}$, HBx$^{1-297}$, 8p11$^{295-674}$, HBx+5aa^{1-312*} did not affect the viability of L02 (Figure 3.14A) augmentation of colony forming growth (P = 0.021) was demonstrated in HBx/8p11$^{1-674}$ expressing cells, while L02 cells expressing HBx$^{1-297}$, 8p11$^{295-674}$, HBx+5aa^{1-312*} remain unaffected (Figure 3.14B). These data strongly supports the role for full-length fusion transcript HBx/8p11$^{1-674}$ in the functional advantages observed, by eliminating the possibility of these phenotypes being contributed from the protein translated by either C-terminus truncated HBx$^{1-297}$, full-length HBx+5aa^{1-312*} or generally non-transcribing 8p11 human repetitive sequences. It is also likely that HBx/8p11$^{1-674}$ exerts its functional phenotypes as a non-protein coding RNA transcript.

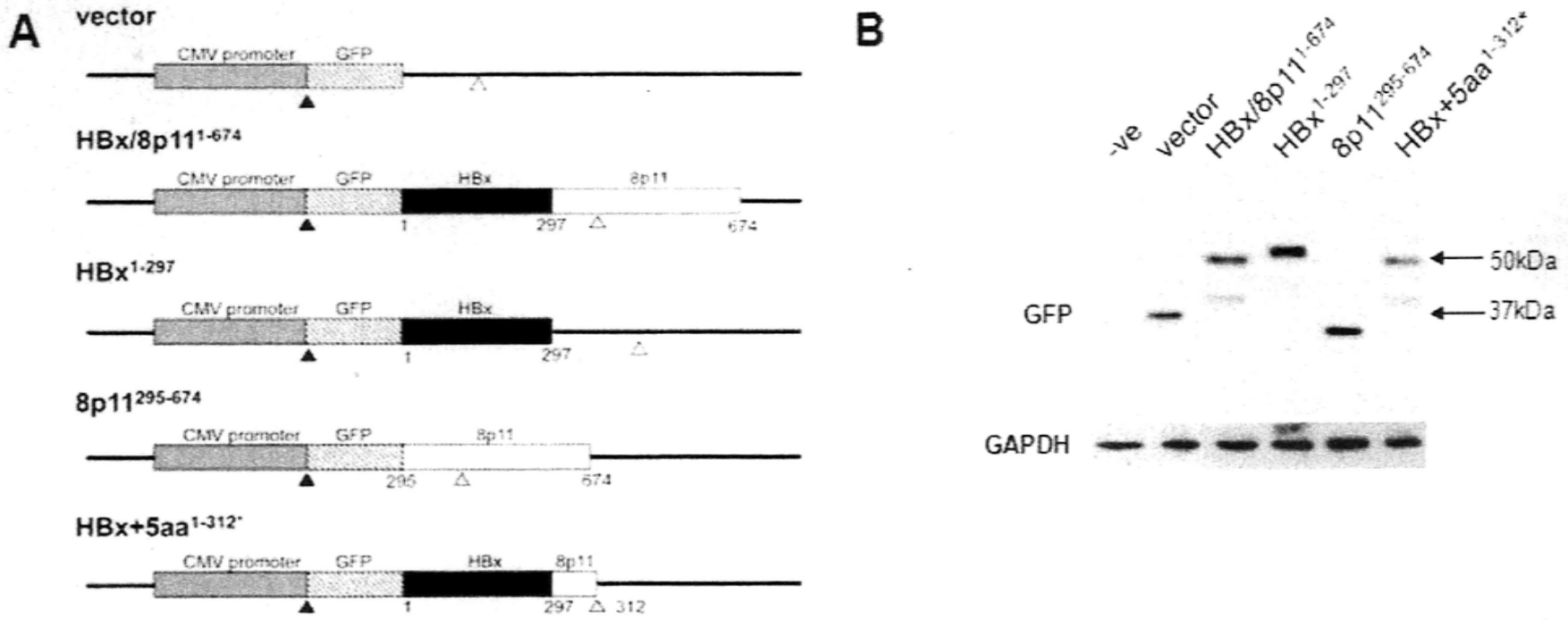

Figure 3.12 Protein translations of HBx/8p11$^{1-674}$, HBx$^{1-297}$, 8p11$^{295-674}$, HBx+5aa^{1-312*}. (A) Expression constructs of GFP conjugated full-length HBx/8p11$^{1-674}$, HBx$^{1-297}$, 8p11$^{295-674}$, HBx+5aa^{1-312*} containing start (▲) and stop (Δ) codon. (B) GFP conjugated protein expression of full-length full-length HBx/8p11$^{1-674}$, HBx$^{1-297}$, 8p11$^{295-674}$, HBx+5aa^{1-312*} were revealed by Western blotting probed against anti-GFP antibody.

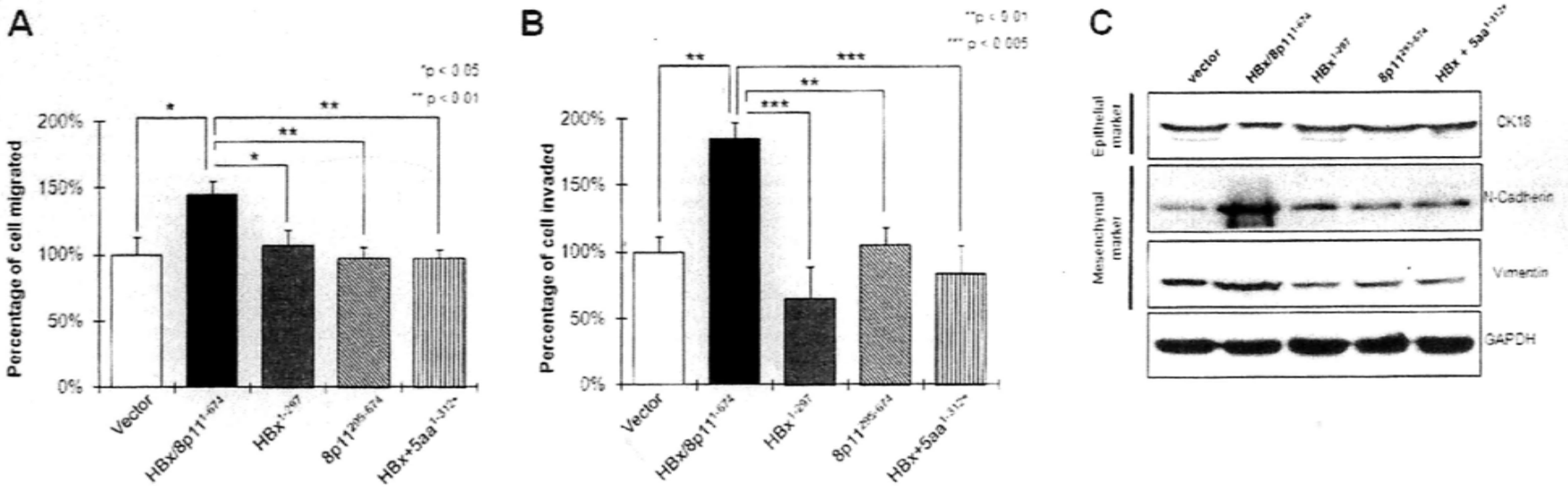

Figure 3.13 Overexpression of full-length HBx/8p11 induces cell motility through EMT. Cell motility of full-length HBx/8p11$^{1-674}$, expressing cells were compared with HBx$^{1-297}$, 8p11$^{295-674}$ and HBx+5aa^{1-312*} expressing cells using (A) migration and (B) Matrigel invasion assay. (C) Western blot analysis showed only the full-length HBx/8p11$^{1-674}$ expressing cells induced EMT by downregulation of epithelial marker CK18 and upregulation of mesenchymal markers N-cadherin and vimentin, compared with vector, HBx$^{1-297}$, 8p11$^{295-674}$ and HBx+5aa^{1-312*} expressing cells.

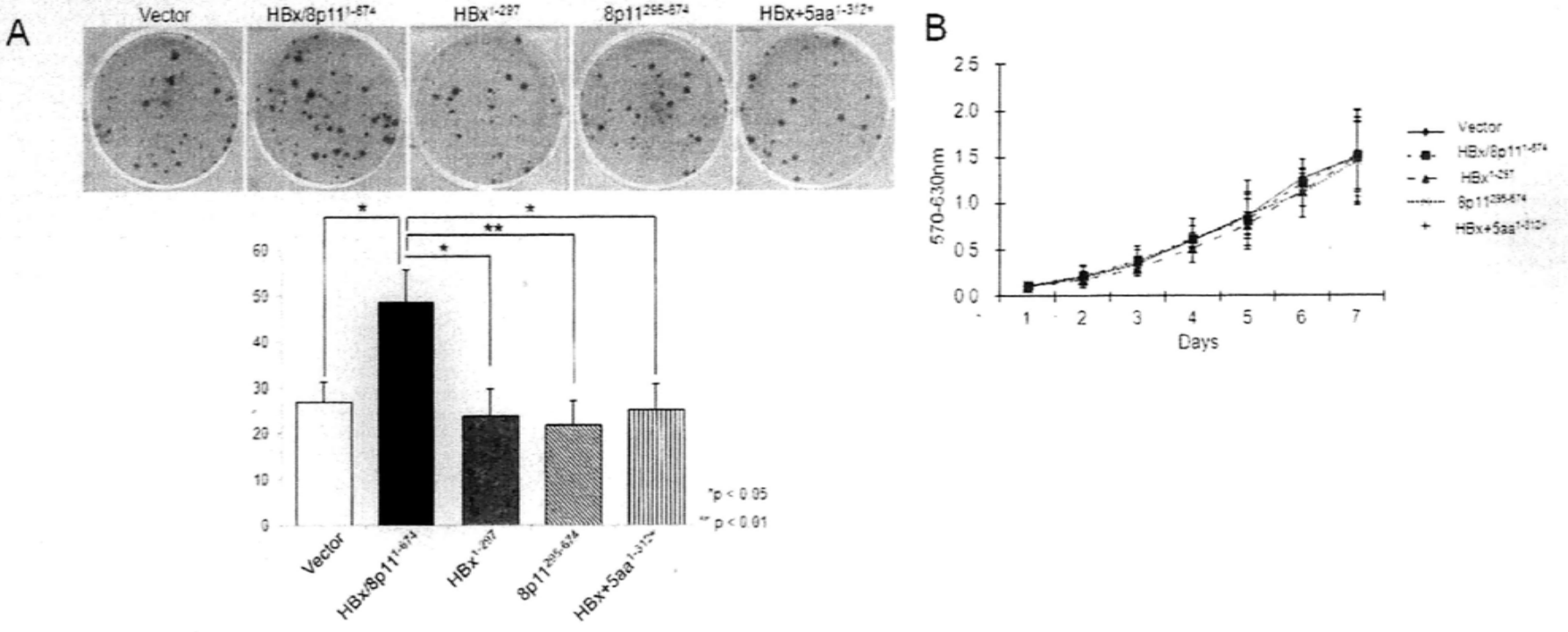

Figure 3.14 Effects of cell viability and growth of full-length HBx/8p11$^{1-674}$, HBx$^{1-297}$, 8p11$^{295-674}$ and HBx+5aa^{1-312*} (A) Colony formation assay demonstrated the induced cell proliferation by full-length HBx/8p11$^{1-674}$ after 21 days of G418 selection. (B) MTT assay demonstrated the unaffected cell viability of full-length HBx/8p11$^{1-674}$, HBx$^{1-297}$, 8p11$^{295-674}$ and HBx+5aa^{1-312*} expressing cells in 7 days.

3.2.6 HBx/8p11 ncRNA affects Wnt signaling pathway

HBx/8p11 knockdown showed a consistent reduction in the transactivation activity of β-catenin. The transactivation activity of β-catenin in full-length HBx/8p11$^{1-674}$ and HBx+5aa$^{1-312}$ overexpressing cells was also investigated. TOP/FOPflash luciferase reporter assay suggested spontaneous activation of β-catenin transactivity in HBx/8p11$^{1-674}$ expressing cells (P = 0.0119) while HBx+5aa^{1-312*} overexpressing cells mimicking HBx/8p11$^{1-674}$ protein expression do not show significant difference (Figure 3.15A).

3.27 HBx/8p11 ncRNA affects immediate neighboring genes in cis-regulating manner

In view of HBx/8p11 exerts functional effects as long ncRNA and the reports of long ncRNA function in cis-regulating the immediate neighboring genes, qPCR was performed to examine the expression level of genes near the site of insertion. By searching public database for the upstream and downstream sequences against 1Mb of chr.8p11, 16 genes and one microRNA were located. qPCR showed a consistent upregulation of these targets upon HBx/8p11 knockdown (Figure 3.15B). Interesting, SFRP1 and DKK4 are Wnt inhibitors in Wnt signaling pathway, showing a significant 3.12 and 1.52 fold upregulation respectively.

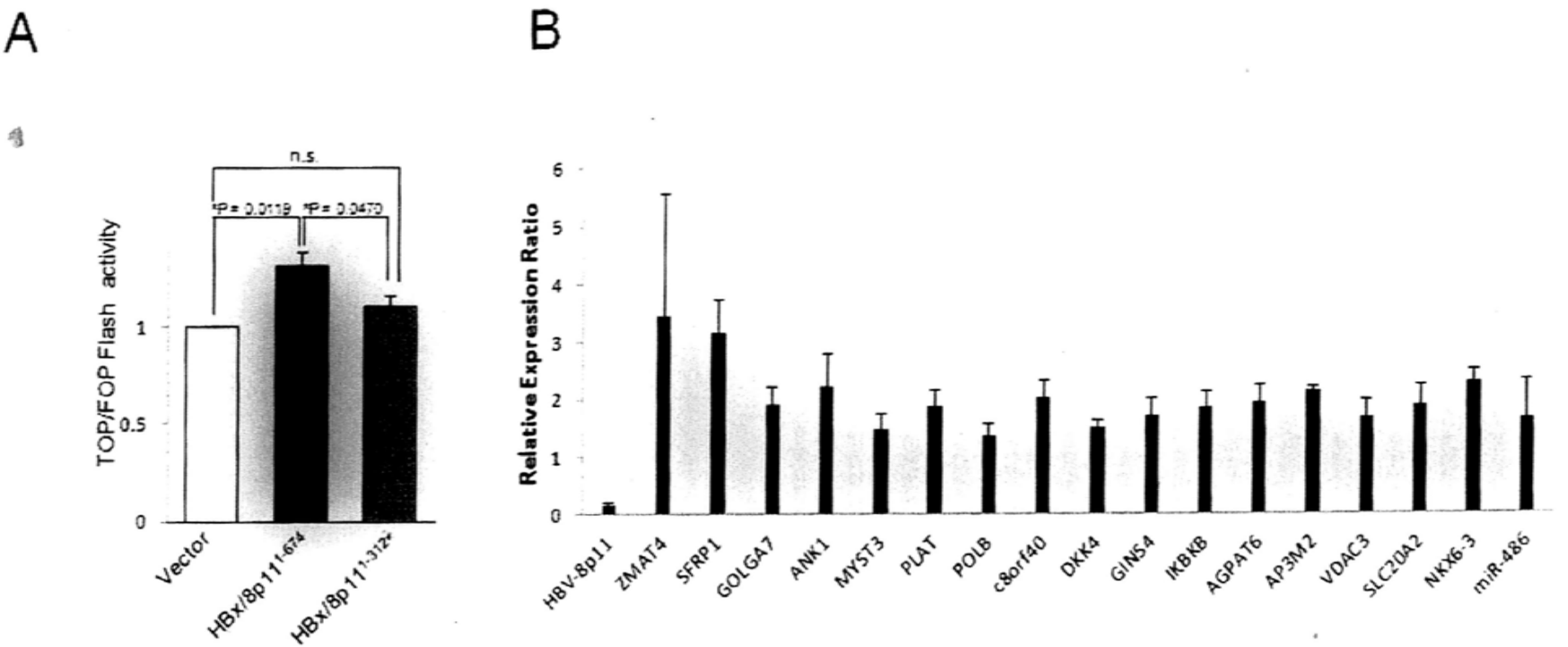

Figure 3.15 HBx/8p11 functions as long ncRNA and Wnt signaling pathway. (A) TOP/FOPflash luciferase reporter assay demonstrated the increase in β-catenin activity only in full-length HBx/8p11$^{1-674}$ expressing cells. (B) HBx/8p11 exerts functional effects as long ncRNA and affect immediate neighboring Wnt inhibitors in cis-regulating manners.

3.28 HBx/8p11 transgene increases susceptibility to DEN-induced hepatocarcinogenesis

The HBx/8p11 TG mice were born normal in terms of body weight and size when compared with their non-transgenic littermate, suggesting the presence of transgene did not affect the development of the animal. Gross examination of liver in HBx/8p11 TG mice revealed more tumor nodules when compared with wild type mice upon DEN induced HCC development at 8 months (Figure 3.16), with hematoxylin and eosin (H&E) staining confirmed the presence of tumors. HBx/8p11 TG mice was significantly more susceptible to more DEN induced tumor (mean = 12.86, $P = 0.0025$) than wild type mice (mean = 3.889).

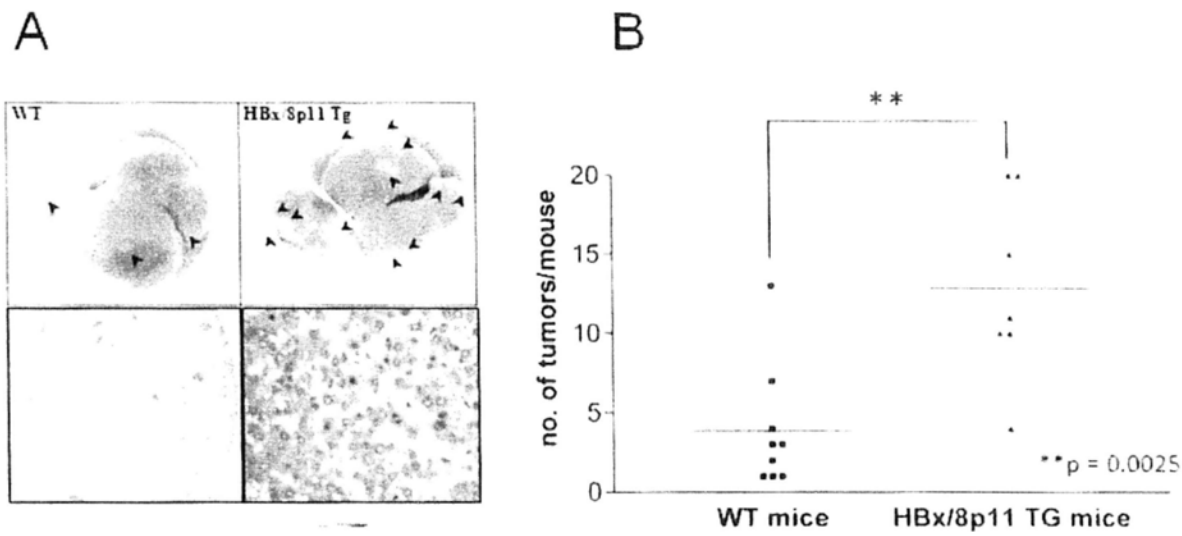

Figure 3.16 HBx/8p11 expression increases susceptibility to DEN-induced hepatocarcinogenesis. **(A)** Typical gross morphology of liver tumors from DEN-treated HBx/8p11 TG mice (right) or wild-type (left) male mice at 8 months. Representative microscopic features of HCC in hematoxylin and eosin (H&E)-stained liver sections of mice. Arrows indicate microscopic HCC. **(B)** The number of HCCs per mouse was counted and expressed as mean.

3.3 DISCUSSION

More than 80% of HCC patients are chronic hepatitis B carriers containing HBV integrations in human genome. As a result, HBV integration into human genome has been hypothesized as one of the mechanisms to induce HBV-related hepatocarcinogenesis. However, only viral integrations in vicinity of cancer-related genes or genes related to cell growth had been identified (Gozuacik et al. 2001; Murakami et al. 2005; Ferber et al. 2003). The significance of viral integrations into intronic or intergenic region had been underestimated. In this study, the functional importance of recurrent HBx integration into intergenic region of chr.8p11 was highlighted. Recurrent HBx/8p11 integration was demonstrated, suggesting preferential integration sites are present in human genome. The human 8p11 region is a repetitive LINE1 sequence. Chromosomal regions containing repetitive sequences have been reported to be HBV integration site, suggesting the integration mechanism is not random (Tsuei et al. 1994; Zhou et al. 1988; Wang et al. 2001).

The expression of HBx/8p11 fusion transcript is possibly driven by HBx enhancer I and HBx promoter sequences, as indicated in RS-PCR. RT-PCR demonstrated a high incidence (~25%) of HBx/8p11 fusion transcript expression in HCC cases, possibly due to clonal expansion of tumor cells carrying this viral integration site. Clinicopathological analysis in the present study supported the pathogenetic importance of recurrent expression of HBx/8p11 fusion transcript particularly during early stage of HCC development, as supported by univariate Kaplan-Meier and multivariate Cox analyses in suggesting HBx/8p11 as an independent prognostic factor for predicting shorter overall

survival but not the disease-free surivial of HCC patients. These data implied the functional importance of HBx/8p11 during HBV-related hepatocarcinogenesis.

Recent studies focusing on the identification and characterization of ncRNAs has been emphasized, especially during tumor development and progression. For example, HULC in HCC (Panzitt et al. 2007), DD3 in prostate cancer (Bussemakers et al. 1999) and BC200 RNA in breast cancer (Iacoangeli et al 2004) were described. It is the first study to describe HBV-human fusion transcript functions as a long ncRNA, as evidenced by the ectopic expressions of full length HBx/8p11$^{1-674}$ and HBx+5aa^{1-312*}. Although full length HBx/8p11$^{1-674}$ showed protein expression which is comparable with HBx+5aa^{1-312*}, functional investigations and luciferase reporter assay suggested the phenotypic advantages and transactivation activity of β-catenin was not conferred by protein expressed by HBx+5aa^{1-312*}. Instead, only full length HBx/8p11$^{1-674}$ expression showed phenotypic advantages and β-catenin transactivation, justifying its action as ncRNA. Western blot analysis reinforced our hypothesis: only full length HBx/8p11$^{1-674}$ expression demonstrated epithelial-to-mesenchymal transition (EMT) as characterized by the upregulation of mesenchymal markers and downregulation of epithelial marker. Although the mechanism of how chimeric HBx/8p11 ncRNA regulates EMT has yet to be determined, our findings suggested HBx/8p11 ncRNA is implicated in Wnt signaling pathway. Based on the knowledge of long ncRNA function in cis-regulating the immediate neighboring coding genes, we speculate the genes upstream and downstream of chr.8p11 are affected. Interesting, by searching public database for the upstream and downstream sequences against chr.8p11, SFRP1 and DKK4 are found within 1Mb of the

HBx/8p11 integration site. SFRP1 and DKK4 are the Wnt inhibitors in Wnt signaling pathway. Silencing of SFRPs and DKKs by hypermethylation were associated with carcinogenesis (Suzuki et al. 2004; Sato et al. 2007). This observation seems to agree with our findings of HBx/8p11 chimeric ncRNA regulate EMT and subsequently control Wnt signaling pathway.

HBx/8p11 ncRNA was demonstrated to exert its functions in cell motility. This finding was supported by the changes in EMT. The increase in E-cadherin was accompanied by lowered active β-catenin and decreased transactivation activity of β-catenin during HBx/8p11 siRNA treatment, suggesting E-cadherin antagonizes Wnt signaling. Studies have shown that E-cadherin binds and sequesters a large pool of β-catenin and preventing its nuclear translocation as well as its function as a component of the TCF/LEF transcription factor complex (Wong et al. 2003; Gottardi et al. 2001). In this study, knockdown of HBx/8p11 ncRNA subsequently caused the upregulation of E-cadherin, resulting in reduced nuclear localization of β-catenin and attenuation of Wnt signaling pathway. Although ectopic expression and knockdown of HBx/8p11 ncRNA do not affect cell viability, HBx/8p11 ncRNA promote tumor growth, as demonstrated by colony formation assay *in vitro* and transgenic model *in vivo* respectively. The role of Wnt signaling pathway on liver tumor growth has been extensively described (Tan et al. 2006; Thompson et al. 2007). One of the possible mechanisms for HBx/8p11 to control cell proliferation is the activation of Wnt signaling pathway, as demonstrated by increased β-catenin transactivity.

Multiple signaling pathways has been identified to play a role in hepatocarcinogenesis, including VEGF, PDGF, EGF, IGF, HGF, PI3K/AKT/mTOR and WNT/β-catenin pathways. In view of this, therapeutic interventions of these pathways were developed for the treatment of HCC. For example, Sorafenib and other anti-angiogenic multi-targeted tyrosine kinase inhibitors such as Sunitinib had been developed recently. However, these treatments are generally palliative in intent and most of these targeted agents have demonstrated a very low response rate when used alone. (Yau et al. 2010). As a result, the development of successful therapeutic targets is still necessary. In recent years, identification of novel fusion transcripts has become a new aspect for therapeutic approach and diagnostic molecular markers (Soda et al. 2007; Ritchie et al. 2008). Our study demonstrated HBx/8p11 fusion transcript expressed in remarkable number of HCC cases (~25%), indicating its potential therapeutic target for HBV carriers during lifelong infection. The involvement of HBx/8p11 fusion transcript in Wnt/β-catenin signaling pathway may contribute, at least in part, 50-70% of dysregulated Wnt/β-catenin signaling pathway in HCC (Wong et al. 2001). This study signifies the potential therapeutic value and importance of HBx/8p11 fusion transcript. Based on significant correlation between HBx/8p11 expression and shorter overall survival as well as the significance as a predictor of HCC development in multivariative analysis, the development of HBx/8p11 as a diagnostic biomarker may substantiate its predictive value for HBV-positive HCC, especially during early pathogenesis.

In this study, a novel recurrent viral integration site leading to the expression of HBx/8p11 fusion transcript was revealed, with its possible functions as ncRNA to

promote cell motility, cell proliferation and tumor growth through alternation of EMT and Wnt signaling pathway. Taken together with its high prevalence and significant effect in overall survival, HBx/8p11 fusion transcript is a potential molecular target for the development of successful therapeutic interventions in HCC.

Chapter 4

Identification and Characterization of HBx/22q11 Fusion Transcript

4.1 INTRODUCTION

In this chapter, the identification of HBx into the intronic region of clathrin (CLTCL1) in chr.22q11.21 leading to the generation of HBx/22q11 fusion transcript was shown. High incidence of 24.9% (12 out of 49 HCC cases) suggested the preferential HBV integration site. Clinicopathological correlations and functional study did not suggest the significance of HBx/22q11 in HBV-induced hepatocarcinogenesis, suggesting some HBV integrations into human genome that might not be contributing to metastasis and tumor development.

4.2 RESULTS

4.2.1 Identification of full-length HBx/22q11 Fusion Transcript by RACE

By 3' RACE for identifying HBx/8p11 fusion transcript using HBx specific primer in the previous chapter, additional fusion transcript was also amplified (Figure 4A, left panel). Sequencing analysis suggested the PCR product contained human chr.22q11 at the 3' end. The 3' end transcript of 22q11 contained a polyadenylation signal AATAAA and poly(A) tail (Figure 4A, left panel) and partial HBx sequence at 5' end. Next we proceeded to 5' RACE for the identification of HBx/22q11 5' end (Figure 4.1, left panel). The 5' end consists of HBx and chr22q11 sequence. The presence of 5' linker suggested the 5' end was achieved (Figure 4.1, right panel). Combining the sequences obtained from 3' and 5' RACE, a full-length HBx/22q11 fusion transcript of 477bp was achieved (Figure 4.2A). The transcript comprised of 302bp from HBx, ranged from 1263-1564bp of HBV genome (accession no.: NC_003977), and 174bp of chr.22q11 ranged from 17,610,727-17,610,900bp which is the 3rd intron of clarthrin (CLTCL1, accession no.: NM_007098.3). Interesting, insertion of G in between the viral and human sequence was observed. The presence of start codon at HBx and stop codon at chr.22q11 in the fusion transcript lead to the possible protein translation, with 64 amino acids contributed by HBx and 3 amino acids from chr.22q11 prior to the stop codon (Figure 4.2B).

4.2.2 HBx/22q11 Fusion Transcript Expression in HCC Cell Lines and Primary Tumors

The high incidence of recurrent HBx/8p11 fusion transcript expression indicated it is a potential prognostic marker of HCC. In this chapter, the incidence of HBx/22q11

expression in HCC was examined. Five out of 12 HCC cell lines (41.7%) and 7 out of 37 primary HCC tumors (18.9%) showed HBx/22q11 expression, with a total incidence of 24.9% (12 out of 49 HCC cases, Figure 4.3A). All PCR products were sequence verified to confirm the presence of viral-human junctions (Figure 4.4). Kaplan-Meier analysis indicated the expression of HBx/22q11 do not correlate to overall (P = 0.4277, Figure 4.3B) or disease-free survival of HCC patients (P = 0.5744, Figure 4.3C). The correlation of clinicopathological parameters suggested HBx/22q11 expression significantly correlated with smaller tumor size (P = 0.0258, Table 4.1).

4.2.3 Functional studies of HBx/22q11 full-length fusion transcript and its components

To study the functional roles of HBx/22q11 and determine individual component contributing to observed phenotypes, if any, HBx/22q11$^{1-477}$, HBx$^{1-303}$, 22q11$^{304-477}$ and HBx^{1-315*} for translated protein were cloned and expressed in immortalized human hepatocyte cell line L02. Migration and Matrigel invasion assay suggested the ectopic expression of full-length$^{1-477}$ and its components do not affect cell motility (Figure 5A and 5B). Next we investigated the effect of cell growth. Similarly, MTT and colony formation assay showed the ectopic expression of full-length$^{1-477}$ and its components do not affect cell viability and proliferation (Figure 5A and 5B).

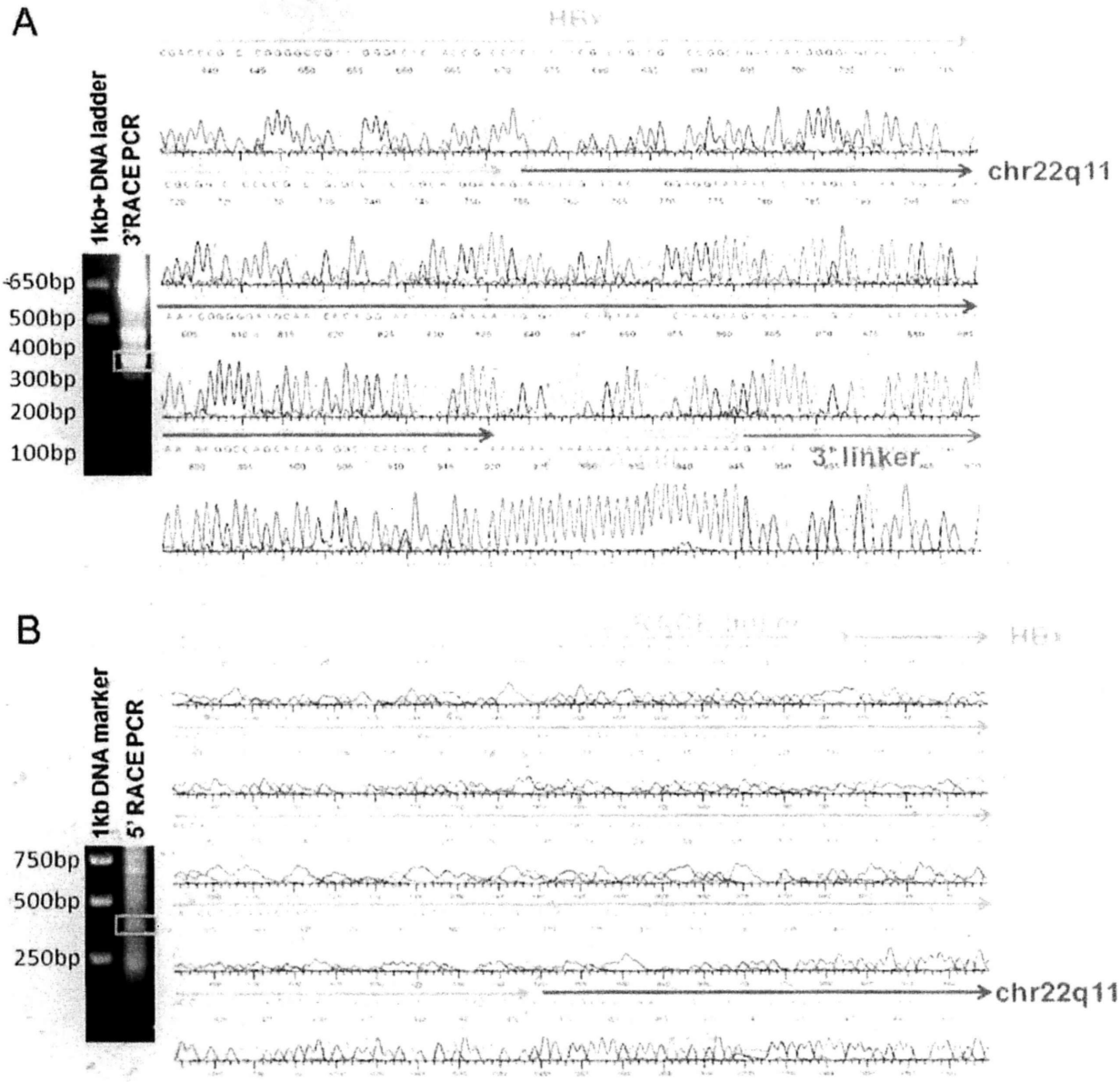

Figure 4.1 RACE for identification of HBx/22q11 fusion transcript. (A) 3' RACE identified the 3' end of HBx/22q11 (red box) consists of HBx, chr.22q11, PolyA signal and PolyA tail. (B) 5' RACE identified the 5' end of HBx/22q11 consists of HBx chr.22q11 sequence (red box). The presence of 5' linker suggested the achievement of 5' end.

A

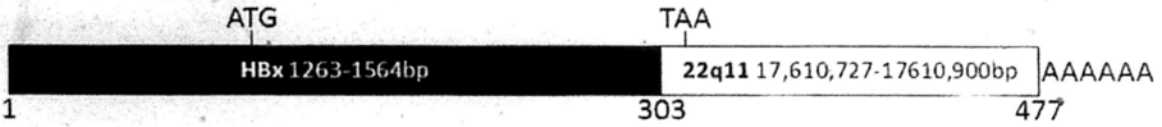

B

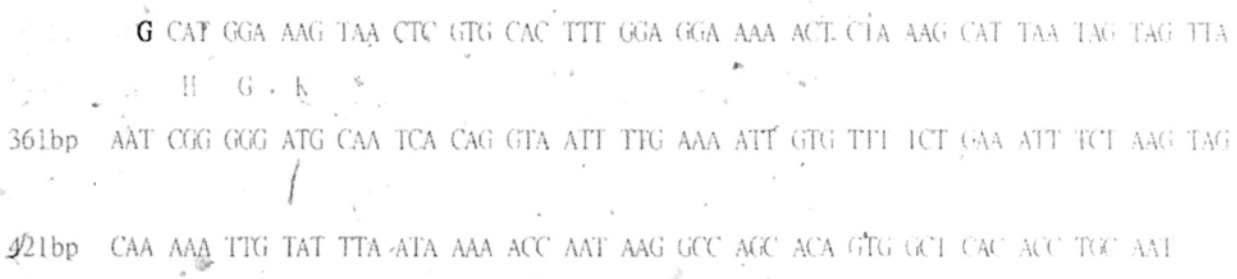

Figure 4.2 Schematic diagram of HBx/22q11. (A) Full-length HBx/22q11 fusion transcript. (B) Translation of HBx/22q11 fusion transcript. Insertion of G between HBx and chr22q (black) was observed.

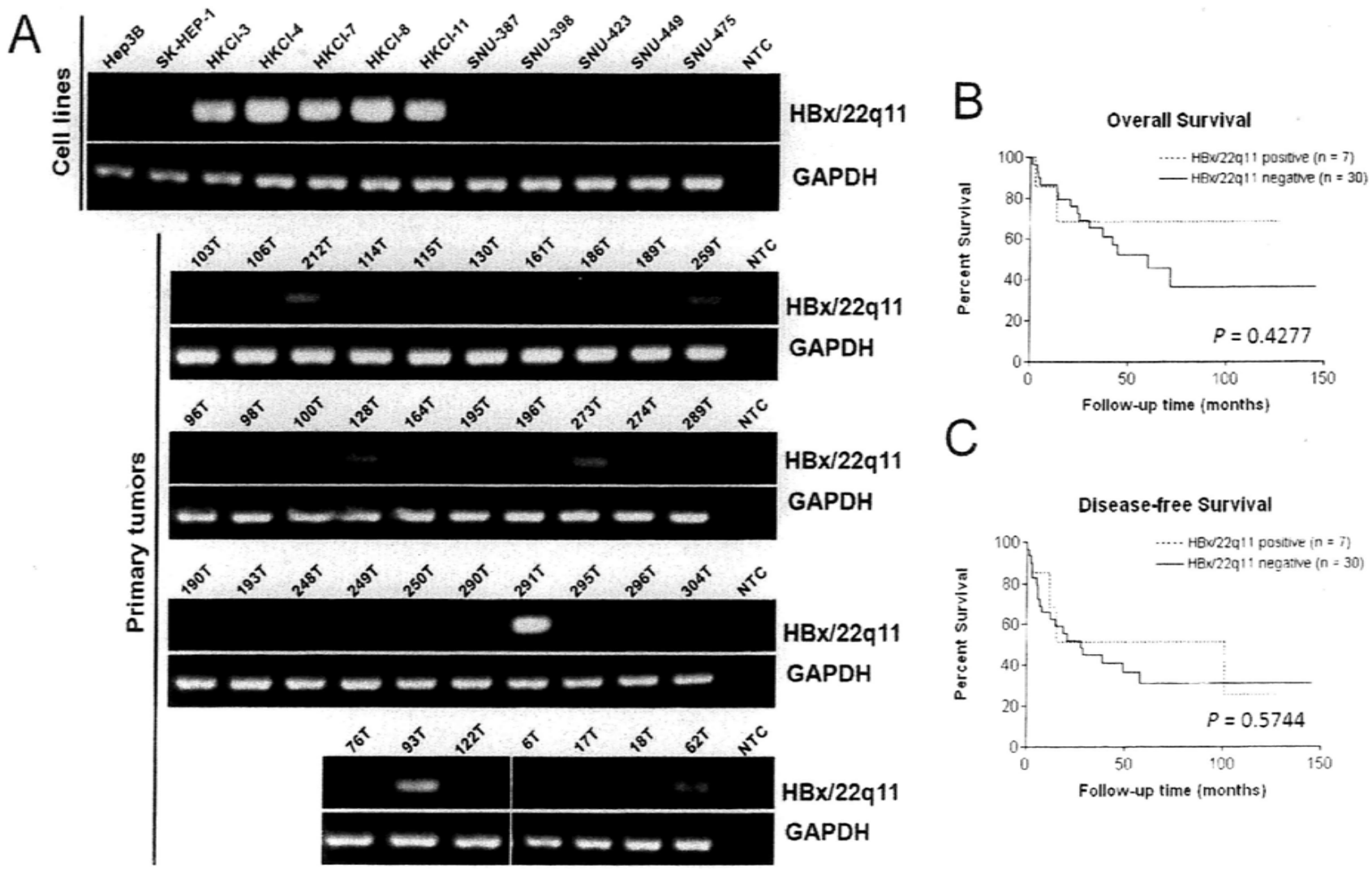

Figure 4.3 HBx/22q11 fusion transcript expression in HCC cell lines and primary tumors. (A) RT-PCR analysis of HBx/22q11 expression in HCC cell lines and primary tumors. Correlation of HBx/22q11 expression with (B) overall and (C) disease-free survival by Kalpan-Meier analysis.

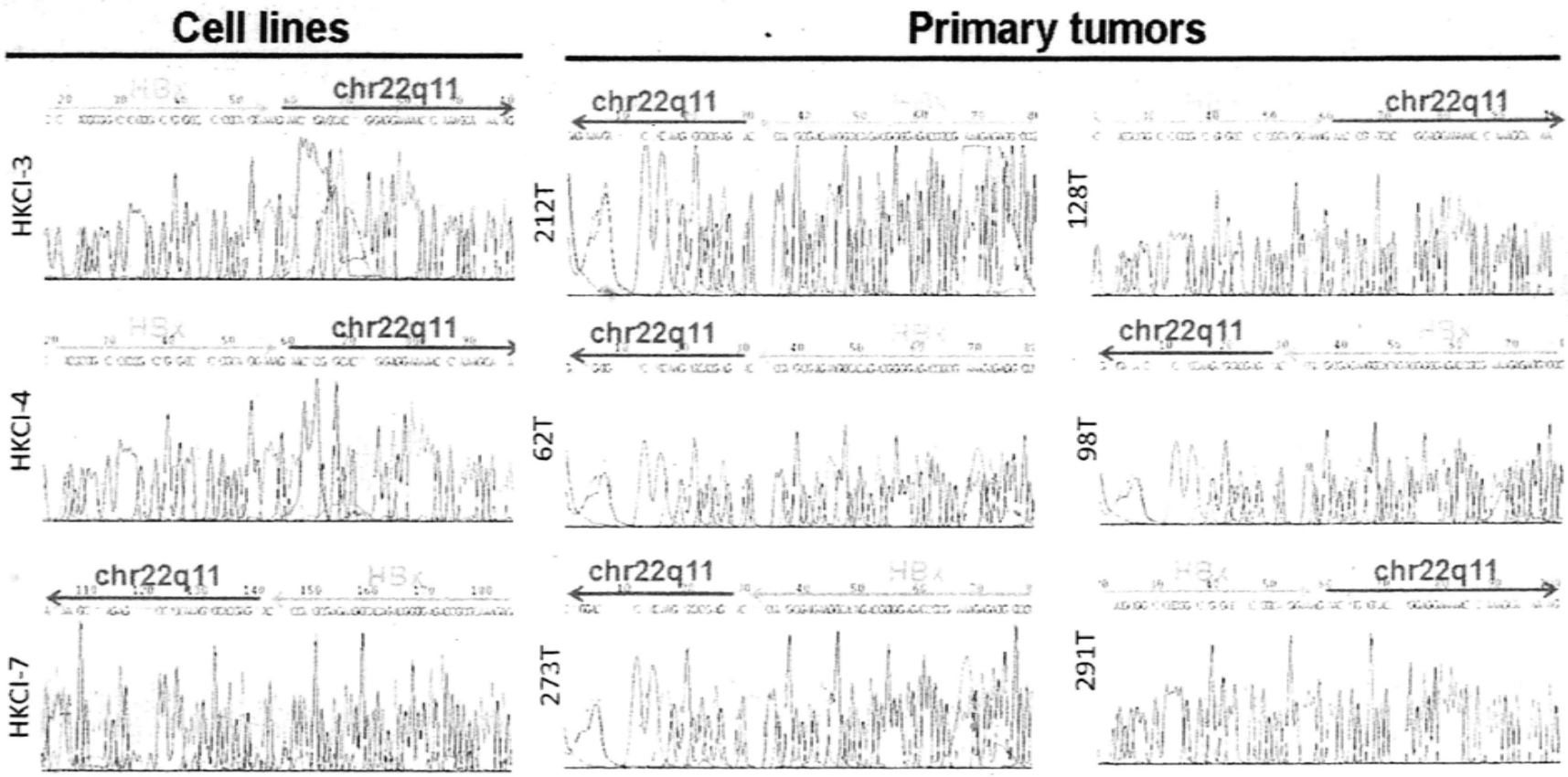

Figure 4.4 Representative DNA sequencing verification of PCR products of HBx/22q11 from HCC cell lines (left panel) and primary tumors (right panel).

Table 4.1 Correlation of clinicopathological parameters with HBx/22q11 expression.

Clinicopathological parameters		HBx/22q11 expression		*P* value
		Positive	Negative	
Sex	Male	5	26	0.32
	Female	2	4	
Age (years, mean±SD)		51.7±13.5	54.9±10.4	0.49
Staging[@]	I	6	16	0.25
	II	1	8	
	III	0	6	
Macrovascular invasion	Yes	0	5	0.26
	No	7	25	
Microvascular invasion	Yes	0	9	0.096
	No	7	21	
Cirrhosis	Yes	7	25	0.25
	No	0	5	
Tumor size (cm, mean±SD)		3.1±0.78	5.1±2.09	0.026*
Tumor Grade[#]	1	1	1	0.47
	2	5	26	
	3	1	3	
Multiple tumor[I]	Yes	2	9	0.94
	No	5	21	

@ Clinical stage: T1, T2 and T3 disease stage of tumors was classified according to the American Joint Committee on Cancer tumor-node-metastasis staging criteria (Greene et al., 2002).

Tumor grade: 1: well-differentiated; 2: moderately differentiated; 3: poorly differentiated

I Tumoral lesions: solitary versus multiple.

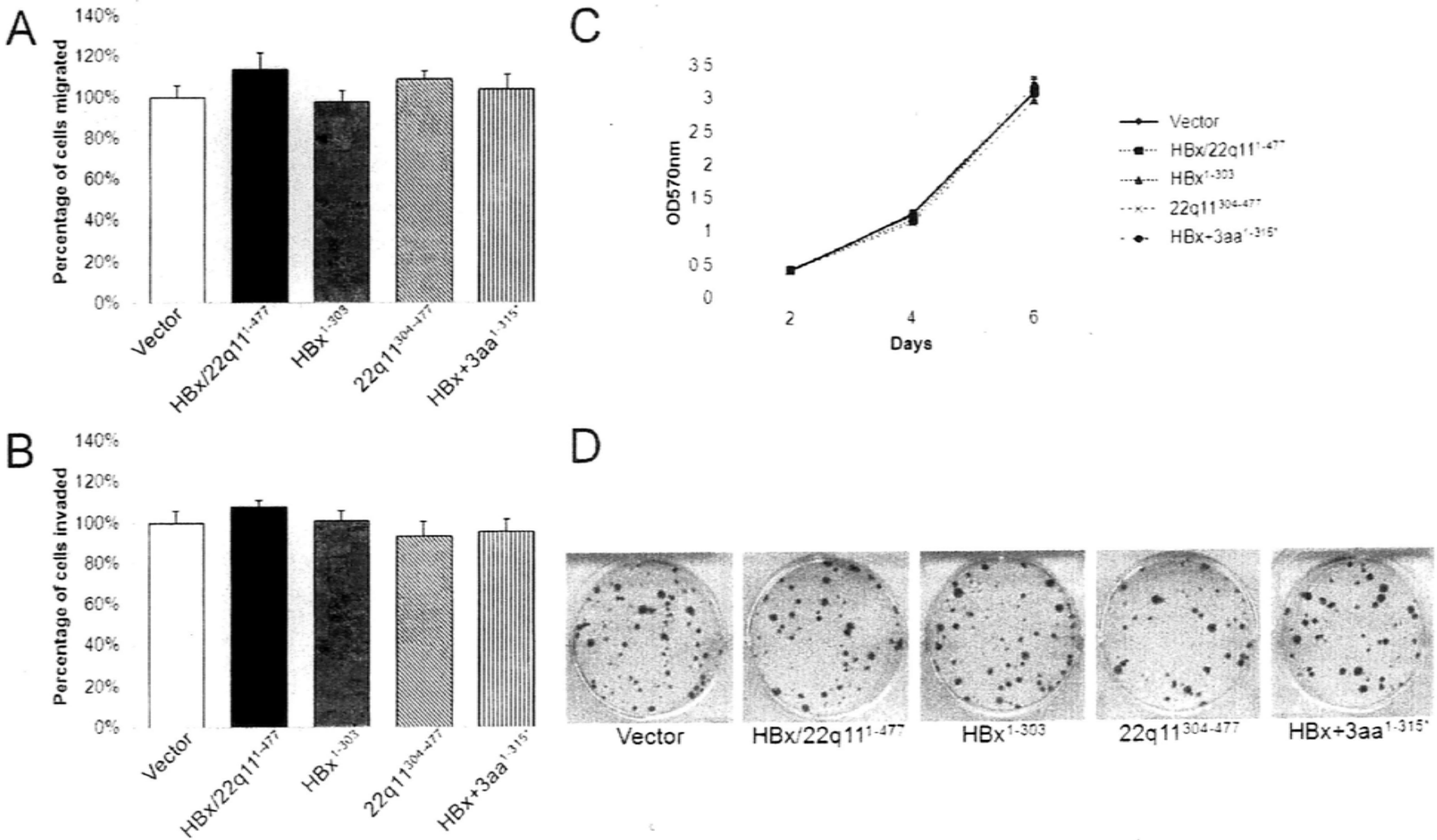

Figure 4.5 Functional studies of HBx/22q11 full-length fusion transcript and its components. (A) Migration assay. (B) Matrigel invasion assay. (C) MTT assay. (D) Colony formation assay.

4.3 DISCUSSION

HBV integration in vicinity of cancer-related genes has been identified to correlate with hepatocarcinogenesis. In this chapter, HBx integration into the intronic region of Clathrin (CLTCL1) in chr22q11.21 was revealed. Human BLAT search suggested the presence of short interspersed nuclear elements (SINE) in chr.22q11.21, which is a repetitive sequence and explained the recurrent HBx integration. Such integration caused a base pair G insertion and maintained in all HCC cell lines and primary cases.

Clinicopathological correlations showed HBx/22q11 expressions in primary HCC tumors do not have implication in prognostic value. In addition, functional study suggested HBx/22q11 is not related to cell motility and growth advantage. However, the high incidence of HBx/22q11 expression not only reaffirmed HBV integration is not a random event, but also implied its significance during the course of HBV infection. For instance, chronic HBV infection is characterized by sustained liver inflammation, which contributes to the development of cirrhosis and hepatocellular carcinoma (Guidotti et al. 2006). Whether HBx/22q11 fusion transcript is involved in thie process remained unstudied. The possibility of identifying other HBV-human fusion transcripts in the future may provide an insight for the mechanisms of HBV-induced carcinogenesis.

Chapter 5

Proposed Future Studies

5.1 Identification of HBV-human integration sites and chimeric fusion transcripts

In this thesis, the role of HBV-human chimeric fusion transcript in hepatocarcinogenesis was clearly demonstrated. As more than 80% of HBV-positive HCC found HBV integration, the identification of HBV integration sites seems to be one of the critical steps in understanding HBV-related HCC development. Previous studies had been focusing on the identification of integrations in vicinity of important genes. However, our results revealed the functional importance of viral integration in repetitive LINE sequence in intergenic regions while some HBV integrations in vicinity of functional genes may be unrelated to carcinogenic process. As a result, the strategy for identifying functional HBV integration sites should be focusing on recurrent HBV integrations and potential expression of HBV-human chimeric fusion transcripts, regardless of the locations of integration. The development of detection methods with high sensitivity and specificity such as real-time PCR would be contributive to the identification and characterization of novel HBV-human chimeric fusion transcripts.

5.2 Identification of HBx/8p11 fusion transcript downstream targets

In chapter 3, we have identified HBx/8p11 fusion transcript promote cell motility through modulation of EMT. Dysregulation of E-cadherin, hallmark of EMT, affect Wnt signaling pathway through disrupting membrane-bound E-cadherin/β-catenin complex. Translocation of β-catenin into nucleus activates Wnt target genes by forming transcriptional complex with TCF/LEF. Although such mechanism has been proposed in our study, downstream target of HBx/8p11 fusion transcript regulating EMT has yet to be

identified. Moreover, upregulation of Wnt inhibitors SFRP1 and DKK4 in siHBx/8p11-treated cells suggested an alternative mechanism to explain the deregulation of Wnt signaling. Confirmation of SFRP1 and DKK4 expression by Western blot is suggested and specific interaction between HBx/8p11 fusion transcript and the promoters of SFRP1 and DKK4 can be further investigated by luciferase reporter assay.

5.3 Development of HBV-human fusion transcript as prognostic marker

Measurement of serum tumor marker alpha-fetoprotein (AFP) is one of the diagnostic methods for HCC. However, the diagnostic accuracy is relatively low. Combination of imaging techniques such as abdominal ultrasonography and computed tomography is required to improve the outcomes. Therefore, the development of a new diagnostic marker for early stage HCC is needed. High incidence and significant correlation with overall survival indicate the prognostic value of HBx/8p11 expression in primary HCC. However, the presence of HBx/8p11 in serum remains to be detected. Real-time PCR with high sensitivity and specificity allow the detection of low copy number in serum. The detection of plasma albumin in HCC patients using real-time PCR has been described (Chan et al. 2010). As a result, the detection of HBx/8p11 in plasma of HCC patients using real-time PCR is a potential new prognostic marker for HBV-positive HCC patients.

Chapter 6

References

REFERENCES

American Cancer Society 2010, liver cancer general treatment information. http://www.cancer.org/Cancer/LiverCancer/DetailedGuide/liver-cancer-treating-general-info

American Cancer Society 2010, survival rates of liver cancer. http://www.cancer.org/Cancer/LiverCancer/DetailedGuide/liver-cancer-survival-rates

Abiru S, Migita K, Maeda Y, Daikoku M, Ito M, Ohata K, Nagaoka S, Matsumoto T, Takii Y, Kusumoto K, Nakamura M, Komori A, Yano K, Yatsuhashi H, Eguchi K, Ishibashi H. Serum cytokine and soluble cytokine receptor levels in patients with non-alcoholic steatohepatitis. Liver Int. 2006 Feb;26(1):39-45.

Bardi G, Sukhikh T, Pandis N, Fenger C, Kronborg O, Heim S. Karyotypic characterization of colorectal adenocarcinomas. Genes Chromosomes Cancer. 1995 Feb;12(2):97-109.

Beasley RP. Hepatitis B virus. The major etiology of hepatocellular carcinoma. Cancer. 1988 May 15;61(10):1942-56.

Bock CT, Tillmann HL, Torresi J, Klempnauer J, Locarnini S, Manns MP, Trautwein C. Selection of hepatitis B virus polymerase mutants with enhanced replication by lamivudine treatment after liver transplantation. Gastroenterology. 2002 Feb;122(2):264-73.

Bonilla Guerrero R, Roberts LR. The role of hepatitis B virus integrations in the pathogenesis of human hepatocellular carcinoma. J Hepatol. 2005 May;42(5):760-77.

Bosch FX, Ribes J, Díaz M, Cléries R. Primary liver cancer: worldwide incidence and trends. Gastroenterology. 2004 Nov;127(5 Suppl 1):S5-S16.

Bréchot C, Gozuacik D, Murakami Y, Paterlini-Bréchot P. Molecular bases for the development of hepatitis B virus (HBV)-related hepatocellular carcinoma (HCC). Semin Cancer Biol. 2000 Jun;10(3):211-31.

Bréchot C. Pathogenesis of hepatitis B virus-related hepatocellular carcinoma: old and new paradigms. Gastroenterology. 2004 Nov;127(5 Suppl 1):S56-61.

Bressac B, Kew M, Wands J, Ozturk M. Selective G to T mutations of p53 gene in hepatocellular carcinoma from southern Africa. Nature. 1991 Apr 4;350(6317):429-31.

Buckwold VE, Xu Z, Chen M, Yen TS, Ou JH. Effects of a naturally occurring mutation in the hepatitis B virus basal core promoter on precore gene expression and viral replication. J Virol. 1996 Sep;70(9):5845-51.

Buendia MA. Hepatitis B viruses and hepatocellular carcinoma. Adv Cancer Res. 1992;59:167-226.

Bussemakers MJ, van Bokhoven A, Verhaegh GW, Smit FP, Karthaus HF, Schalken JA, Debruyne FM, Ru N, Isaacs WB. DD3: a new prostate-specific gene, highly overexpressed in prostate cancer. Cancer Res. 1999 Dec 1;59(23):5975-9.

Caldwell S, Park SH. The epidemiology of hepatocellular cancer: from the perspectives of public health problem to tumor biology. J Gastroenterol. 2009;44 Suppl 19:96-101.

Carman WF, Jacyna MR, Hadziyannis S, Karayiannis P, McGarvey MJ, Makris A, Thomas HC. Mutation preventing formation of hepatitis B e antigen in patients with chronic hepatitis B infection. Lancet. 1989 Sep 9;2(8663):588-91.

Carman WF, Zanetti AR, Karayiannis P, Waters J, Manzillo G, Tanzi E, Zuckerman AJ, Thomas HC. Vaccine-induced escape mutant of hepatitis B virus. Lancet. 1990 Aug 11;336(8711):325-9.

Cha MY, Kim CM, Park YM, Ryu WS. Hepatitis B virus X protein is essential for the activation of Wnt/beta-catenin signaling in hepatoma cells. Hepatology. 2004 Jun;39(6):1683-93.

Chan HL, Tse CH, Mo F, Koh J, Wong VW, Wong GL, Lam Chan S, Yeo W, Sung JJ, Mok TS. High viral load and hepatitis B virus subgenotype ce are associated with increased risk of hepatocellular carcinoma. J Clin Oncol. 2008 Jan 10;26(2):177-82.

Chan HL, Tsui SK, Tse CH, Ng EY, Au TC, Yuen L, Bartholomeusz A, Leung KS, Lee KH, Locarnini S, Sung JJ. Epidemiological and virological characteristics of 2 subgroups of hepatitis B virus genotype C. J Infect Dis. 2005 Jun 15;191(12):2022-32.

Chan KY, Lai PB, Squire JA, Beheshti B, Wong NL, Sy SM, Wong N. Positional expression profiling indicates candidate genes in deletion hotspots of hepatocellular carcinoma. Mod Pathol. 2006 Dec;19(12):1546-54.

Chan RW, Wong J, Chan HL, Mok TS, Lo WY, Lee V, To KF, Lai PB, Rainer TH, Lo YM, Chiu RW. Aberrant concentrations of liver-derived plasma albumin mRNA in liver pathologies. Clin Chem. 2010 Jan;56(1):82-9.

Chisari FV, Ferrari C. Hepatitis B virus immunopathogenesis. Annu Rev Immunol. 1995;13:29-60.

Choo QL, Kuo G, Weiner AJ, Overby LR, Bradley DW, Houghton M. Isolation of a cDNA clone derived from a blood-borne non-A, non-B viral hepatitis genome. Science. 1989 Apr 21;244(4902):359-62.

Cseh B, Fernandez-Sauze S, Grall D, Schaub S, Doma E, Van Obberghen-Schilling E. Autocrine fibronectin directs matrix assembly and crosstalk between cell-matrix and cell-cell adhesion in vascular endothelial cells. J Cell Sci. 2010 Nov 15;123(Pt 22):3989-99.

Dandri M, Burda MR, Bürkle A, Zuckerman DM, Will H, Rogler CE, Greten H, Petersen J. Increase in de novo HBV DNA integrations in response to oxidative DNA damage or inhibition of poly(ADP-ribosyl)ation. Hepatology. 2002 Jan;35(1):217-23.

Daniele B, Bencivenga A, Megna AS, Tinessa V. Alpha-fetoprotein and ultrasonography screening for hepatocellular carcinoma. Gastroenterology. 2004 Nov;127(5 Suppl 1):S108-12.

Dejean A, Bougueleret L, Grzeschik KH, Tiollais P. Hepatitis B virus DNA integration in a sequence homologous to v-erb-A and steroid receptor genes in a hepatocellular carcinoma. Nature. 1986 Jul 3-9;322(6074):70-2.

Doherty GJ, McMahon HT. Mediation, modulation, and consequences of membrane-cytoskeleton interactions. Annu Rev Biophys. 2008;37:65-95.

Donato F, Tagger A, Gelatti U, Parrinello G, Boffetta P, Albertini A, Decarli A, Trevisi P, Ribero ML, Martelli C, Porru S, Nardi G. Alcohol and hepatocellular carcinoma:

the effect of lifetime intake and hepatitis virus infections in men and women. Am J Epidemiol. 2002 Feb 15;155(4):323-31.

Elgouhari HM, Abu-Rajab Tamimi TI, Carey WD. Hepatitis B virus infection: understanding its epidemiology, course, and diagnosis. Cleve Clin J Med. 2008 Dec;75(12):881-9.

Elmore LW, Hancock AR, Chang SF, Wang XW, Chang S, Callahan CP, Geller DA, Will H, Harris CC. Hepatitis B virus X protein and p53 tumor suppressor interactions in the modulation of apoptosis. Proc Natl Acad Sci U S A. 1997 Dec 23;94(26):14707-12.

El-Serag HB, Rudolph KL. Hepatocellular carcinoma: epidemiology and molecular carcinogenesis. Gastroenterology. 2007 Jun;132(7):2557-76.

Erhardt A, Hassan M, Heintges T, Häussinger D. Hepatitis C virus core protein induces cell proliferation and activates ERK, JNK, and p38 MAP kinases together with the MAP kinase phosphatase MKP-1 in a HepG2 Tet-Off cell line. Virology. 2002 Jan 20;292(2):272-84.

Feitelson MA, Lee J. Hepatitis B virus integration, fragile sites, and hepatocarcinogenesis. Cancer Lett. 2007 Jul 18;252(2):157-70.

Ferber MJ, Montoya DP, Yu C, Aderca I, McGee A, Thorland EC, Nagorney DM, Gostout BS, Burgart LJ, Boix L, Bruix J, McMahon BJ, Cheung TH, Chung TK, Wong YF, Smith DI, Roberts LR. Integrations of the hepatitis B virus (HBV) and human papillomavirus (HPV) into the human telomerase reverse transcriptase (hTERT) gene in liver and cervical cancers. Oncogene. 2003 Jun 12;22(24):3813-20.

Ferlay J, Shin HR, Bray F, Forman D, Mathers C, Parkin DM. Estimates of worldwide burden of cancer in 2008: GLOBOCAN 2008. Int J Cancer. 2010 Dec 15;127(12):2893-917.

Fernandez AF, Esteller M. Viral epigenomes in human tumorigenesis. Oncogene. 2010 Mar 11;29(10):1405-20.

Fidler IJ. The pathogenesis of cancer metastasis: the 'seed and soil' hypothesis revisited. Nat Rev Cancer. 2003 Jun;3(6):453-8.

Friedman SL, Arthur MJ. Activation of cultured rat hepatic lipocytes by Kupffer cell conditioned medium. Direct enhancement of matrix synthesis and stimulation of cell proliferation via induction of platelet-derived growth factor receptors. J Clin Invest. 1989 Dec;84(6):1780-5.

Friedman SL. Mechanisms of hepatic fibrogenesis. Gastroenterology. 2008 May;134(6):1655-69.

Greene FL, American Joint Committe on Cancer, American Cancer Society. AJCC cancer staging manual. pp. xiv 421–i411. New York: Springer-Verlag; 2002.

Gorunova L, Höglund M, Andrén-Sandberg A, Dawiskiba S, Jin Y, Mitelman F, Johansson B. Cytogenetic analysis of pancreatic carcinomas: intratumor heterogeneity and nonrandom pattern of chromosome aberrations. Genes Chromosomes Cancer. 1998 Oct;23(2):81-99.

Gottardi CJ, Wong E, Gumbiner BM. E-cadherin suppresses cellular transformation by inhibiting beta-catenin signaling in an adhesion-independent manner. J Cell Biol. 2001 May 28;153(5):1049-60.

Gozuacik D, Murakami Y, Saigo K, Chami M, Mugnier C, Lagorce D, Okanoue T, Urashima T, Bréchot C, Paterlini-Bréchot P. Identification of human cancer-related genes by naturally occurring Hepatitis B Virus DNA tagging. Oncogene. 2001 Sep 27;20(43):6233-40.

Graef E, Caselmann WH, Wells J, Koshy R. Insertional activation of mevalonate kinase by hepatitis B virus DNA in a human hepatoma cell line. Oncogene. 1994 Jan;9(1):81-7.

Guidotti LG, Chisari FV. Immunobiology and pathogenesis of viral hepatitis. Annu Rev Pathol. 2006;1:23-61.

Heinlein CA, Chang C. Androgen receptor (AR) coregulators: an overview. Endocr Rev. 2002 Apr;23(2):175-200.

Hoek JB, Pastorino JG. Ethanol, oxidative stress, and cytokine-induced liver cell injury. Alcohol. 2002 May;27(1):63-8.

Hogan B, Costantini F and Lacy E. Manipulating the mouse embryo: a laboratory manual. New York, Cold Spring Harbour Laboratory Press. 1986.

Hoofnagle JH. Course and outcome of hepatitis C. Hepatology. 2002 Nov;36(5 Suppl 1):S21-9.

Hosono S, Tai PC, Wang W, Ambrose M, Hwang DG, Yuan TT, Peng BH, Yang CS, Lee CS, Shih C. Core antigen mutations of human hepatitis B virus in hepatomas accumulate in MHC class II-restricted T cell epitopes. Virology. 1995 Sep 10;212(1):151-62.

Hsu IC, Metcalf RA, Sun T, Welsh JA, Wang NJ, Harris CC. Mutational hotspot in the p53 gene in human hepatocellular carcinomas. Nature. 1991 Apr 4;350(6317):427-8.

Hung T, Chang HY. Long noncoding RNA in genome regulation: prospects and mechanisms. RNA Biol. 2010 Sep-Oct;7(5):582-5

Hussain SP, Schwank J, Staib F, Wang XW, Harris CC. TP53 mutations and hepatocellular carcinoma: insights into the etiology and pathogenesis of liver cancer. Oncogene. 2007 Apr 2;26(15):2166-76.

Iacoangeli A, Lin Y, Morley EJ, Muslimov IA, Bianchi R, Reilly J, Weedon J, Diallo R, Böcker W, Tiedge H. BC200 RNA in invasive and preinvasive breast cancer. Carcinogenesis. 2004 Nov;25(11):2125-33.

Javier RT, Butel JS. The history of tumor virology. Cancer Res. 2008 Oct 1;68(19):7693-706.

Koch S, Freytag von Loringhoven A, Kahmann R, Hofschneider PH, Koshy R. The genetic organization of integrated hepatitis B virus DNA in the human hepatoma cell line PLC/PRF/5. Nucleic Acids Res. 1984 Sep 11;12(17):6871-86.

Koch S, von Loringhoven AF, Hofschneider PH, Koshy R. Amplification and rearrangement in hepatoma cell DNA associated with integrated hepatitis B virus DNA. EMBO J. 1984 Sep;3(9):2185-9.

Koshy R, Koch S, von Loringhoven AF, Kahmann R, Murray K, Hofschneider PH. Integration of hepatitis B virus DNA: evidence for integration in the single-stranded gap. Cell. 1983 Aug;34(1):215-23.

Kremsdorf D, Soussan P, Paterlini-Brechot P, Brechot C. Hepatitis B virus-related hepatocellular carcinoma: paradigms for viral-related human carcinogenesis. Oncogene. 2006 Jun 26;25(27):3823-33.

Kuper H, Ye W, Broomé U, Romelsjö A, Mucci LA, Ekbom A, Adami HO, Trichopoulos D, Nyrén O. The risk of liver and bile duct cancer in patients with chronic viral hepatitis, alcoholism, or cirrhosis. Hepatology. 2001 Oct;34(4 Pt 1):714-8.

Kwun HJ, Jung EY, Ahn JY, Lee MN, Jang KL. p53-dependent transcriptional repression of p21(waf1) by hepatitis C virus NS3. J Gen Virol. 2001 Sep;82(Pt 9):2235-41.

Laskus T, Radkowski M, Wang LF, Nowicki M, Rakela J. Detection and sequence analysis of hepatitis B virus integration in peripheral blood mononuclear cells. J Virol. 1999 Feb;73(2):1235-8.

Lavanchy D. The global burden of hepatitis C. Liver Int. 2009 Jan;29 Suppl 1:74-81.

Lee YH, Yun Y. HBx protein of hepatitis B virus activates Jak1-STAT signaling. J Biol Chem. 1998 Sep 25;273(39):25510-5.

Lee YI, Kang-Park S, Do SI, Lee YI. The hepatitis B virus-X protein activates a phosphatidylinositol 3-kinase-dependent survival signaling cascade. J Biol Chem. 2001 May 18;276(20):16969-77.

Lev S, Moreno H, Martinez R, Canoll P, Peles E, Musacchio JM, Plowman GD, Rudy B, Schlessinger J. Protein tyrosine kinase PYK2 involved in Ca(2+)-induced regulation of ion channel and MAP kinase functions. Nature. 1995 Aug 31;376(6543):737-45.

Liu X, Wang L, Zhang S, Lin J, Zhang S, Feitelson MA, Gao H, Zhu M. Mutations in the C-terminus of the X protein of hepatitis B virus regulate Wnt-5a expression in hepatoma Huh7 cells: cDNA microarray and proteomic analyses. Carcinogenesis. 2008 Jun;29(6):1207-14.

Lu B, Guo H, Zhao J, Wang C, Wu G, Pang M, Tong X, Bu F, Liang A, Hou S, Fan X, Dai J, Wang H, Guo Y. Increased expression of iASPP, regulated by hepatitis B virus X protein-mediated NF-κB activation, in hepatocellular carcinoma. Gastroenterology. 2010 Dec;139(6):2183-2194.

Ma NF, Lau SH, Hu L, Xie D, Wu J, Yang J, Wang Y, Wu MC, Fung J, Bai X, Tzang CH, Fu L, Yang M, Su YA, Guan XY. COOH-terminal truncated HBV X protein plays key role in hepatocarcinogenesis. Clin Cancer Res. 2008 Aug 15;14(16):5061-8.

Ma WL, Hsu CL, Wu MH, Wu CT, Wu CC, Lai JJ, Jou YS, Chen CW, Yeh S, Chang C. Androgen receptor is a new potential therapeutic target for the treatment of hepatocellular carcinoma. Gastroenterology. 2008 Sep;135(3):947-55.

Majumder M, Steele R, Ghosh AK, Zhou XY, Thornburg L, Ray R, Phillips NJ, Ray RB. Expression of hepatitis C virus non-structural 5A protein in the liver of transgenic mice. FEBS Lett. 2003 Dec 18;555(3):528-32.

Matouk IJ, Abbasi I, Hochberg A, Galun E, Dweik H, Akkawi M. Highly upregulated in liver cancer noncoding RNA is overexpressed in hepatic colorectal metastasis. Eur J Gastroenterol Hepatol. 2009 Jun;21(6):688-92.

Matouk IJ, DeGroot N, Mezan S, Ayesh S, Abu-lail R, Hochberg A, Galun E. The H19 non-coding RNA is essential for human tumor growth. PLoS One. 2007 Sep 5;2(9):e845.

Matsubara K, Tokino T. Integration of hepatitis B virus DNA and its implications for hepatocarcinogenesis. Mol Biol Med. 1990 Jun;7(3):243-60.

Matsuzaki K. Modulation of TGF-beta signaling during progression of chronic liver diseases. Front Biosci. 2009 Jan 1;14:2923-34.
McLaughlin-Drubin ME, Munger K. Viruses associated with human cancer. Biochim Biophys Acta. 2008 Mar;1782(3):127-50.
McMahon BJ. The natural history of chronic hepatitis B virus infection. Hepatology. 2009 May;49(5 Suppl):S45-55.
Mertens F, Johansson B, Höglund M, Mitelman F. Chromosomal imbalance maps of malignant solid tumors: a cytogenetic survey of 3185 neoplasms. Cancer Res. 1997 Jul 1;57(13):2765-80.
Moinzadeh P, Breuhahn K, Stützer H, Schirmacher P. Chromosome alterations in human hepatocellular carcinomas correlate with aetiology and histological grade--results of an explorative CGH meta-analysis. Br J Cancer. 2005 Mar 14;92(5):935-41.
Moradpour D, Penin F, Rice CM. Replication of hepatitis C virus. Nat Rev Microbiol. 2007 Jun;5(6):453-63.
Murakami Y, Saigo K, Takashima H, Minami M, Okanoue T, Bréchot C, Paterlini-Bréchot P. Large scaled analysis of hepatitis B virus (HBV) DNA integration in HBV related hepatocellular carcinomas. Gut. 2005 Aug;54(8):1162-8.
Nakatani T, Roy G, Fujimoto N, Asahara T, Ito A. Sex hormone dependency of diethylnitrosamine-induced liver tumors in mice and chemoprevention by leuprorelin. Jpn J Cancer Res. 2001 Mar;92(3):249-56.
Naugler WE, Sakurai T, Kim S, Maeda S, Kim K, Elsharkawy AM, Karin M. Gender disparity in liver cancer due to sex differences in MyD88-dependent IL-6 production. Science. 2007 Jul 6;317(5834):121-4.
Ng IO, Guan XY, Poon RT, Fan ST, Lee JM. Determination of the molecular relationship between multiple tumour nodules in hepatocellular carcinoma differentiates multicentric origin from intrahepatic metastasis. J Pathol. 2003 Mar;199(3):345-53.
Nusse R. Wnt signaling in disease and in development. Cell Res. 2005 Jan;15(1):28-32.
Ogata N, Tokino T, Kamimura T, Asakura H. A comparison of the molecular structure of integrated hepatitis B virus genomes in hepatocellular carcinoma cells and hepatocytes derived from the same patient. Hepatology. 1990 Jun;11(6):1017-23.
Ogura Y, Kurosaki M, Asahina Y, Enomoto N, Marumo F, Sato C. Prevalence and significance of naturally occurring mutations in the surface and polymerase genes of hepatitis B virus. J Infect Dis. 1999 Nov;180(5):1444-51.
Okamoto CT, McKinney J, Jeng YY. Clathrin in mitotic spindles. Am J Physiol Cell Physiol. 2000 Aug;279(2):C369-74.
Oliva J, Bardag-Gorce F, French BA, Li J, French SW. The regulation of non-coding RNA expression in the liver of mice fed DDC. Exp Mol Pathol. 2009 Aug;87(1):12-9.
Onder TT, Gupta PB, Mani SA, Yang J, Lander ES, Weinberg RA. Loss of E-cadherin promotes metastasis via multiple downstream transcriptional pathways. Cancer Res. 2008 May 15;68(10):3645-54.
Pang E, Wong N, Lai PB, To KF, Lau WY, Johnson PJ. Consistent chromosome 10 rearrangements in four newly established human hepatocellular carcinoma cell lines. Genes Chromosomes Cancer. 2002 Feb;33(2):150-9.
Pang EY, Bai AH, To KF, Sy SM, Wong NL, Lai PB, Squire JA, Wong N. Identification of PFTAIRE protein kinase 1, a novel cell division cycle-2 related gene, in the

motile phenotype of hepatocellular carcinoma cells. Hepatology. 2007 Aug;46(2):436-45.

Panzitt K, Tschernatsch MM, Guelly C, Moustafa T, Stradner M, Strohmaier HM, Buck CR, Denk H, Schroeder R, Trauner M, Zatloukal K. Characterization of HULC, a novel gene with striking up-regulation in hepatocellular carcinoma, as noncoding RNA. Gastroenterology. 2007 Jan;132(1):330-42.

Parada LA, Bardi G, Hallén M, Hägerstrand I, Tranberg KG, Mitelman F, Johansson B. Cytogenetic abnormalities and clonal evolution in an adult hepatoblastoma. Am J Surg Pathol. 1997 Nov;21(11):1381-6.

Parada LA, Hallén M, Tranberg KG, Hägerstrand I, Bondeson L, Mitelman F, Johansson B. Frequent rearrangements of chromosomes 1, 7, and 8 in primary liver cancer. Genes Chromosomes Cancer. 1998 Sep;23(1):26-35.

Parsons CJ, Takashima M, Rippe RA. Molecular mechanisms of hepatic fibrogenesis. J Gastroenterol Hepatol. 2007 Jun;22 Suppl 1:S79-84. Review. Erratum in: J Gastroenterol Hepatol. 2008 Mar;23(3):501-2.

Paterlini-Bréchot P, Saigo K, Murakami Y, Chami M, Gozuacik D, Mugnier C, Lagorce D, Bréchot C. Hepatitis B virus-related insertional mutagenesis occurs frequently in human liver cancers and recurrently targets human telomerase gene. Oncogene. 2003 Jun 19;22(25):3911-6.

Perz JF, Armstrong GL, Farrington LA, Hutin YJ, Bell BP. The contributions of hepatitis B virus and hepatitis C virus infections to cirrhosis and primary liver cancer worldwide. J Hepatol. 2006 Oct;45(4):529-38.

Pinkert CA. Transgenic animal technology – A laboratory handbook. San Diego, Academic Press, Inc. 1994.

Pinzani M, Milani S, Herbst H, DeFranco R, Grappone C, Gentilini A, Caligiuri A, Pellegrini G, Ngo DV, Romanelli RG, Gentilini P. Expression of platelet-derived growth factor and its receptors in normal human liver and during active hepatic fibrogenesis. Am J Pathol. 1996 Mar;148(3):785-800.

Polyak K, Weinberg RA. Transitions between epithelial and mesenchymal states: acquisition of malignant and stem cell traits. Nat Rev Cancer. 2009 Apr;9(4):265-73.

Ritchie DS, McBean M, Westerman DA, Kovalenko S, Seymour JF, Dobrovic A. Complete molecular response of e6a2 BCR-ABL-positive acute myeloid leukemia to imatinib then dasatinib. Blood. 2008 Mar 1;111(5):2896-8.

Saigo K, Yoshida K, Ikeda R, Sakamoto Y, Murakami Y, Urashima T, Asano T, Kenmochi T, Inoue I. Integration of hepatitis B virus DNA into the myeloid/lymphoid or mixed-lineage leukemia (MLL4) gene and rearrangements of MLL4 in human hepatocellular carcinoma. Hum Mutat. 2008 May;29(5):703-8.

Sarkar G, Turner RT, Bolander ME. Restriction-site PCR: a direct method of unknown sequence retrieval adjacent to a known locus by using universal primers. PCR Methods Appl. 1993 May;2(4):318-22.

Sato H, Suzuki H, Toyota M, Nojima M, Maruyama R, Sasaki S, Takagi H, Sogabe Y, Sasaki Y, Idogawa M, Sonoda T, Mori M, Imai K, Tokino T, Shinomura Y. Frequent epigenetic inactivation of DICKKOPF family genes in human gastrointestinal tumors. Carcinogenesis. 2007 Dec;28(12):2459-66.

Schmid SL. Clathrin-coated vesicle formation and protein sorting: an integrated process. Annu Rev Biochem. 1997;66:511-48.

Shin JY, Hur W, Wang JS, Jang JW, Kim CW, Bae SH, Jang SK, Yang SH, Sung YC, Kwon OJ, Yoon SK. HCV core protein promotes liver fibrogenesis via up-regulation of CTGF with TGF-beta1. Exp Mol Med. 2005 Apr 30;37(2):138-45.

Soda M, Choi YL, Enomoto M, Takada S, Yamashita Y, Ishikawa S, Fujiwara S, Watanabe H, Kurashina K, Hatanaka H, Bando M, Ohno S, Ishikawa Y, Aburatani H, Niki T, Sohara Y, Sugiyama Y, Mano H. Identification of the transforming EML4-ALK fusion gene in non-small-cell lung cancer. Nature. 2007 Aug 2;448(7153):561-6.

Suzuki H, Watkins DN, Jair KW, Schuebel KE, Markowitz SD, Chen WD, Pretlow TP, Yang B, Akiyama Y, Van Engeland M, Toyota M, Tokino T, Hinoda Y, Imai K, Herman JG, Baylin SB. Epigenetic inactivation of SFRP genes allows constitutive WNT signaling in colorectal cancer. Nat Genet. 2004 Apr;36(4):417-22.

Takahashi K, Akahane Y, Hino K, Ohta Y, Mishiro S. Hepatitis B virus genomic sequence in the circulation of hepatocellular carcinoma patients: comparative analysis of 40 full-length isolates. Arch Virol. 1998;143(12):2313-26.

Tan X, Behari J, Cieply B, Michalopoulos GK, Monga SP. Conditional deletion of beta-catenin reveals its role in liver growth and regeneration. Gastroenterology. 2006 Nov;131(5):1561-72.

Terradillos O, Billet O, Renard CA, Levy R, Molina T, Briand P, Buendia MA. The hepatitis B virus X gene potentiates c-myc-induced liver oncogenesis in transgenic mice. Oncogene. 1997 Jan 30;14(4):395-404.

Thompson MD, Monga SP. WNT/beta-catenin signaling in liver health and disease. Hepatology. 2007 May;45(5):1298-305.

Thorland EC, Myers SL, Gostout BS, Smith DI. Common fragile sites are preferential targets for HPV16 integrations in cervical tumors. Oncogene. 2003 Feb 27;22(8):1225-37.

Tipples GA, Ma MM, Fischer KP, Bain VG, Kneteman NM, Tyrrell DL. Mutation in HBV RNA-dependent DNA polymerase confers resistance to lamivudine in vivo. Hepatology. 1996 Sep;24(3):714-7.

Tokino T, Fukushige S, Nakamura T, Nagaya T, Murotsu T, Shiga K, Aoki N, Matsubara K. Chromosomal translocation and inverted duplication associated with integrated hepatitis B virus in hepatocellular carcinomas. J Virol. 1987 Dec;61(12):3848-54.

Tong WM, Lee MK, Galendo D, Wang ZQ, Sabapathy K. Aflatoxin-B exposure does not lead to p53 mutations but results in enhanced liver cancer of Hupki (human p53 knock-in) mice. Int J Cancer. 2006 Aug 15;119(4):745-9.

Tsai WL, Chung RT. Viral hepatocarcinogenesis. Oncogene. 2010 Apr 22;29(16):2309-24.

Tsuei DJ, Hsu TY, Chen JY, Chang MH, Hsu HC, Yang CS. Analysis of integrated hepatitis B virus DNA and flanking cellular sequences in a childhood hepatocellular carcinoma. J Med Virol. 1994 Mar;42(3):287-93.

Tu H, Bonura C, Giannini C, Mouly H, Soussan P, Kew M, Paterlini-Bréchot P, Bréchot C, Kremsdorf D. Biological impact of natural COOH-terminal deletions of hepatitis B virus X protein in hepatocellular carcinoma tissues. Cancer Res. 2001 Nov 1;61(21):7803-10.

Tung-Ping Poon R, Fan ST, Wong J. Risk factors, prevention, and management of postoperative recurrence after resection of hepatocellular carcinoma. Ann Surg. 2000 Jul;232(1):10-24.

Turner PC, Sylla A, Diallo MS, Castegnaro JJ, Hall AJ, Wild CP. The role of aflatoxins and hepatitis viruses in the etiopathogenesis of hepatocellular carcinoma: A basis for primary prevention in Guinea-Conakry, West Africa. J Gastroenterol Hepatol. 2002 Dec;17 Suppl:S441-8.

Wang HP, Zhang L, Dandri M, Rogler CE. Antisense downregulation of N-myc1 in woodchuck hepatoma cells reverses the malignant phenotype. J Virol. 1998 Mar;72(3):2192-8.

Wang J, Chenivesse X, Henglein B, Bréchot C. Hepatitis B virus integration in a cyclin A gene in a hepatocellular carcinoma. Nature. 1990 Feb 8;343(6258):555-7.

Wang PC, Hui EK, Chiu JH, Lo SJ. Analysis of integrated hepatitis B virus DNA and flanking cellular sequence by inverse polymerase chain reaction. J Virol Methods. 2001 Mar;92(1):83-90.

Wang Y, Lau SH, Sham JS, Wu MC, Wang T, Guan XY. Characterization of HBV integrants in 14 hepatocellular carcinomas: association of truncated X gene and hepatocellular carcinogenesis. Oncogene. 2004 Jan 8;23(1):142-8.

Wong AS, Gumbiner BM. Adhesion-independent mechanism for suppression of tumor cell invasion by E-cadherin. J Cell Biol. 2003 Jun 23;161(6):1191-203.

Wong CM, Fan ST, Ng IO. beta-Catenin mutation and overexpression in hepatocellular carcinoma: clinicopathologic and prognostic significance. Cancer. 2001 Jul 1;92(1):136-45.

Yang J, Weinberg RA. Epithelial-mesenchymal transition: at the crossroads of development and tumor metastasis. Dev Cell. 2008 Jun;14(6):818-29.

Yau T, Pang R, Chan P, Poon RT. Molecular targeted therapy of advanced hepatocellular carcinoma beyond sorafenib. Expert Opin Pharmacother. 2010 Sep;11(13):2187-98.

Yim HJ. [Hepatitis B virus genetic diversity and mutant]. Korean J Hepatol. 2008 Dec;14(4):446-64.

Zhao LJ, Wang L, Ren H, Cao J, Li L, Ke JS, Qi ZT. Hepatitis C virus E2 protein promotes human hepatoma cell proliferation through the MAPK/ERK signaling pathway via cellular receptors. Exp Cell Res. 2005 Apr 15;305(1):23-32.

Zhong S, Chan JY, Yeo W, Tam JS, Johnson PJ. Frequent integration of precore/core mutants of hepatitis B virus in human hepatocellular carcinoma tissues. J Viral Hepat. 2000 Mar;7(2):115-23.

Zhou YZ, Slagle BL, Donehower LA, vanTuinen P, Ledbetter DH, Butel JS. Structural analysis of a hepatitis B virus genome integrated into chromosome 17p of a human hepatocellular carcinoma. J Virol. 1988 Nov;62(11):4224-31.